THE TRANSFER OF MOMENTUM, MASS AND HEAT BETWEEN A CROP AND THE ATMOSPHERE

Thesis

Submitted by

ALEXANDER STRANG THOM, B.Sc. (Natural Philosophy, Glasgow)

for the degree of

DOCTOR OF PHILOSOPHY

University of Edinburgh,

October, 1967.

THE UNIVERSITY *of* EDINBURGH

ACKNOWLEDGEMENTS

I should like to thank Mr. James Paton for the chance of pursuing research in a Scottish University Department of Meteorology; Professor N. Feather for use of a wind-tunnel and associated facilities in the Department of Natural Philosophy; and Sir Frederick Bawden for the privilege of spending part of my research course under supervision at Rothamsted Experimental Station.

Also, I should like to express my gratitude to Dr. J.L. Monteith of Rothamsted, effectively my "external" supervisor, for introducing me to the subject and for continued patient guidance, both in person and in correspondence; to Dr. H.L. Penman, head of the Physics Department at Rothamsted, for accommodating my presence over several months; to the people of Rothamsted in general, but especially Dr. P.H. Gregory for access to a wind-tunnel and I.F. Long and T. Bull for provision of necessary field data: to Dr. D.H. McIntosh of the Meteorology Department, my "resident" supervisor, for his help at all times and in all matters; to Drs. M.A.S. Ross and J.G. Burns of Natural Philosophy for ready advice and pertinent discussion: to Mr. A. Headridge and his workshop staff, Mr. W. Wilson, and Mr. J. Whittaker, each of whom has catered in the best of humour with the experimental eccentricities involved; to Mrs. R.W. Chester for her accurate and patient typing of this thesis: and finally to the Science Research Council for financial support during the two years occupied by this work.

CONTENTS

C O N T E N T S (Contd.)

C O N T E N T S (Contd.)

C O N T E N T S (Contd.)

C O N T E N T S (Contd.)

SUMMARY

The crop is treated as a complex rough surface, to which transfer of mass or heat encounters greater resistance than transfer of momentum. This excess resistance is expressed in terms of the parameter B^{-1} (used by Chamberlain, 1966), and incorporated in Monteith's (1963, 1965) method of estimating surface vapour pressures and temperatures.

An explicit expression for B^{-1} is developed, in part from appropriate resistances of individual crop elements. Also, a general empirical relationship is proposed between B^{-1} and the ratio μ of the normal pressure drag to the tangential skin friction drag on any rough surface: μ, alone or implicit in B^{-1}, is claimed to be a more useful parameter of surface roughness than the roughness length z_o when effectiveness of transfer at the surface itself is under consideration. It is further argued that a universal threshold value of μ, and not the roughness Reynolds' number $R_o = 2.4$, specifies the transition to the "fully rough" flow regime.

The nature of the drag on surface elements exposed to highly sheared and turbulent flow is investigated by direct measurement with a simple moment balance of the drag on several elements of an artificial crop. This experiment gives rise to a technique for procuring an "equilibrium" wind profile (i.e. a profile largely invariant in the direction of flow) with the shortest possible extent of crop; an expression relating the behaviour of z_o to that of the drag coefficient of an individual surface element; an analytical method of estimating the turbulent resistance of the canopy flow; and a plausible electrical analogue to the crop as a momentum sink.

Direct measurement of the dimensionless coefficients, C_d, C_v and C_h for transfer of momentum, mass and heat (molecular diffusivities ν, D and κ, respectively) between an artificial leaf (a typical element of a natural rough surface) and the airflow in a wind-tunnel leads to the result $C_{v,h} = C_o(D/\nu, \kappa/\nu)$, where C_o is practically independent of the angle of incidence ϕ of the leaf to the airflow and in a regime of fully forced convection is proportional to (wind speed)$^{-\frac{1}{2}}$. C_d however, made up of a (usually) dominant pressure part C_b in addition to the molecular skin friction part C_f, is found to depend strongly on ϕ and, except near $\phi = 0^o$, to be much greater than C_o. A proposed equality between C_o and C_f is reduced by argument to the form $C_f = \beta C_o$, where β lies between unity and (about) 10^{-1}, depending on the type and inclination (ϕ) of the roughness elements, and on wind speed. (The sensitive moment balance developed for the crop drag experiment is used to determine both C_d and C_v.)

Examination of a set of Rothamsted field data shows that shelter of several leaves by an upstream neighbour restricts the transfer of momentum to a real crop (beans). It is suggested that the corresponding restriction to mass or heat transfer is somewhat less effective, and the magnitude 4 ± 2 is derived for B^{-1}. Finally, a universal value of B^{-1} is proposed for any suitably vegetated natural surface: namely $B^{-1} = 4$, provided the friction velocity u_* lies between the arbitrary limits 15 and 45 cm. sec.$^{-1}$.

SYMBOLS AND SUBSCRIPTS

Each symbol without exception is defined at its point of introduction in the text, It should be noted however that a few symbols have different meanings according to context.

Use of subscripts is extensive. Where a subscript is attached to a dimensionless transfer coefficient C, or to the corresponding resistance r, the following case convention is adopted.

An upper case subscript is used when transfer is between an extended rough surface and the airflow at some level above: e.g. the drag coefficient C_D; and the resistance to heat transfer r_H.
(Such coefficients and resistances refer to unit area in the horizontal plane.)

A lower case subscript is used for transfer between an element of a rough surface and air flowing past the element, whether the element remains part of the surface or is isolated in a wind-tunnel. e.g. the generalised coefficient for transfer of mass or heat C_o; and the resistance to momentum transfer r_d.
(Such quantities refer to unit plan area of the element - i.e. one half of the total surface area of a leaf, but only about $1/\pi$ times the surface area of a cylindrical element.)

N.B. several subscripts, notably "o", have meanings which depend on the parent symbol.

LIST OF FIGURES

LIST OF FIGURES (Contd.)

LIST OF FIGURES (Contd.)

LIST OF TABLES

LIST OF TABLES (Contd.)

REFERENCES

1. Barry, P.J. 1965 'Exchange rates of radioactive tracers between the atmosphere and snow,' Presented at First Canadian Conference in Micro-meteorology, Toronto, AECL-2232.

2. Blasius, H. 1908 'Grenzschichten in Flüssigkeiten mit kleiner Reibung,' Z. Math. u. Physik, 56, p.1.

3. Chamberlain, A.C. 1966 'Transport of gases to and from grass and grass-like surfaces,' Proc. Roy. Soc., A, 290, p. 236.

4. Cowan, I.R. and Milthorpe, F.L. 1967 'Physiological responses in relation to the environment within the plant cover,' Proceedings, First Symposium on Ecosystems, Copenhagen 1965, UNESCO, Paris.

5. Davies, C.N., 1966, 'Aerosol Science', Academic Press, p. 393.

6. Deacon, E.L. 1957 'Wind profiles and the shearing stress - an anomaly resolved,' Quart. J.R. Met. Soc., 83, p. 537.

7. Goldstein, S. 1938 'Modern Developments in Fluid Mechanics,' 2 vols., Clarendon Press, Oxford.

8. Impens, I. 1964 'Experimentele studie van de physische en biologische aspeken van de transpiratie in de verschillende lagen van de vegetatie,' Doctoral thesis, Laboratorium voor Plantecologie, Ghent.

9. Kusuda, T. 1965 'Calculation of the temperature of a flat plate wet surface with respect to the Lewis relation,' in Humidity and Moisture Measurement and Control in Science and Industry, Vol. 1.

10. Long, I.F. 1957 'Instruments for micro-meteorology,' Quart. J.R. Met. Soc., 83, p.202.

11. Monteith, J.L. 1963 'Gas exchange in plant communities,' in Environmental Control of Plant Growth, L.T. Evans, (ed.), p. 95.

12. Monteith, J.L. 1965 'Evaporation and Environment,' Symp. Soc. expl. Biol., XIX, p. 205.

13. Owen, P.R. and Thomson, W.R. 1963 'Heat transfer across rough surfaces,' J. Fluid Mech., 15, p. 321.

REFERENCES (Contd.)

14. Paeschke, W. 1937 'Experimentelle Untersuchungen zum Rauhigkeits - und Stabilitätsproblem in der bodennahen Luftschicht,' Thesis, Göttingen.

15. Pasquill, F. 1949 'Eddy diffusion of water vapour and heat near the ground,' Proc. Roy, Soc. A, 198, p. 116.

16. Penman, H.L. and Long, I.F. 1960 'Weather in wheat: an essay in micro-meteorology,' Quart. J.R. Met. Soc., 86, p. 16.

17. Philip, J.R. 1966 'Plant water relations: some physical aspects,' Ann. Rev. of Plant Physiology, Vol. 17.

18. Plate, E.J. and Quraishi, A.A. 1965 'Modeling of velocity distributions inside and above tall crops,' J. Appl. Met. 4 (June), p. 400.

19. Pohlhausen, E. 1921 'Der Wärmeaustausch zwischen festen Körpern and Flüssigkeiten mit kleiner Reibung und kleiner Warmeleitung,' Z. angew Math. Mech., 1, p. 115.

20. Powell, R.W. 1940 'Further experiments on the evaporation of water from saturated surfaces,' Trans. Inst. Chem. Engrs., 18, p. 36.

21. Priestley, C.H.B. 1959 'Turbulent Transfer in the Lower Atmosphere,' University of Chicago Press.

22. Raschke, K. 1956 'Über die physikalischen Beziehungen zwischen Wärmeübergangszahl, Strahlungsaustausch, Temperatur und Transpiration eines Blattes,' Planta, 48, p. 200.

23. Rider, N.E. 1954 'Eddy diffusion of momentum, water vapour and heat near the ground,' Phil. Trans. A, 246, p. 481.

24. Schlichting, H. 1955 'Boundary Layer Theory,' Pergamon Press, London.

25. Sheppard, P.A. 1947 'The aerodynamic drag of the earth's surface and the value of von Karman's constant in the lower atmosphere,' Proc. Roy. Soc. A, 188, p. 208.

REFERENCES (Contd.)

26. Sheppard, P.A. 1958 'Transfer across the earth's surface and through the air above,' Quart. J.R. Met. Soc., 84, p. 205.

27. Simmons, L.F.G. 1949 'A shielded, hot-wire anemometer for low speeds,' J. Sci. Instrum., 26, p. 407.

28. Smith, M.C. and Kuethe, A.M. 1966 'Effects of turbulence on Laminar Skin Friction and Heat Transfer,' Phys. Fluids, 9 (Dec.), p. 2337.

29. Sutton, O.G. 1953 'Micrometeorology,' New York, McGraw-Hill.

30. Tanner, C.B. and Pelton, W.L. 1960 J. Geophys. Research 65, 3391.

31. Thom, A.S. 1968 'The exchange of momentum, mass and heat between an artificial leaf and the airflow in a wind-tunnel,' Quart. J.R. Met. Soc. 94, (in the press).

32. Uchijima, Z., and Wright, J.L. 1963 'An experimental study of air flow in a corn plant-air layer.' Department of Agriculture and Cornell University, Ithaca, N.Y. Research Report No. 369, Interim Report 63-1 (DDC)

INTRODUCTION

The aerodynamic properties and behaviour of individual roughness elements of an extended natural surface, such as the leaves and stems of a field crop, dictate the magnitude of the atmospheric wind drag on the surface as a whole. Under conditions of fully forced convection this drag force, or downward turbulent flux of momentum, specifies completely the intensity and scale of turbulence in the boundary layer flow above the surface; and in turn this turbulence promotes vertical transfer of mass or heat towards or away from the surface. Between any two levels within such a turbulent boundary layer, Reynolds' analogy between the transfer of momentum and the simultaneous transfer of any property entrained in the turbulent flow can be properly invoked. (Whether or not Reynolds' analogy is ever exactly upheld, even under neutral stability conditions, is not a consideration of this thesis).

However, as explained by Owen and Thomson (1963), Reynolds' analogy breaks down where transfer to or from the surface itself is concerned: briefly, normal pressure or "bluff-body" forces acting on individual elements of a rough surface greatly augment the transfer of momentum to the surface, but have no analogue in the transfer of mass or heat (see 1.3(c)). In effect, greater (non-dimensional) differences of temperature or humidity than of wind speed are maintained between a rough surface

and the airflow above it. This in itself is a fundamental objection to Monteith's (1963) determination of surface properties by extrapolation to zero wind speed of the atmospheric wind versus property relations. The present work examines the forced convective transfer of momentum, mass and heat to or from rough surfaces in general and natural rough surfaces in particular, emphasis being placed on the role played by individual surface elements; and seeks a quantitative improvement to Monteith's method of estimating "mean surface conditions" of temperature and humidity.

The complex form of natural surface roughnesses, in comparison with Nikuradse's simple sand roughness, leads the author into discussion of the nature of the flow regime over, and the behaviour of the roughness length z_o of, a typical vegetated surface (see 1.1(b)).

Any serious attempt to calculate the drag on a field crop from the wind profile within the canopy should (if possible) avoid the over-simplification made by Uchijima and Wright (1963) that the drag coefficients of crop elements can be assumed independent of wind speed. Also, following Philip (1966), it is possible that the drag coefficient of a leaf or stem exposed to a highly sheared and turbulent mean flow within a crop canopy differs significantly from the coefficient found for an identical leaf or stem exposed, in isolation, to a uniform laminar airflow. The artificial crop experiment (Chapters 2 and 3) is designed primarily to test this latter point by

direct measurement of the force (or rather the moment) on a single crop element of known "isolated" drag coefficient. This experiment demonstrates also the nature of the airflow into, over and through a densely "planted" area; gives realistic values for the vertical exchange coefficient for momentum within the artificial canopy; and provides general insight into the behaviour of the roughness length, z_o, and the zero plane displacement, d_o, of a complex rough surface.

In the artificial leaf experiment (Chapter 4), coefficients are measured (independently) for the transfer of momentum, mass and heat between a single leaf and a uniform airflow: results are obtained for several values of ϕ, the angle between the leaf and the incident airflow. (Previous work has not considered momentum, mass and heat transfer to (or from) the self-same surface or surface element). Also, a relationship is sought between the measured transfer coefficient of a property and its molecular diffusivity. These coefficients are required initially in Chapter 5 ("Application to a field crop"), but are needed for any realistic analysis of exchange processes within a crop canopy. Chapter 5 is of an exploratory nature and includes the introduction of a "shelter factor" to account for direct aerodynamic sheltering of some leaves by their upstream neighbours.

CHAPTER 1

THE FLOW OF AIR ABOVE AND WITHIN A CROP CANOPY.

1.1 Turbulent Shear Flow over a Complex Rough Surface

1.1(a) The profile of mean wind speed

Prandtl assumed that the shearing stress, or downward flux of momentum, in a fully developed turbulent boundary layer is independent of the height z above the boundary and equal to the stress τ on the boundary. This allowed the gradient of mean fluid velocity at z to be expressed as

$$\frac{\partial u(z)}{\partial z} = \frac{u_*}{kz} \qquad (1.1)$$

where kz is the Prandtl mixing length, k being von Karman's constant, and u_* is the friction velocity defined in a fluid of density ρ by

$$\tau = \rho u_*^2 \quad . \qquad (1.2)$$

Provided that buoyancy effects due to vertical temperature gradients in the fluid can be neglected, Eq. (1.1) can be integrated in the form

$$\frac{u(z)}{u_*} = \frac{1}{k} \ell n \, (z/z_o) \qquad (1.3)$$

where z_o, which accounts for the constant of integration, is termed the roughness length of the surface. It has been found that, when $k = 0.40$, Eq. (1.3) gives the

profile of mean wind speed in turbulent shear flow over any level surface, whether smooth or uniformly rough, in the laboratory (Schlichting, 1955) or in the field (Sheppard, 1947; Rider, 1954).

1.1(b) The roughness length, z_o

For flow over a rough surface z_o is a measure of the associated scale of turbulence, and is usually about an order of magnitude less than the average height of the surface irregularities (see also 3.3(b)). From Eq. (1.3), z_o can be written

$$z_o = z\, e^{-k(u(z)/u_*)} \qquad (1.4)$$

so that z_o will be independent of wind speed if the dimensionless ratio $(u(z)/u_*)$ is independent of wind speed; but if τ is written in the form

$$\tau = \rho . u^2(z)\, C_D(z) \qquad (1.5)$$

where $C_D(z)$ is the surface drag coefficient, then comparison with Eq. (1.2) gives

$$C_D(z) = (u(z)/u_*)^{-2} \qquad (1.6)$$

Thus constancy of z_o implies constancy of $C_D(z)$, and vice-versa.

For flow over a surface with a roughness of closely packed sand grains of height h_s, Nikuradse (see Schlichting, 1955) showed experimentally that

$$z_o = h_s/30 = \text{a constant},$$
$$\text{when } R_o = u_* z_o/\nu > 2.4 \tag{1.7}$$

where ν is the appropriate kinematic viscosity and R_o the roughness Reynolds' number. In this flow regime, which is termed "fully rough", constancy of z_o and hence of $C_D(z)$ demonstrates a quadratic relationship between τ and $u(z)$. This implies that by far the greatest part of τ is due to "bluff-body" (or normal pressure) drag on the individual sand grains: i.e. the Reynolds' number R of the flow past the roughness elements is high enough (greater than a critical value R_c) for their individual drag coefficients, $C_d(u)$, to be independent of wind speed when $(u_* h_s/\nu)$ is greater than about 70. This critical Reynolds' number can be estimated for sand roughness by writing

$$(R_c)_s = \frac{u(h_s)h_s}{\nu} \tag{1.8}$$

where h_s is a representative cross-stream dimension of a surface element. Eqs. (1.3) and (1.7) combine to give

$$\frac{u(z)}{u_*} = \frac{1}{k} \ell n(z/h_s) + 8.5 \tag{1.9}$$

from which $u(h_s) = 8.5\, u_*$. The critical value of

u_* is $70\nu/h_s$, so that $(R_c)_s \doteqdot 600$ which is safely into the regime of dominant pressure drag for a bluff object.

Although Eq. (1.3) holds for the complex forms of surface roughness which occur in nature, care must be taken in applying (as did Sutton, 1953) the relations of Eq. (1.7), which were obtained for the simple sand roughness only. For example, when Paeschke (1937) used the height h of vegetative growth on the surface of the earth as a roughness parameter, Eq. (1.3) took the form

$$\frac{u(z)}{u_*} = \frac{1}{k} \ell n(z/h) + 5 \qquad (1.10)$$

which corresponds to $z_o = h/7.5$. However, use of the criterion $R_o > 2.4$ to imply constancy of z_o assumes implicitly that the vegetation can be treated aerodynamically as a roughness comprised of closely packed sand "grains" of height $h_s = 30z_o = 4h$, which is physically incongruous. If Eq. (1.8) is written, for a vegetative surface roughness, in the form

$$(R_c)_{veg} = \frac{u(h)\, d}{\nu} \qquad (1.11)$$

where d is a typical <u>minimum</u> cross-stream dimension, and $(R_c)_{veg}$ is equated to $(R_c)_s$, then as d is of the order h/10 it can be shown from Eq. (1.10) that

$$z_o = \text{a constant when } (R_o)_{veg} > 150 \quad (1.12)$$

i.e. $R_o = 150$ is suggested for the lower limit of the "fully rough" flow regime over a vegetated surface. This is in partial agreement with Deacon (1957), who analysed Rider's (1954) data to show the critical value of R_o for short grass to be about 40.

Thus, for $(R_o)_{veg} < 150$, z_o cannot be assumed independent of wind speed, even although the roughness elements project fully into the turbulent boundary layer and there is no laminar sublayer (in the commonly accepted sense). The roughness length z_o is related by Eqs. (1.4) and (1.6) to $C_D(z)$, a drag coefficient of the surface as a whole; and if the drag force on the surface is not primarily due to pressure forces (i.e. if $(R_o)_{veg}$ is less than 150) $C_D(z)$ and hence z_o must be a decreasing function of wind speed.

A further decrease in z_o with increasing wind speed will occur (for any value of R_o) if flexible roughness elements change their geometry in accord with changing wind speed (e.g. streamlining of leaves or stems). Such a reduction in z_o is recorded for long grass by Priestley (1959).

In general, if the drag coefficient C_d of a typical element of a rough surface is written as $C_d(u, \phi)$, where ϕ is the angle of inclination of the element to air flowing past with speed u, then z_o will decrease with wind speed if C_d, and hence $C_D(z)$, decreases with

wind speed. If C_d decreases with wind speed solely because ϕ decreases with wind speed then the flow regime can genuinely be termed "fully rough". However if C_d decreases with u at constant ϕ the flow regime must be termed "transitional". (For flow regimes over a rough surface see, e.g., Schlichting, 1955).

1.1(c) The Zero Plane Displacement, d_o

When the surface roughness consists of high vegetation, such as a cereal or bean crop, an empirical constant in the form of a zero plane displacement must be introduced into Eq. (1.3), such that

$$\frac{u(z)}{u_*} = \frac{1}{k} \ell n((z - d_o)/z_o) \quad . \qquad (1.13)$$

This empirical displacement is the value of d_o for which the plot of $\ell n(z - d_o)$ versus $u(z)$ is judged to be linear. d_o is always somewhat less than the height h of a crop canopy, and is a larger fraction of h for more densely planted crops. (Note: in the limits of zero and maximum density, d_o must equal zero and h respectively.) In terms of Eq. (1.13), the plane $z = d_o$ can be designated a virtual surface (see also 3.3(f)); and $u(z) = 0$ at $z = d_o + z_o$. However, Eq. (1.13) describes the real wind speed profile down to $z = h$ only.

1.1(d) The Eddy Viscosity, K_M

The eddy viscosity of a turbulent shear flow can be defined as a function of z by writing the shearing stress in the form

$$\tau = \rho K_M(z) \frac{\partial u}{\partial z} \qquad (1.14)$$

$$z \geqslant h$$

The quantity $K_M(z)$ is the vertical diffusivity of momentum, or the inverse of the specific resistance to momentum transfer in the vertical, at the level z; and on combining Eqs. (1.1), (1.2) and (1.14) can be written as

$$K_M(z) = ku_*(z - d_o) \qquad (1.15)$$

$$z \geqslant h$$

i.e. $K_M(z)$ increases linearly with height above the canopy.

For the purposes of this thesis, the corresponding turbulent diffusivities of mass, K_V, and heat, K_H, are assumed equal to each other (K_O) and to K_M, so that

$$K_O(z) = K_M(z) \qquad (1.16)$$

$$z \geqslant h$$

(This equation expresses Reynolds' analogy between the transfer of mass or heat on the one hand and momentum on the other.)

1.2 Turbulent Shear Flow Past the Roughness Elements of a Complex Surface.

1.2(a) Drag on the surface elements

In Section 1.1 the crop is introduced as a complex roughness of uniform density (spacing) covering a level ground surface to a uniform height, h. Here the crop is considered as the region in which a turbulent shearing stress, τ , in the flow over the crop is transferred to the ground surface via the stresses on individual crop elements. Assuming that within the crop canopy mean wind speed can be defined and its profile measured, then the force f on an "equivalent" vertical column of crop, of cross-section 1 cm.^{2}, can be written in the form

$$f = \rho \int_0^h u^2(z) \sum_j (A_j(z).(C_d)_j)\, dz \quad (1.17)$$

where ρ is the density of air, each $A_j(z)$ is the surface area per unit volume of each type of crop element (leaf, stalk etc.) and $(C_d)_j$ is the corresponding drag coefficient. Direct wind drag on a ground surface covered by dense (or high) vegetation is negligible, so that τ can be equated to f.

Thus Eq. (1.17) would allow τ to be calculated from a knowledge of $u(z)$ within the canopy (i.e. between $z = 0$ and $z = h$), provided that each $(C_d)_j$ can be assigned a value relevant to conditions within the canopy. However, available values of C_d apply to isolated

objects exposed in wind-tunnel conditions of smooth flow, whereas in the canopy, (i), the flow is turbulent and highly sheared (especially between d_o and h), and (ii), complete sheltering of one or more leaves by an upstream neighbour may well occur. "(i)" is investigated in Chapter 3 for a leaf-less artificial crop, and evidence of "(ii)" is found for a field crop (beans) in Chapter 5.

1.2(b) τ within the canopy.

The shearing stress in the turbulent flow at level z within the canopy can be written, from Eq. (1.17), as

$$\tau(z) = \tau - \rho \int_z^h u^2(z) \sum_j (A_j(z).(C_d)_j)\, dz \qquad 0 \leq z \leq h \qquad (1.18)$$

The stress $\tau(z)$ decreases most rapidly in the uppermost layers of the crop where the wind speed is highest and momentum absorption is accordingly most efficient.

1.2(c) K_M within the canopy.

It is possible to define $K_M(z)$ for $0 \leq z \leq h$ by writing

$$K_M(z) = \tau(z)/(\rho \frac{\partial u}{\partial z}) \qquad (1.19)$$

where $\tau(z)$ can be obtained from Eq. (1.18). (For

$z \geqslant h$, Eq. (1.19) reduces to Eq. (1.15)). The magnitude of K_M within a crop canopy is required for comparison with, or substitution for, corresponding values of K_V and K_H which are being determined by independent means at Rothamsted Experimental Station.

When Uchijima and Wright (1963) use Eq. (1.19) to determine K_M within a corn canopy they find that $K_M(z)$ decreases exponentially with distance below $z = h$, in such a way that $K_M(0.75h) \doteq 0.5\, K_M(h)$. However, in obtaining τ as a function of z within the canopy they consider the drag on the leaves only, and also assume that C_d has the same constant value at all levels (i.e. implicitly at all wind speeds) within the canopy (although they have to choose different "constant" values on different occasions). It is likely that C_d is relatively large at lower levels in the canopy and relatively small at upper levels where higher wind speeds promote streamlining (i.e reduction in ϕ; and/or increase in shelter effect due to bunching of leaves - see 5.2(d)). If such a variation in C_d with height within the canopy is accepted, then it can be shown that K_M has larger values within the canopy than those calculated by Uchijima and Wright.

The magnitude and behaviour of $K_M(z)$ is studied in Section 3.4(a) for the artificial crop and in Section 5.3(a) for the 1966 bean crop at Rothamsted.

1.3 The Transfer Resistances of a Complex Rough Surface

1.3(a) Definition of transfer resistance, r

The effectiveness of transfer of a property between height z, where $u = u(z)$, and a surface on which u is everywhere zero can be represented by a dimensionless transfer coefficient $C(z)$ defined by

$$q = C(z)\, u(z)\, \delta\chi \qquad (1.20)$$

where, in consistent units, q is the rate of convective transfer of the property across unit horizontal area and $\delta\chi$ is the difference in concentration of the property between z, where its concentration is $\chi(z)$ and the surface on which its mean concentration is χ_s. The product $u(z)\, C(z)$ can be regarded as a conductance through which the potential difference $\delta\chi$ drives the current or flux density q. The corresponding resistance is

$$r(z) = (u(z)\, C(z))^{-1} \qquad (1.21)$$

and is termed a transfer resistance: with $u(z)$ expressed in cm. sec.$^{-1}$, $r(z)$ has units of sec. cm.$^{-1}$.

For transfer of momentum to a surface, $q = \tau = \rho u_*^2$; $\chi(z) = \rho u(z)$; and χ_s is zero; so that $C(z) = (u_*/u(z))^2$ which is equal to the drag coefficient $C_D(z)$ defined by Eq. (1.6). A resistance $r_D(z)$ can then be defined, namely

$$r_D(z) = u(z)/u_*^2 \qquad (1.22)$$

which, for a crop of height h, is the total resistance to the transfer of momentum to the crop from a height z greater than or equal to h .

The corresponding resistances $r_V(z)$ and $r_H(z)$ to the transfer of mass or heat to or from the crop can be defined in terms of the appropriate values of q, $\chi(z)$ and χ_s. However, difficulties in measuring or even defining χ_s for the complex vegetated surfaces which occur in nature have hindered direct measurement of r_V and r_H. Conversely, without an estimate of the size of $r_V(z)$ or $r_H(z)$, it is not possible to predict each χ_s from a knowledge of appropriate q and $\chi(z)$. Monteith (1963) has used a simple model, in which $r_W(z)$ for water vapour and $r_H(z)$ for heat are each implicitly assumed equal to $r_D(z)$, to determine representative values of vapour pressure and temperature on various vegetated surfaces. That this assumption is an over-simplification (even within the terms of the model) is discussed in the following Sections; while the model itself is discussed in Section 5.4(b).

1.3(b) Differences between r_D, r_V and r_H.

It has long been recognised that the resistance of a rough surface to momentum transfer is usually much less than the corresponding resistance to a simultaneous transfer of mass or heat. The transfer of any property to a

rough surface can be considered as taking place through two resistances in series: i.e. r_D, r_V and r_H can each be separated into two parts; (a), and (b). Part (a) is the resistance to transfer across the turbulent boundary layer. If Reynolds' analogy between the transfer of momentum on the one hand and mass or heat on the other can be invoked, then (a) can be assumed the same for all properties in transfer, including momentum (i.e the resistances given by the integrals of dz/K_O and dz/K_M across the turbulent boundary layer are identical - see Eq. (1.16)). The other resistance (b) is that of the surface itself. This (aerodynamic, as distinct from stomatal) resistance differs for mass, heat and momentum to an extent depending on the size of the appropriate molecular diffusivities and on the shape, size and inclination of each element of roughness on the surface. Owen and Thomson (1963) measured the discrepancy between the resistance to the transfer of mass or heat and the resistance to the transfer of momentum between a rough glass plate and a turbulent air-stream. They analyse their results in terms of the quantity B^{-1}, the inverse of a sublayer Stanton number defined for the surface: B^{-1} is a non-dimensional form of the extra resistance encountered by mass or heat at the surface over that encountered by momentum. Owen and Thomson find that

$$B^{-1} = a \left(\frac{u_* h_s}{\nu}\right)^m \left(\frac{\nu}{D}, \frac{\nu}{\kappa}\right)^n \qquad (1.23)$$

where ν, D, and κ are the molecular diffusivities of momentum, mass, and heat; where m and n were found to have the values 0.45 and 0.8 respectively; and where α was found to be constant for a given type of surface roughness. Thus B^{-1} increases with surface roughness, or rather with surface roughness as specified by h_s, and decreases with an increase in diffusivity of the property in transfer. That α is a surface parameter, and not an absolute constant, demonstrates the inability of the roughness length z_o (equal to $h_s/30$) to specify fully the effectiveness of transfer of mass or heat to or from a rough surface (see also 1.3(c) and 5.4(a)).

1.3(c) The "bluff-body" effect

At any rough surface normal pressure or "bluff-body" forces acting on individual roughness elements greatly augment the transfer of momentum by molecular diffusion (manifested by skin friction), whereas simultaneous transfer of mass or heat to or from the surface is restricted to the mechanism of molecular diffusion alone. Chamberlain (1966) measured the deposition rate of thorium-B on to artificial grass and other rough surfaces from a turbulent air-stream. He reports that the enhancement of momentum transfer is much less for the artificial grass and other fibrous surfaces (B^{-1} of order 5) than for rough glass surfaces (B^{-1} of order 25). Because "bluff-body" forces constitute a relatively small proportion of

the total drag on such fibrous surfaces, Barry (1965) has equated the mass transfer coefficient (for $D = \nu$) of a natural surface to that part of its total drag coefficient not due to pressure forces, i.e. to its skin friction drag coefficient. That this cannot be true in general is shown in Section 4.4.

If μ is the ratio between the "bluff-body" and skin friction forces acting on the elements of a rough surface and E is an absolute constant, then the relation

$$B^{-1} = E\mu \left(\frac{\nu}{D}, \frac{\nu}{\kappa}\right)^{n} \qquad (1.24)$$

should provide an estimate of the size of B^{-1}; for in the limit of a smooth surface (and D or $\kappa = \nu$) both B^{-1} and μ must be zero: also, large μ implies large B^{-1}, and vice versa. If μ varies little from one type of "fibrous" roughness element to another, which indeed is likely, then Chamberlain's statement that B^{-1} varies little with roughness length (over a factor of 20 in z_o), "provided the roughness elements are of fibrous character," gives qualitative support to Eq. (1.24). It is therefore suggested that the product $\alpha((u_* h_s)/\nu)^{0.45}$ in Eq. (1.23) could reasonably be replaced by the product $E\mu$ (Note: μ must have a wind speed dependence close to u^4; at least for rigid roughness elements.)

Thus the ratio μ (alone or implicit in B^{-1}) is a more representative parameter of surface roughness than is z_o when the nature or effectiveness of transfer at

at the surface itself is being considered, although the scale of turbulence specified by z_o controls the transfer towards or away from the surface. It is likely that there exists a universal threshold value of μ, (of order 10), which delineates the transition to or from the "fully rough" flow regime over any rough surface, a transition not fully specified by a universal value of the roughness Reynolds' number R_o, equal to $(u_* z_o)/\nu$ (see 1.1(b)).

1.3(d) B^{-1} for a crop

As introduced initially by Owen and Thomson (1963)

$$B^{-1} = u_* r_{V,H}(z) - \frac{(u(z) - u(h_s))}{u_*} \qquad (1.25)$$

which is the non-dimensional resistance of the surface region (defined for $z < h_s$) to mass or heat transfer. However, they subsequently set $(u(h_s)/u_*)$ equal to zero, equivalent to re-defining B^{-1} as the extra non-dimensional resistance encountered by mass or heat, over that encountered by momentum, at the surface: i.e.

$$B^{-1} = u_* r_{V,H}(z) - \frac{u(z)}{u_*} \qquad (1.26)$$

This is the definition of B^{-1} used by Chamberlain (1966) in a study of the transfer resistances of a complex rough surface consisting of uniformly "planted" artificial grass ($h = 7.5$ cm.), exposed to a turbulent

air-stream in a wind-tunnel.

Provided Eq. (1.16) is valid, B^{-1} is independent of the level of observation, z : also, B^{-1} is free from any assumptions concerning the nature of the flow below $z = h$. Assuming that the log-linear wind speed profile (Eq. (1.13)) holds down to $z = h$, a condition found for both real and artificial crops (neglecting spatial departures close to each roughness element), then Eq. (1.26) holds down to $z = h$ also. Thus, for a crop, Eq. (1.26) can conveniently be written (using Eq. (1.22)) as

$$B^{-1} = u_* (r_0(h) - r_D(h)) \qquad (1.27)$$

where the subscript "0" refers to the transfer of a generalised property with diffusivity equal to ν .

It is proposed that each resistance, $r_0(h)$ or $r_D(h)$, can be separated into two parts. One is the mean turbulent resistance to vertical transfer within the canopy, $\overline{R}$, and is termed the canopy resistance. The other is the mean resistance of the crop elements themselves, $\overline{r}/S$, where S is the area of crop element per unit area of horizontal surface. The canopy resistance can usefully be considered as the turbulent resistance between $z = h$ and some mean level $\overline{z}$ within the canopy (but see also 3.4(b), 3.4(c) and 5.3(b)), so that for a turbulent diffusivity $K(z)$

$$\overline{R} = R(h \leftrightarrow \overline{z}) = \int_{\overline{z}}^{h} \frac{dz}{K(z)} \qquad (1.28)$$

Appropriate parallel definition of $\bar{r}$ results from considering the crop elements to be localised at $z = \bar{z}$ where $u = \bar{u} = u(\bar{z})$, and writing $\bar{r}$ equal to $r(\bar{u})$, (3.3(d), 3.4(d)).

In consistent symbolism, therefore

$$r_D(h) = \bar{R}_D + \bar{r}_d/S_d \qquad (1.29)$$

and

$$r_O(h) = \bar{R}_O + \bar{r}_o/S_o \qquad (1.30)$$

where

$$\bar{R}_D = R_D(h \leftrightarrow \bar{z}_D) = \int_{\bar{z}_D}^{h} dz/K_M(z) \qquad (1.31)$$

and

$$\bar{R}_O = R_O(h \leftrightarrow \bar{z}_O) = \int_{\bar{z}_O}^{h} dz/K_O(z) \qquad (1.32)$$

The resistance $\bar{r}_o/S_o$ usually accounts for transfer to or from leaves only, so that $S_o = L$, the leaf area index; whereas $\bar{r}_d/S_d$ should be derived to include momentum transfer to stalks etc. as well as to leaves (see 5.3(b)). However, as a first approximation $S_d = S_o = S$, so that Eqs. (1.29) and (1.30) can be combined to give Eq. (1.27) in the form

$$B^{-1} = u_*((\bar{r}_o - \bar{r}_d)/S + (\bar{R}_O - \bar{R}_D)) \qquad (1.33)$$

This is a full expression for B^{-1} in any crop or vegetation canopy of height h. If the "turbulent" contribution $(\bar{R}_O - \bar{R}_D)$ can be neglected in comparison with $(\bar{r}_o - \bar{r}_d)/S$ contributed by the "bluff-body" effect, then

$$B^{-1} = u_*(\bar{r}_o - \bar{r}_d)/S \qquad (1.34)$$

This equation will be exact only if $\overline{R}_0 = \overline{R}_D$, a condition not likely to be fulfilled unless $K_0(z) = K_M(z)$ within the canopy and $\overline{z}_0 = \overline{z}_D$. The former equality may or may not be true in general, while the latter requires that the sources and/or sinks of momentum, mass and heat be similarly distributed in the vertical within the canopy.

Eq. (1.34) can be used to estimate the size of B^{-1} for a given crop, thus determining the discrepancy in resistance between the transfer of mass or heat and the transfer of momentum to that crop. In Section 5.4(b), B^{-1} is incorporated in Monteith's (1963) method of estimating "mean surface conditions" of vapour pressure and of temperature, thereby improving the accuracy of the method while accounting for relevant criticisms made by Philip and by Swinbank (see Monteith, 1963; Discussion).

CHAPTER 2

DESIGN OF THE ARTIFICIAL CROP EXPERIMENT

2.1 The Artificial Crop

2.1(a) Choice of crop element

Several requirements influenced the choice of the size and shape of the elements and of their subsequent density and mode of array as an artificial crop:

(i) that the drag coefficient $C_d(u)$ of an isolated element be well enough known to allow calculation of the mean drag force, f, on a typical crop element from a knowledge of the profile of mean wind speed within the canopy (i.e. of $u(z)$ for $0 \leqslant z \leqslant h$);

(ii) that it be possible to traverse an anemometer head (vertically) between $z = 0$ and $z = h$ to determine the required $u(z)$;

(iii) that it be possible to attach one or more of the elements to a drag meter, thereby confirming f (or rather C_d) by direct measurement (see 1.2(a));

(iv) that the crop be sufficiently tall and dense to prevent measureable shearing stress reaching the substrate directly, so that, if n is the number of elements per $cm.^2$ of horizontal surface, nf can be equated to the shearing stress ;

and (v) that $C_d(u)$ should decrease greatly with increase in wind speed, so that the associated decrease in z_o could be investigated ("transitional" flow regime: see 1.1(b)).

These requirements led to the construction of an artificial crop from a large number of rigid circular cylinders of diameter 1 mm., set (vertically) to a height h of 14.3 cm. and with a uniform density of one per cm.^{2} of base (i.e. $n = 1$). Fig. 2.1 shows the drag coefficient $C_d(u)$ of a long circular cylinder of 1 mm. diameter placed at right angles to a uniform airflow. The curve (from Goldstein's (1938) treatise) is experimental above and theoretical below the wind speed (15 cm. sec.$^{-1}$) corresponding to a Reynolds' number R equal to 10. The product $u^2C_d(u)$, required to calculate f, is shown on Fig. 2.1 also.

2.1(b) Construction of the crop

Polystyrene sheet was chosen as a suitable substance in which to "plant" the crop. Twelve interchangeable sections, each 2.3 cm. thick and (accurately) 30 cm. square, were "planted" with 6.5 in. lengths of 1 mm. diameter steel rod in the regular pattern shown in Fig. 2.2, so that either orientation X or Y was available. Except at the edges A and B of each section the crop density n was precisely unity.

The actual "planting" of close to eleven thousand crop elements was a formidable task. An accurately made brass jig, 30 cm. in length, 1.45 cm. in width and about 1 cm. thick, was drilled, 0.50 cm. from one edge, with 30 equally spaced guide-holes of 1.1 mm. diameter, and used

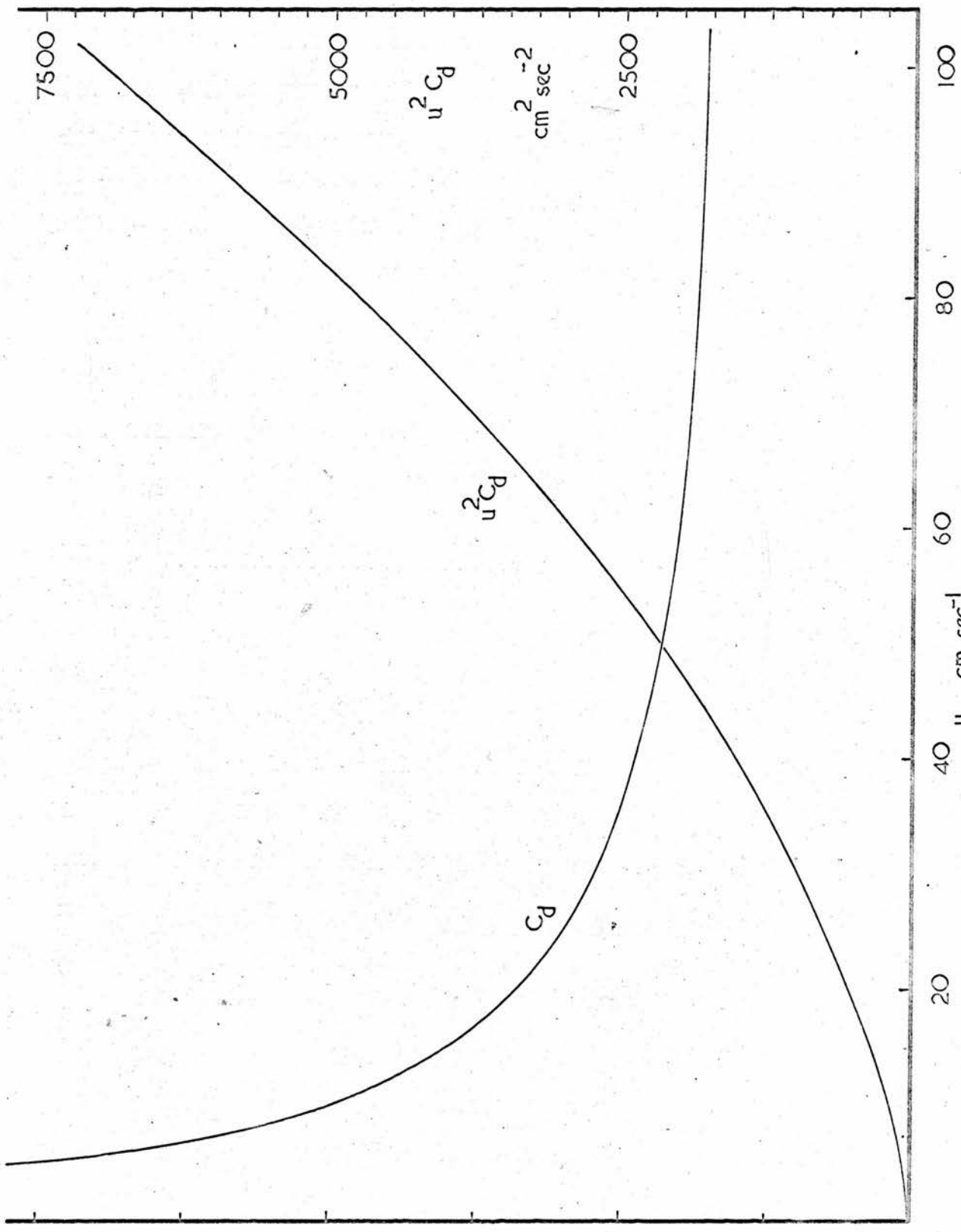

FIGURE 2.1 Drag coefficient $C_d(u)$ of a 1 mm. diameter circular cylinder, versus wind speed u : also, $u^2 C_d(u)$ versus u.

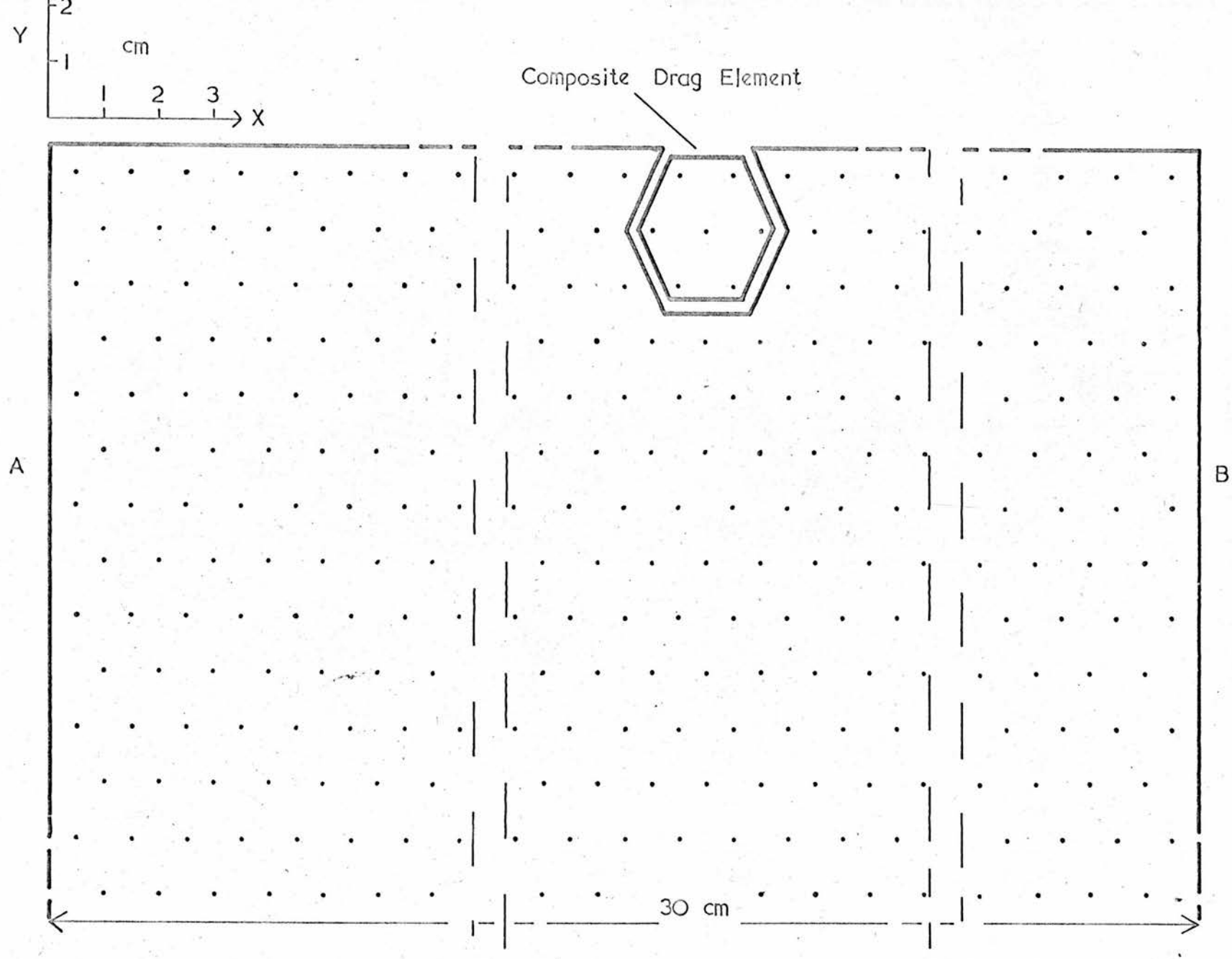

FIGURE 2.2 "Planting" pattern for artificial crop (to scale): for symbols see 2.1(b): for Composite drag element see 2.5(c).

to "plant" the steel rods one row at a time. The 0.1 mm. clearance between the steel rods and the guide holes was necessary to provide unrestricted passage of the one end of each rod which had been slightly damaged by a cutting tool. This clearance combined with slight curvature of many of the rods to produce a random departure from the vertical of any given rod by an angle not (usually) exceeding 5°. Thus, in the upper levels of the crop, the array of elements departed randomly from the rigid pattern set out in Fig. 2.2 (see, e.g., Fig. 2.11).

2.2 The Wind-Tunnel

2.2(a) Section of the tunnel used

The closed-circuit wind-tunnel in the Natural Philosophy Department at the University of Edinburgh was used for the artificial crop experiment. The section chosen, to conduct the experiment within, lies between the 3rd and 4th corners (counting from the high speed working section) of this low turbulence tunnel, and is vented to atmospheric pressure. The relatively low wind speeds required (of order 5 ft. sec.$^{-1}$) could be maintained in this section while running the fan at moderate and therefore stable speeds. Also, atmospheric pressure within this section permitted the use of a simple moment balance (see 2.5) to determine the drag force on a single crop element. The relevant area cross-section of the

tunnel appears in Fig. 2.3, and the floor plan in Fig. 2.4.

2.2(b) Positioning of the crop

Cross-sections of axial wind speed were measured at aa' and bb' (Fig. 2.4) using a propellor anemometer mounted on a specially designed spring-loaded mast. These cross-sections (Figs. 2.3(a) and 2.3(b)) showed that the crop could reasonably be placed in this part of the tunnel if it (the crop) was restricted to the cross-stream region $0 < Y < 3$ ft. A typical position of the crop is shown on Fig. 2.4.

2.2(c) Need for a wind-channel with a graded approach

As the crop covered so little of the total width of the tunnel, it was apparent that side walls of sufficient height would be required to contain the retarded flow (in the boundary layer) above the crop and separate it from the unretarded flow on either side: i.e. the need for a wind-channel within the wind-tunnel was recognized.

To lessen the effect of the massive change of surface roughness from wind-tunnel floor to artificial crop, Chamberlain (1966) set the crop into the tunnel floor to a depth equal to the estimated zero plane displacement of the crop. Although this was not possible in the Edinburgh tunnel, it was possible, and necessary to raise the level of entry of the airflow into the crop by building a

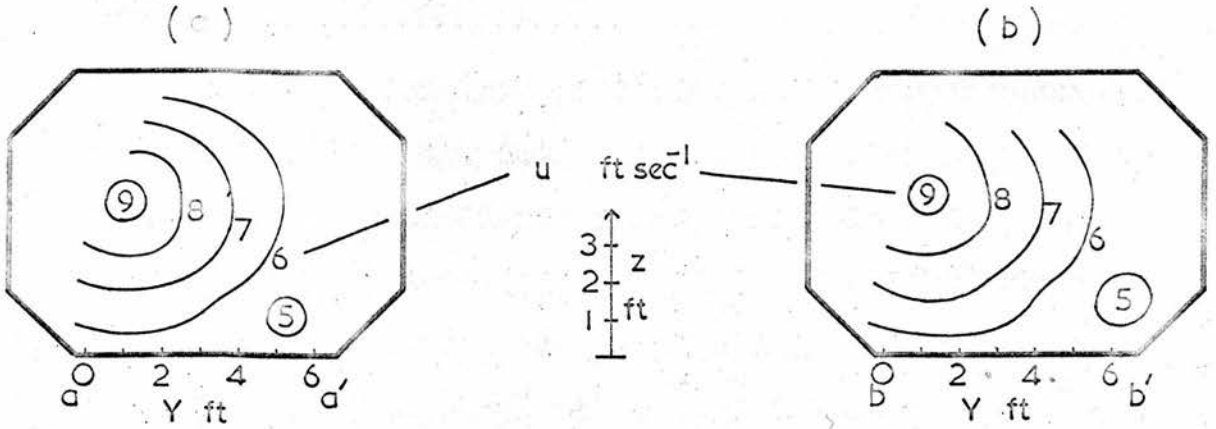

FIGURE 2.3 Area and axial wind speed cross-sections of wind-tunnel at aa' and bb' (see below).

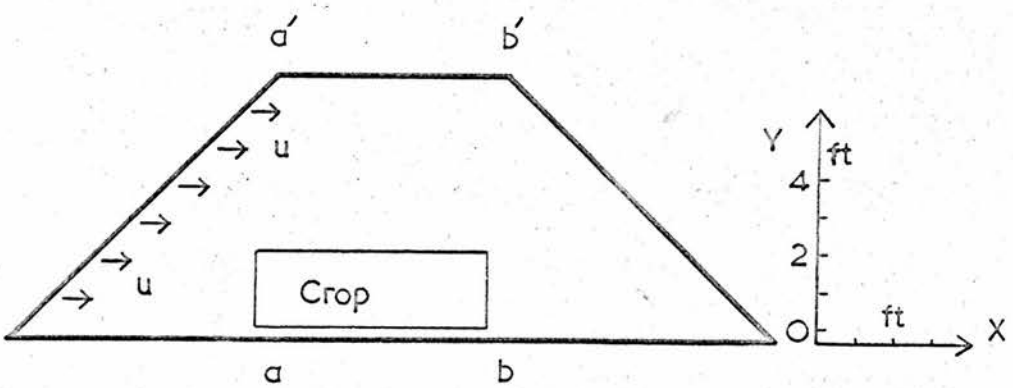

FIGURE 2.4 Floor plan of section of wind-tunnel used.

graded approach to the leading edge of the crop (see 2.4(c) and 3.1(a)).

2.3 The Hot-Wire Anemometer

2.3(a) Choice of anemometer

A Simmons shielded hot-wire anemometer (by H. Tinsley and Co. Ltd.) was chosen for measuring the wind speed profiles both above and within the artificial canopy. This instrument consists of a hot wire mounted in one of the fine bores of a twin bore silica tube: the other bore contains the hot junction of a thermo-couple used to determine the temperature difference between the hot wire and the incident air-stream (to which the cold junction is exposed). The silica tube, which is about 3 cm. long, protects the hot wire (of the same length) from deposits and/or minor injury, thereby ensuring permanency of calibration of the instrument. The output from the thermo-couple gives a measure of the speed of the incident air-stream, and is read on the 150 mm. scale of a reflecting galvanometer: calibration figures were provided by the makers for the anemometer head in a vertical position, normal to a horizontal airflow. Fig. 2.5 shows the corresponding calibration curve, (ON), in the wind speed range zero to 200 cm. sec.$^{-1}$. This curve shows the instrument to be most sensitive in the wind speed range expected within the canopy (10 to 75 cm. sec.$^{-1}$), but to be

adequately sensitive up to about 180 cm. sec.$^{-1}$ - the highest wind speed expected above the crop canopy.

2.3(b) Use of anemometer

To determine the wind speed profile over a horizontal surface the wind speed at each of several precise levels is required, so that the anemometer head must be held in a horizontal position, normal to the airflow, and not in a vertical position. This does not change the calibration of the instrument at wind speeds high enough to ensure cooling of the hot wire by forced convection alone. However, at the lower wind speeds measured by the instrument, free convection does play a part, and the calibration is then a function of the orientation of the hot wire.

At the limit of zero wind speed, cooling of the wire is by free convection alone; and is more effective when the wire is horizontal than when it is vertical. This causes a shift in the instrument zero from O to O' (Fig. 2.5). Consultation of the original paper by Simmons (1949) shows that the "horizontal" calibration of the instrument is of the form given by the curve O'PN in Fig. 2.5. The point O' and the minimum value M were found (for the Tinsley instrument) by observing the galvanometer scale deflection under calm and slightly disturbed conditions, respectively. The point P is based on information, supplied by the National Physical Laboratory on request, that the difference in the two calibrations at

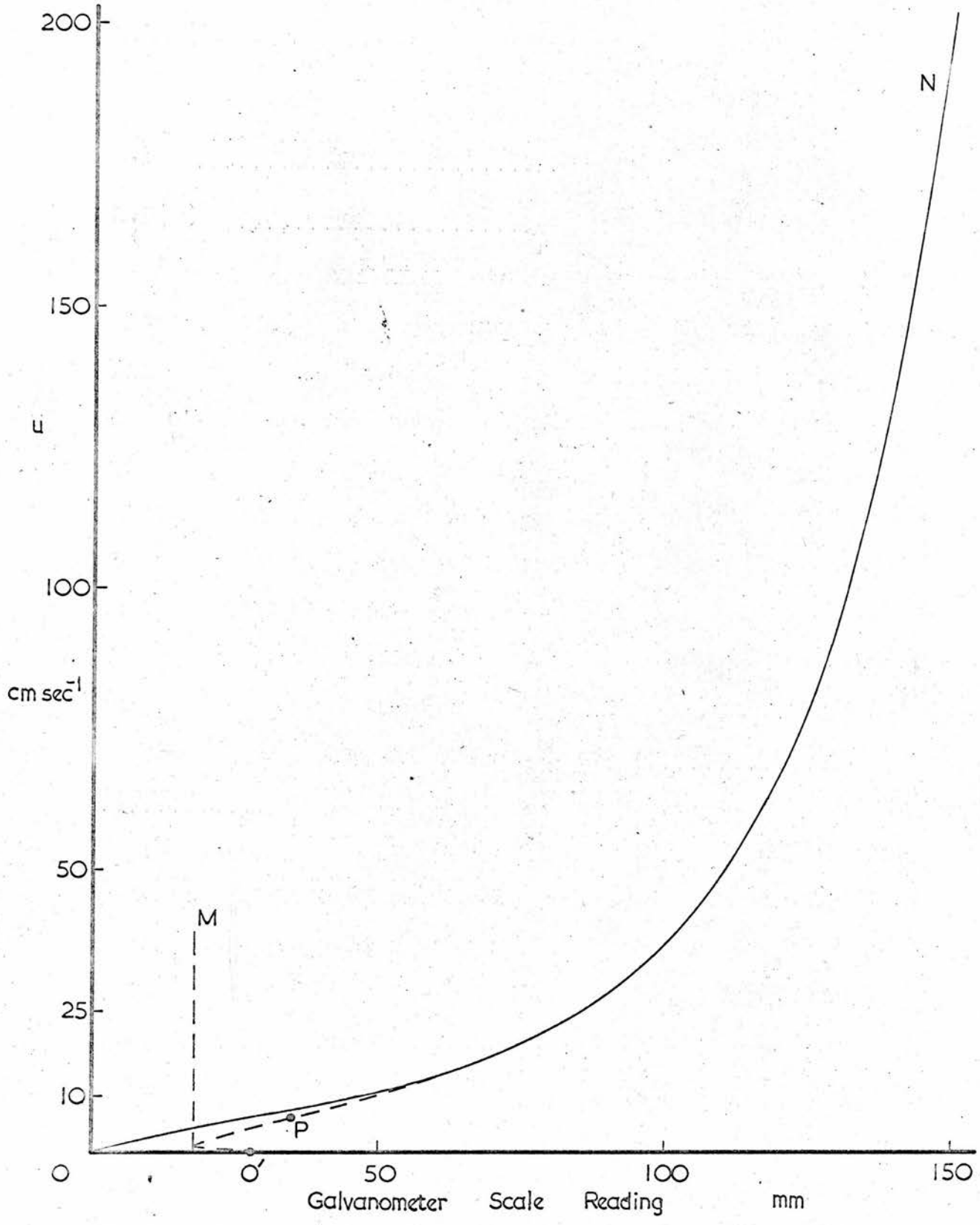

FIGURE 2.5 Calibration curves for Simmons shielded hot-wire anemometer: curve ON, anemometer head vertical: curve O'PN, head horizontal. (For significance of O', M and P, see Section 2.3(b)).

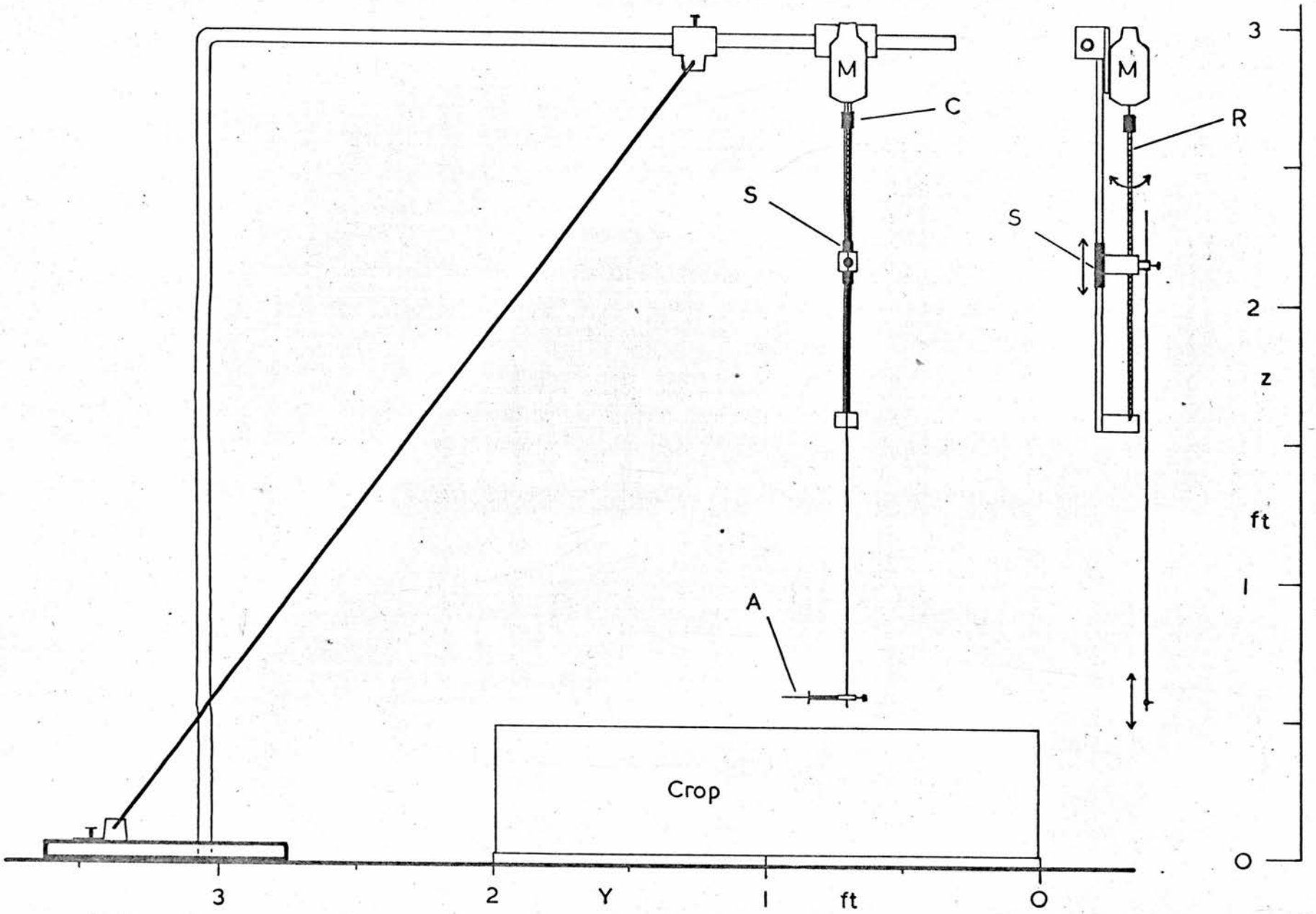

FIGURE 2.6 Anemometer traversing mechanism.

A : anemometer head.
C : rubber coupling.
M : motor
R : screwed rod.
S : sleeve.

$u = 7.5$ cm. sec.$^{-1}$ "is about 15 per cent on velocity."

The curve O'PN in Fig. 2.5 was assumed to represent the "horizontal" calibration of the instrument accurately enough for wind speeds in excess of 5 cm. sec.$^{-1}$ (but see 3.3(c)).

2.3(c) The traversing mechanism

The traversing mechanism for the anemometer head is sketched in Fig. 2.6. The mechanism was held on a rigid cantilevered support attached to a heavy cast iron base. This support could be moved to position the anemometer head vertically above any chosen point in the X,Y-plane, while a worm drive system, operated by a Meccano motor, enabled the anemometer head to be traversed, remotely, in the vertical, over any chosen 25 cm. range between $z = 1$ cm. and $z = 50$ cm. The motor operated on 4 volts d.c. from accumulators outside the tunnel, a gear box giving a choice of traverse speeds.

The control switch for the motor was positioned, together with the (Tinsley) galvanometer, on a specially constructed control panel. This panel was attached to the outside of the wind-tunnel, just below the vents, and a make-shift platform was built to support the observer. The z-coordinate of the anemometer head was determined by eye from the position of a known mark against a millimetre scale attached to the standing part of the traversing mechanism.

2.4 Exploratory Wind Speed and Profile Measurements

2.4(a) The "instantaneous" wind speed

The horizontal extent of the hot wire meant that the deflection registered at any instant by the galvanometer gave a measure of the average wind speed over a cross-stream distance of about 3 cm. This was especially useful within the canopy, where, unlike in the true boundary layer flow above, the time mean of the wind speed at a given value of z does depend on cross-stream position, i.e. on the proximity of the crop elements and the behaviour of their wakes. The hot wire was always positioned across the wakes of three crop elements and the reading of the galvanometer at any instant was taken to define the corresponding "instantaneous" wind speed.

2.4(b) The mean wind speed

Turbulence in the highly sheared flow both above and within the crop canopy caused the deflection registered by the galvanometer to fluctuate about a mean value. This value was judged to the nearest millimetre, by observing the motion of the spot on the galvanometer scale for about twenty seconds, and then converted to a mean wind speed from a table prepared from Fig. 2.5.

2.4(c) Profiles of mean wind speed.

The crop was positioned on the tunnel floor as shown in Fig. 2.4, and side walls of polystyrene sheet were erected to a height $z = 28$ cm. (Fig. 2.7(a)). With the

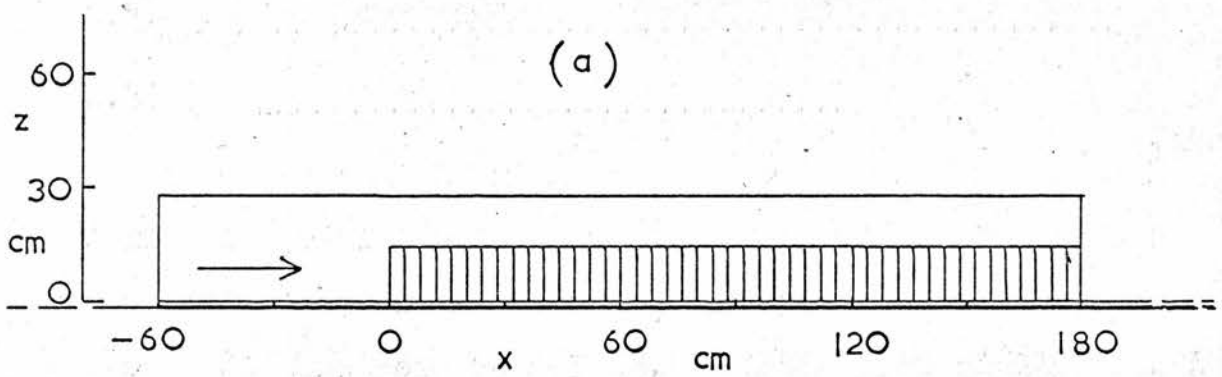

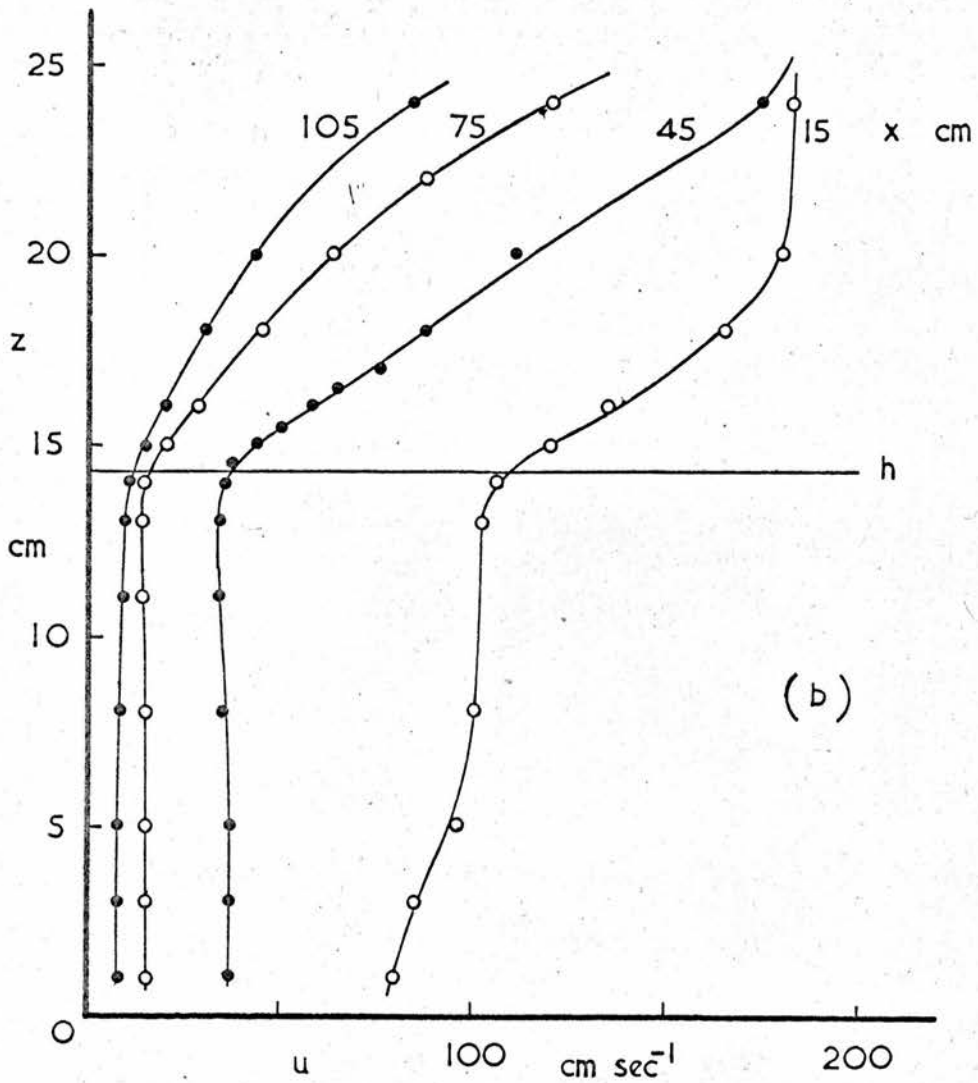

FIGURE 2.7 (a) Cross-section of crop (with side walls); and (b) corresponding wind speed profiles: open leading edge (b = 0).

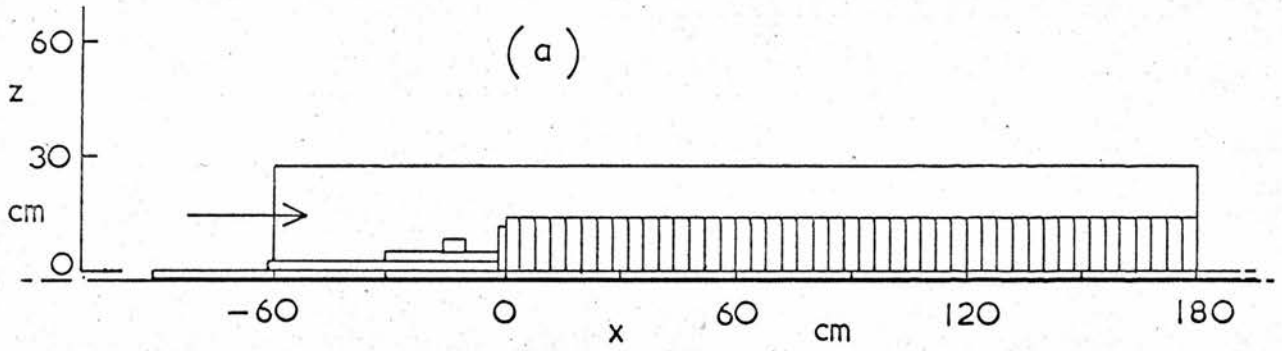

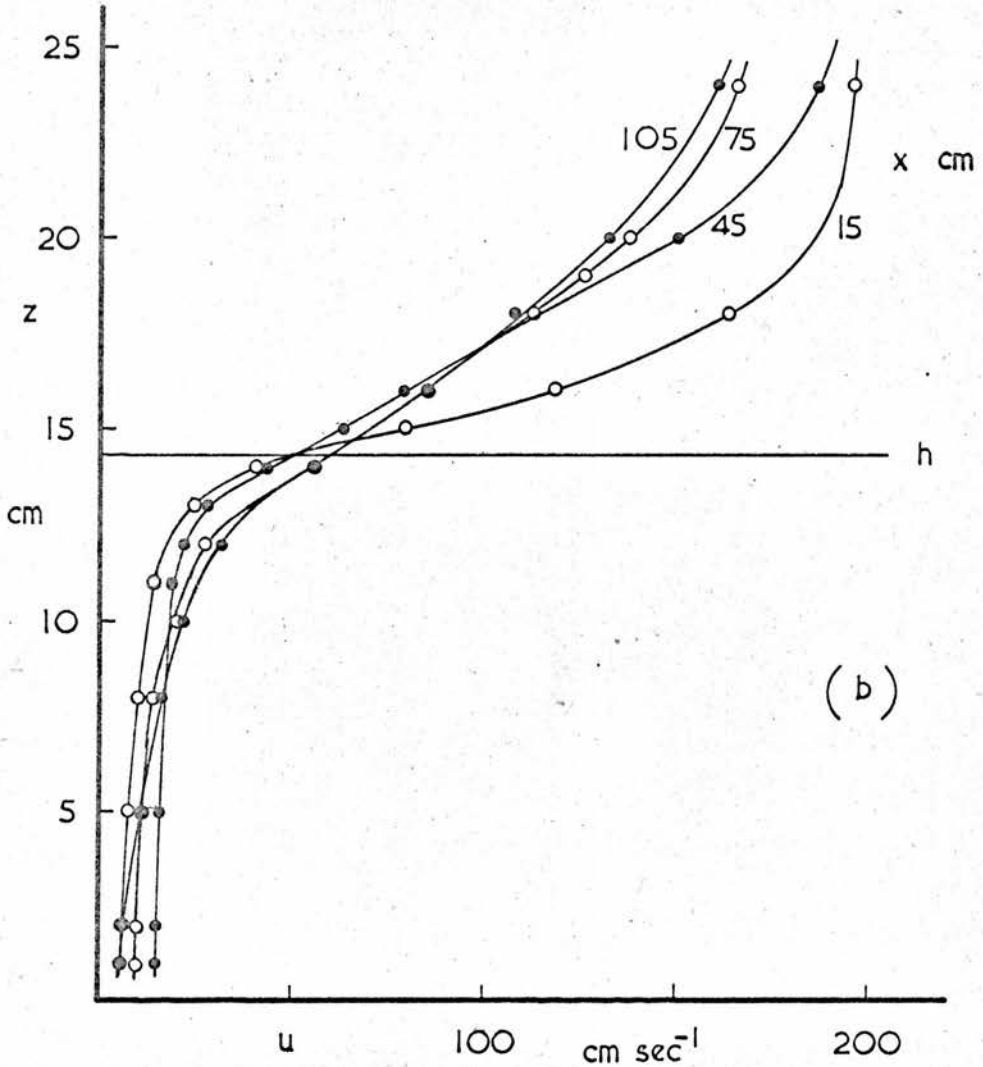

FIGURE 2.8 (a) Cross-section of crop (with side walls); and (b) corresponding wind speed profiles: restricted leading edge (b ≒ 12 cm.)

wind-tunnel running at a constant shaft speed, T, of 200 units, the mean wind speed $u(z)$ was determined at several values of z between 1 cm. and 34 cm., for x (distance downstream from leading edge of crop) equal to 15, 45, 75 and 105 cm. The resulting profiles of mean wind speed, in Fig. 2.7(b) (for z less than 26 cm. only), show a rapid deceleration of the airflow entering the leading edge of the crop, followed by upward emergence of this decelerated flow to form a grossly swollen boundary layer. There was obviously little hope that the wind profile would settle down to an "equilibrium" shape by $x = 180$ cm. unless, as mentioned in Section 2.2(c), some means could be found to restrict the mass flow of air into the leading edge of the crop.

Figs. 2.8(a) and 2.8(b) show the method and success of the first tentative attempt to promote rapid attainment of "equilibrium" flow conditions both within and above the canopy. The leading edge was blocked (using materials immediately available) to a height $z = b$ of close to 12 cm., the estimated zero plane displacement for the crop. The wind profile below $z = h$ gave appearance of settling, towards an "equilibrium" shape (i.e. of tending to become invariant with x), while above $z = h$ the boundary layer increased smoothly in depth with x.

From the results of these preliminary measurements, it was decided to experiment with different levels (b) of smoothly constructed approach to the leading edge of the crop; thus to determine the value of b which gives

the most rapid development of the ("equilibrium") wind speed profile characteristic of the crop. Furthermore, it was evident that side walls higher than 28 cm. were required.

2.5 The Moment Balance

2.5(a) The force to be measured

The drag force f on a single crop element at x = 105 cm., due to the corresponding wind speed profile in Fig. 2.8(b), was calculated (assuming applicability of coefficient $C_d(u)$, Fig. 2.1) to be about 0.5 dynes - a small force on any account. It was decided, therefore, to measure the moment ,M, on seven neighbouring elements about a point some 10 to 15 cm. below z = 0, a moment large enough (about 100 dyne cm.) to be accurately measureable with simple apparatus. The force f could then be determined from a knowledge of its own level of action on one of the elements, i.e. of the centre of pressure c (see 3.2(a)).

2.5(b) Design of the balance

The simple moment balance shown in Fig. 2.9 was constructed, using the agate knife-edge suspension of a standard laboratory balance. The relative sensitivity of the instrument can be adjusted by raising or lowering the centre of gravity of the suspended system, while a high

absolute sensitivity was ensured by making the suspended part as light as possible. Due to fluctuations about the mean of the force on an object exposed to a turbulent flow, oil damping of the suspended systems was included. Four rider weights were made of approximately 500, 200, 50 and 10 mgm. At its maximum sensitivity this balance can measure moments to an accuracy of $\pm$ 5 dyne cm.

2.5(c) The composite drag element

Seven crop elements were removed from the edge of one of the 30 cm. square sections of crop, and a hexagonal gap was cut in the polystyrene base (see Fig. 2.2). A smaller hexagon was cut from 1 cm.-thick polystyrene sheet and seven suitable lengths of 1 mm. diameter steel rod were glued firmly into this chassis, the central rod being long enough (about 24 cm.) to reach through a hole bored in the floor of the tunnel and be attached to the suspension of the moment balance, which was mounted below, Fig. 2.10. The composite drag element is shown in position in Fig. 2.11.

Reliable use of this moment balance technique required that there be no detectable force on the hexagonal chassis, or on the rod holding the chassis, due to any flow of air through the access hole in the tunnel floor, nor any measureable drag force on the chassis itself, due to wind within the canopy. Although venting of (that part

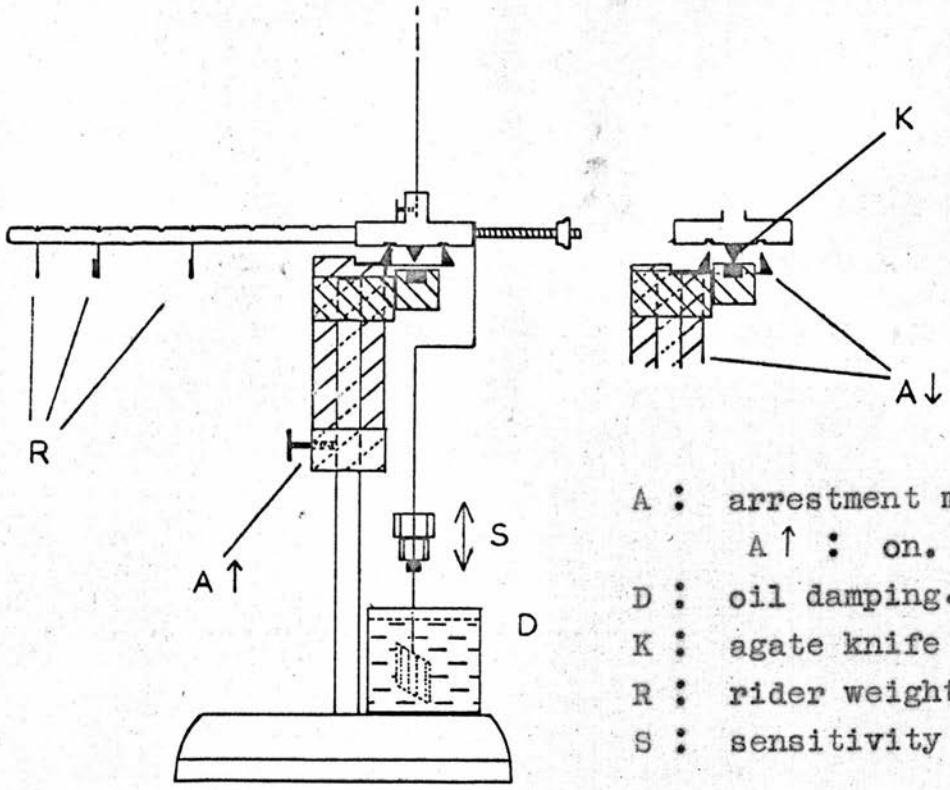

A : arrestment mechanism,
A↑ : on. A↓ : off.
D : oil damping.
K : agate knife edge suspension.
R : rider weights.
S : sensitivity adjustment.

FIGURE 2.9 Sketch of Moment Balance.

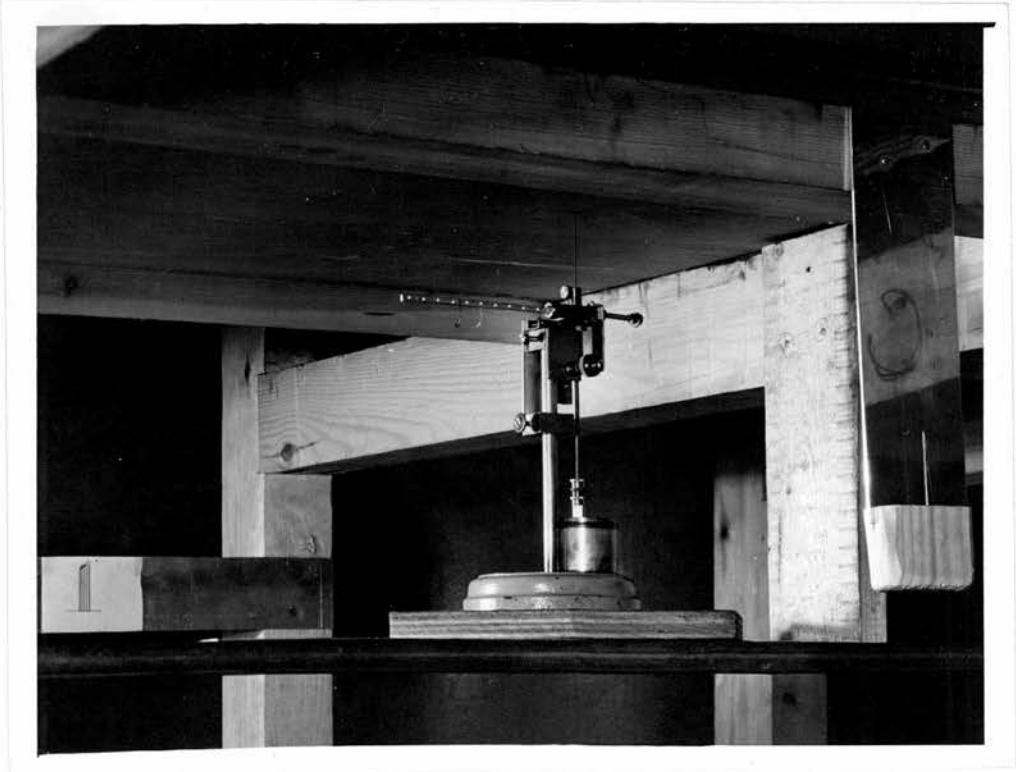

FIGURE 2.10 Moment balance mounted below tunnel

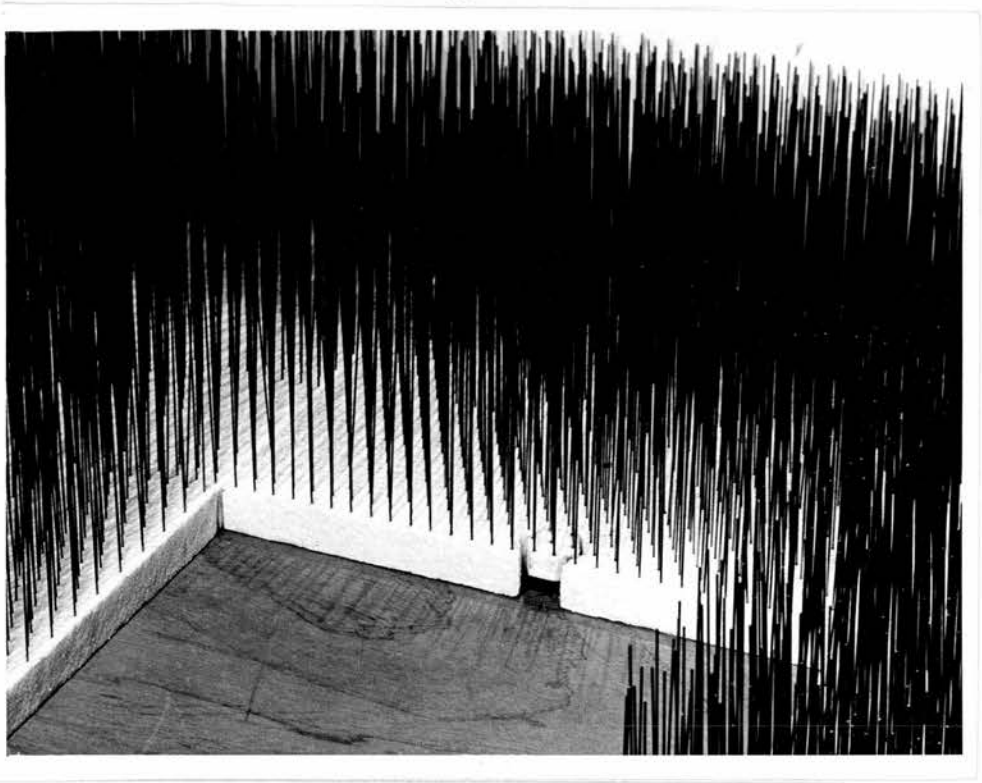

FIGURE 2.11 The composite drag element (attached to suspension of balance below).

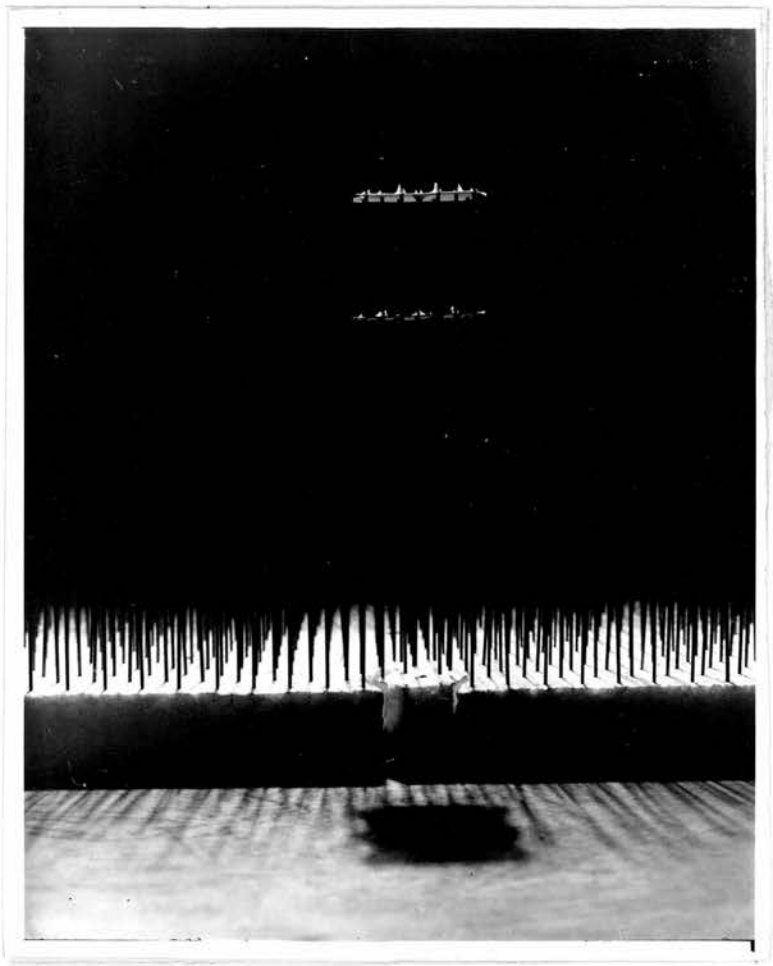

FIGURE 2.12 Dummy hexagonal chassis, with elements suspended above it (see 2.5(c)).

of) the wind tunnel to atmospheric pressure ensured the minimum possible flow of air through the access hole, and although wind speeds within the canopy were known to be small, it was decided to check that the resultant moment due to the above mentioned forces was in practice negligible. A duplicate hexagonal chassis, with seven (shortened) crop elements suspended carefully above it, was substituted for the composite drag element, as shown in Fig. 2.12. No measureable net force on this dummy chassis could indeed be detected, even at the highest wind speeds available, thus confirming under dynamic conditions, the reliability of the moment balance technique.

2.5(d) Use of the balance

With the composite drag element centrally balanced under calm conditions, the position of the lower end of the suspended system against the vertically ruled background (Fig. 2.10) was determined accurately by viewing through the appropriately placed slit. For any subsequent airflow in the tunnel, the suspended system was returned to this central position by requisite movement, along the moment arm, of one or more of the rider weights. In this way the moment M was measured absolutely.

As the moment balance was of necessity at a fixed point in the tunnel, values of M for different values of x (distance from leading edge of crop) could be obtained only by moving the crop relative to the balance. The

CHAPTER 3

RESULTS OF THE ARTIFICIAL CROP EXPERIMENT

3.1 Measured Moments and Wind Profiles

3.1(a) Experimental data

The profile of mean wind speed both above and within the artificial crop was determined at x = 10.5, 40.5, 70.5, 100.5, 130.5 and 160.5 cm., together with the moment M due to the wind drag on the seven mounted crop elements at x = 14, 44, 74, 104, 134 and 164 cm. These measurements were obtained for each of the five chosen values of b shown in Fig. 3.1, where $z = b$ is the level at which the airflow entered the leading edge of the crop. The complete, heightened, side wall construction is shown in Fig. 3.2, on which the broken curve indicates the upper limit of a typical boundary layer region appropriate to $b = 0$. A short addition to the crop, at the trailing edge, is also shown.

The wind speeds measured at selected values of z between 1 cm. and 25 cm. are recorded in Tables 3.1 to 3.5 inclusive, together with the corresponding values of M for each of b = 0, 7.4, 11.7, 12.9 and 14.1 cm., respectively. All data were obtained with the tunnel drive speed T held constant at 200 units.

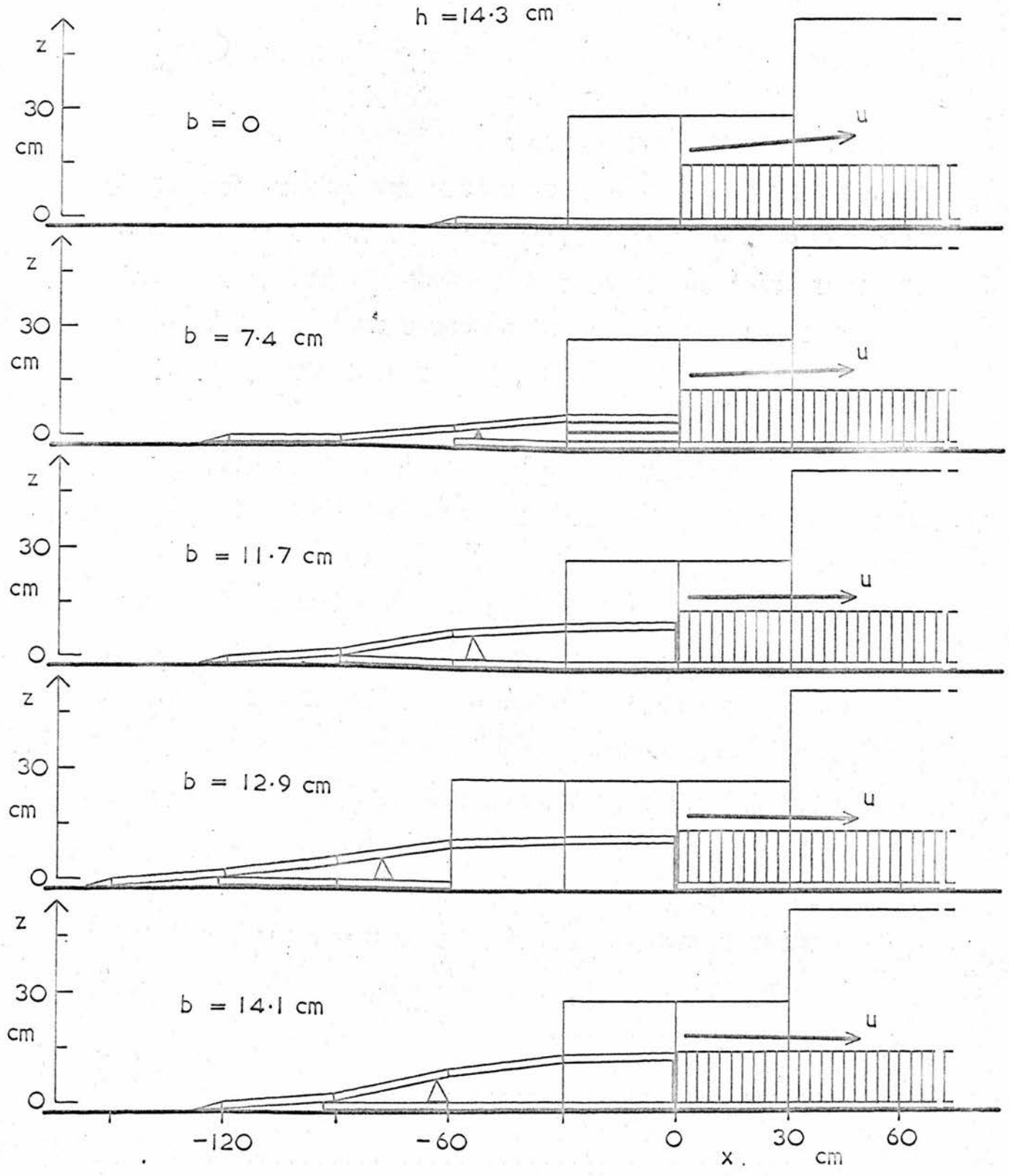

FIGURE 3.1 Cross-section of crop leading edge region (with improved side walls) for each chosen value of b . (The arrows indicate likely streamlines of flow: see also Figs. 3.3 and 3.4.)

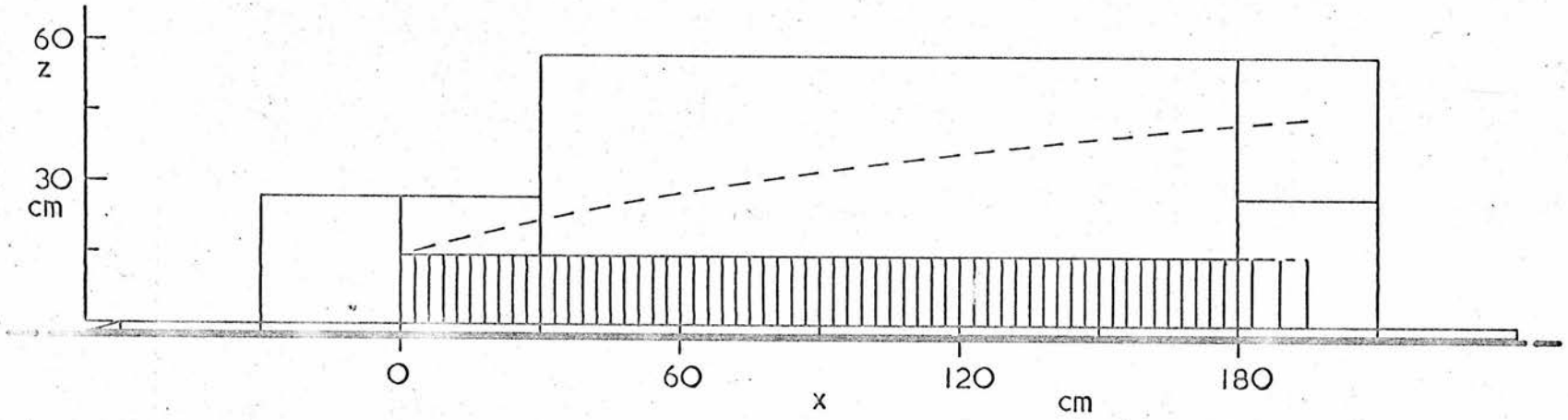

FIGURE 3.2 Cross-section of entire crop (with improved side walls). The broken curve delineates the boundary layer region for b = 0 (when T = 200 units).

3.1(b) The x-component u_x of the mean wind speed u

The negative values of the moment M which were found for $x > 120$ cm. when b was zero, (Table 3.1), served as a reminder that the quantity u measured by the hot-wire anemometer was the mean of the speed of the wind in the x,z-plane. (The anemometer is relatively insensitive to a wind component along the hot-wire axis.) It was however assumed that the x-component of wind speed u_x, responsible for M, was equal to u except where the direction of the mean flow deviated considerably from +x. Where u_x could be demonstrated, or argued, to be negative, the prefix (-) appears with the corresponding value of u in Tables 3.1 to 3.5; and where u_x could be demonstrated, or argued, to be zero (static turbulence; or $u = u_z$ only) the prefix (z) is included.

3.1(c) Flow visualisation by liquid nitrogen

Because of possible damage to fine hot-wires in the high-speed section of the tunnel, a particulate smoke could not be used for flow visualisation. However, the nature of specific parts of the flowwas investigated successfully by observing and photographing the fog of water droplets which streamed behind a shallow tray of liquid nitrogen, appropriately placed. Fig. 3.3. demonstrates the emergence of the streamlines of flow from the top of the crop when b = zero. Fig. 3.4 shows, in contrast, that when b = 11.7 cm., streamlines entering

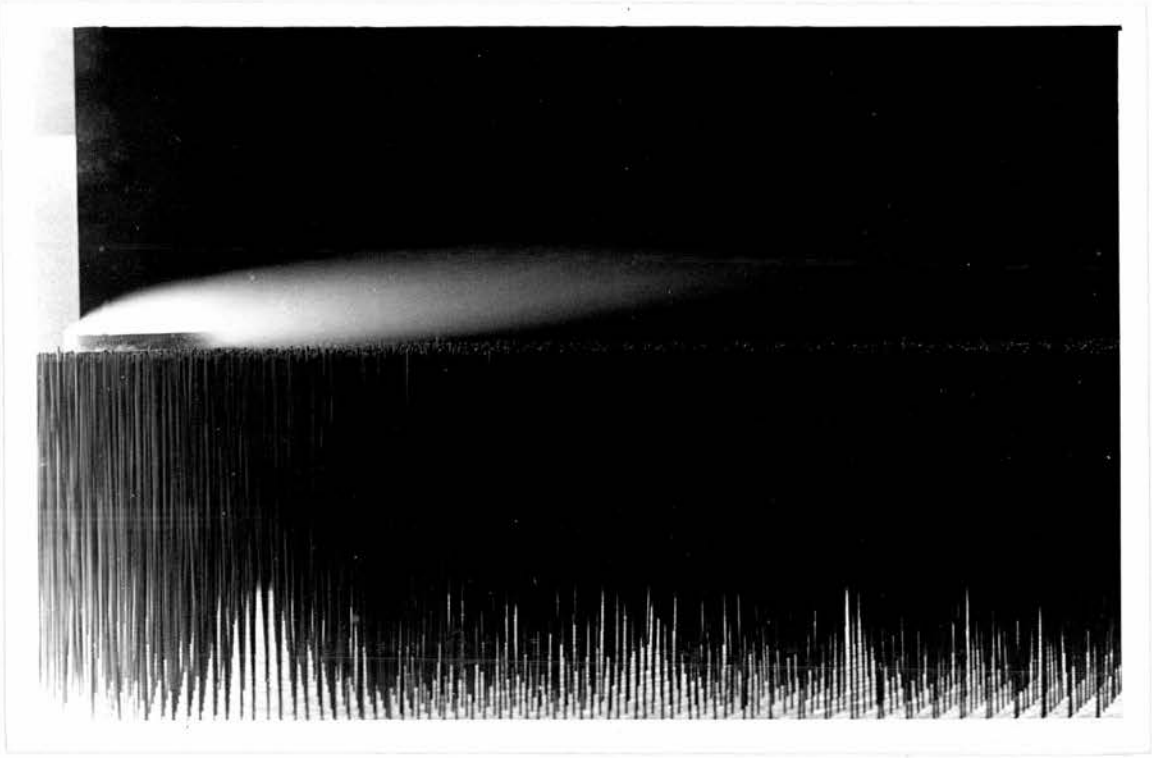

FIGURE 3.3 b = zero: water droplet source (liquid nitrogen) at $x \doteq 5$ cm.

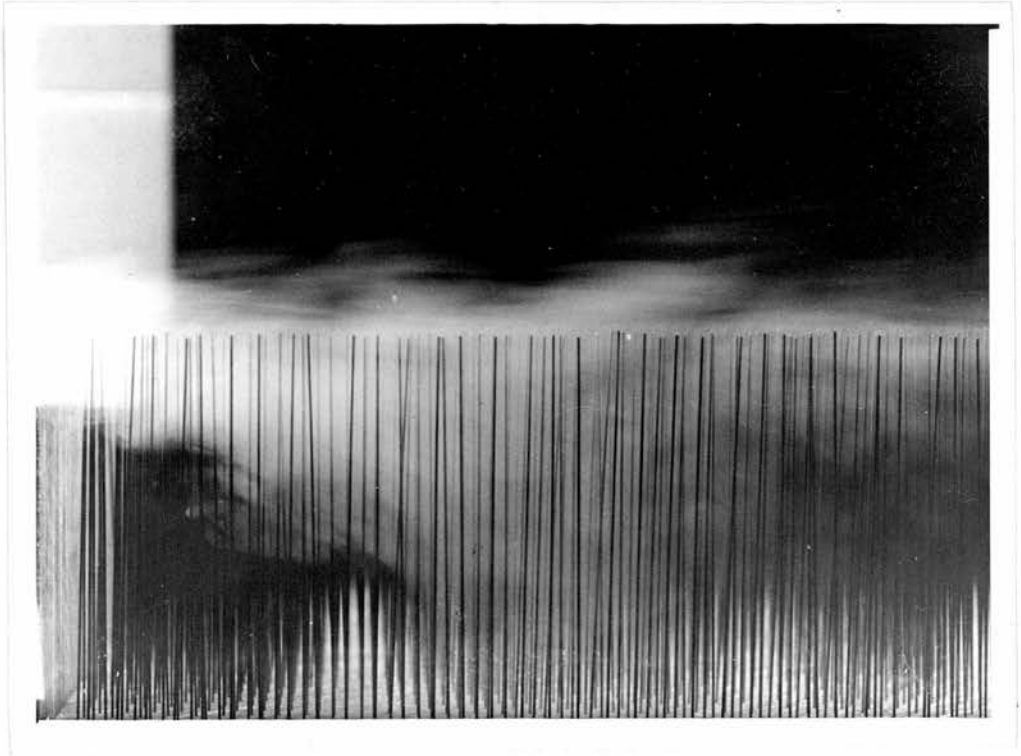

FIGURE 3.4 b = 11.7 cm.: water droplet source at $x \doteq -20$ cm.

TABLE 3.1 b = 0 cm. T = 200 units

x cm.	10.5	40.5	70.5	100.5	130.5	160.5
z cm.	Mean wind speed, u cm. sec.$^{-1}$					
25	166	162	84	55	38.7	37
24	-	-	-	-	-	33
23	163	139	68	38	27.9	-
22	-	-	-	-	-	25
21	160	99	47.6	26.5	17.2	-
20	-	-	-	23.3	15.2	(z) 24
19	157	74.4	35.1	18.2	(z) 13.6	-
18	-	61.6	-	16.9	(z) 11.4	(z) 18
17	152	56.0	25.4	14.4	(z) 9.4	(z) 15.2
16	129	44.5	-	12.5	(z) 9.4	(z) 13.6
15	101	37.8	17.2	8.3	(z) 8.5	(z) 13.0
14.5	-	-	-	-	-	-
14	87.6	31.5	13.2	7.0	(z) 8.5	(-) 11.1
13.5	-	-	-	-	-	-
13	84.8	30.6	13.2	7.0	(z) 8.0	-
12.5	-	-	-	-	-	-
12	84.8	31.5	-	-	(z) 6.9	(-) 8.8
11	84.8	32.4	13.4	6.9	(z) 7.4	-
10	84.8	-	-	-	(z) 6.7	(-) 7.7
9	84.8	32.4	13.6	6.3	(z) 6.9	-
8	84.8	-	-	-	(-) 6.9	(-) 5.9
7	82.0	32.8	14.0	6.2	(-) 6.7	-
6	80.0	-	-	-	(-) 6.2	(-) 5.4
5	77.8	-	14.6	5.6	(-) 5.9	-
4	75.4	33.3	-	-	(-) 5.6	(-) 4.6
3	73.0	-	14.6	5.4	(-) 4.8	-
2	66.0	33.3	-	-	-	-
1	64.1	32.8	14.6	5.4	(-) 4.3	(-) 3.4
M dyne cm.	800	173	48	14	-5	-22
x cm.	14	44	74	104	134	164

TABLE 3.2 b = 7.4 cm. T = 200 units

x cm.	10.5	40.5	70.5	100.5	130.5	160.5
z cm.	Mean wind speed, u cm. sec.$^{-1}$					
25	183	185	179	147	129	123
24	-	-	-	-	-	-
23	179	185	157	126	114	110
22	-	-	-	-	-	-
21	179	177	126	98	93	92
20	-	-	-	-	-	-
19	177	146	92.5	76.5	75	78.5
18	-	-	83.6	-	-	67.0
17	174	102	67.7	61.3	59.8	58.9
16	-	-	56.0	-	47.7	53.8
15	137	58.9	44.5	38.3	38.7	48.6
14.5	108	-	-	-	-	-
14	77	37.4	29.7	25.2	27.9	34.8
13.5	-	-	-	-	-	-
13	77	33.0	21.7	21.6	21.7	20.5
12.5	-	-	-	-	-	-
12	77	31.2	19.2	18.3	16.4	18.2
11	74.4	30.3	16.4	13.5	14.0	15.5
10	70.2	29.4	15.2	13.0	12.0	12.6
9	-	30.3	14.9	10.5	9.4	11.6
8	65.6	31.2	14.6	8.5	9.1	9.3
7	59.5	31.2	-	8.2	8.0	7.4
6	52.5	30.3	14.9	8.0	7.7	-
5	41.7	32.1	-	7.1	7.1	6.9
4	23.7	32.1	14.9	6.7	6.7	-
3 (z)	12.0	32.1	15.2	-	-	-
2 (z)	5.9	32.1	15.6	5.9	5.6	-
1 (-)	6.7	32.1	15.6	5.4	4.0	5.1
M dyne cm.	540	180	74	25	22	34
x cm.	14	44	74	104	134	164

TABLE 3.3 b = 11.7 cm. T = 200 units

x cm.	10.5	40.5	70.5	100.5	130.5	160.5
z cm.	Mean wind speed, u cm. sec^{-1}					
25	168	168	171	168	154	150
24	168	168	-	-	-	143
23	-	168	168	154	138	135
22	168	168	-	-	-	125
21	-	165	157	138	121	117
20	165	162	147	132	111	107.3
19	-	-	131	118	102.0	99.8
18	165	157	117	108.7	91.6	91.6
17	160	147	103.0	87.1	80.7	83.6
16	155	117	83.6	84.4	74.5	74.4
15	147	89.4	72.3	70.9	61.0	63.0
14.5	124	-	-	-	-	-
14	82	59.5	52.5	51.2	47.0	45.5
13.5	-	-	-	-	-	-
13	64	36.0	36.9	37.2	34.8	33.6
12.5	-	-	-	-	-	-
12	58.3	22.1	24.0	26.4	23.5	26.3
11	42.0	15.6	18.4	18.6	17.8	19.7
10	22.0	13.6	14.6	15.3	17.2	16.1
9	(z) 5.5	11.4	11.4	12.1	12.6	13.8
8	(z) 5.5	10.8	9.7	10.1	10.4	11.4
7	(-) 6.5	10.5	8.2	-	9.1	9.5
6	(-) 6.2	10.5	7.4	6.8	7.7	7.8
5	-	-	6.5	-	7.1	6.8
4	(-) 4.6	10.8	5.9	6.2	-	6.1
3	-	-	-	-	5.9	5.2
2	(-) 2.3	11.4	5.4	-	-	4.8
1	(-) 2	11.4	5.1	4.6	4.6	4.2
M dyne cm.	175	112	106	95	96	94
x cm.	14	44	74	104	134	164

TABLE 3.4 b = 12.9 cm. T = 200 units

x cm.	10.5	40.5	70.5	100.5	130.5	160.5
z cm.	Mean wind speed, u cm. sec^{-1}					
25	200	200	196	-	181	177
24	-	-	-	-	-	172
23	200	196	190	-	169	166
22	-	-	-	-	-	159
21	200	191	185	-	156	150
20	-	-	-	-	-	139
19	193	185	172	-	141	130
18	-	-	-	-	125	118
17	185	171	146	-	111	102.0
16	179	150	121	-	96.0	95.2
15	165	126	95.1	-	80.7	78.5
14.5	108	99	-	-	-	-
14	86.3	83.6	69.5	-	63.0	61.0
13.5	-	-	-	-	-	-
13	54.3	41.7	48.6	-	45.5	44.1
12.5	-	-	-	-	-	-
12	35.1	27.9	31.2	-	34.8	34.8
11	15.2	17.6	24.1	-	25.2	26.0
10	(z) 5.1	12.0	17.8	-	21.5	22.9
9	(z) 7.0	7.7	13.2	-	17.5	18.6
8	-	-	-	-	-	15.1
7	(-) 6.5	5.6	9.0	-	13.0	12.3
6	-	-	-	-	-	-
5	(-) 4.8	4.8	7.1	-	9.7	9.6
4	-	-	-	-	-	-
3	(-) 3.4	4.0	5.4	-	8.2	7.1
2	-	-	-	-	-	-
1	(-) 2.3	4.0	4.8	-	6.9	7.0
M dyne cm.	109	133	144	-	147	145
x cm.	14	44	74	104	134	164

TABLE 3.5 b = 14.1 cm. T = 200 units

x cm.		10.5	40.5	70.5	100.5	130.5	160.5
z cm.		Mean wind speed, u cm. sec.$^{-1}$					
25		183	182	185	182	178	173
24		-	-	-	-	-	-
23		180	182	182	173	169	161
22		-	-	-	-	-	156
21		180	177	174	154	150	146
20		-	-	-	-	148	135
19		174	167	162	140	136	125
18		-	-	152	-	125	115
17		165	152	142	119	108	106.6
16		160	134	124	-	92.7	95.0
15		142	105	92.0	83.3	79.7	80.7
14.5		-	-	-	-	-	-
14		76.0	63.5	67.4	67.3	61.9	62.9
13.5		43.0	-	-	-	-	-
13		17.2	39.0	44.4	47.4	43.2	44.1
12.5	(z)	10.8	-	-	-	-	-
12	(z)	9.4	22.5	30.5	35.0	35.2	35.6
11	(z)	8.5	17.2	22.5	26.1	25.5	26.0
10	(-)	7.7	9.9	18.7	20.6	21.8	24.0
9		-	8.0	14.6	16.0	18.5	18.2
8	(-)	6.9	7.0	11.4	14.9	14.9	15.8
7	(-)	5.9	4.6	9.4	11.7	12.0	13.5
6	(-)	5.4	4.6	8.2	10.5	10.0	11.6
5	(-)	4.0	3.7	6.7	8.2	-	10.4
4	(-)	3.5	3.7	5.4	7.7	8.2	9.3
3		-	3.2	-	-	-	9.0
2	(-)	< 2	3.2	4.6	6.5	7.1	8.8
1	(-)	< 2	3.2	4.3	6.2	7.1	8.4
M dyne cm.		67	116	152	162	161	159
x cm.		14	44	74	104	134	164

The following Figures (3.5 to 3.9, inclusive) have been prepared from the preceding Tables (3.1 to 3.5, inclusive), and from Table 3.8(a).

Each Figure shows

(a) : the measured wind speed profiles at

x = 10.5, 40.5, 70.5, 100.5, 130.5 and 160.5 cm., numbered 1, 2, 3, 4, 5, and 6;,

and the (partly) estimated profile at x = 0 cm., numbered 0;

and

(b) : the behaviour with x of the measured moment M and the calculated moment M_p, (the latter from Table 3.8(a)).

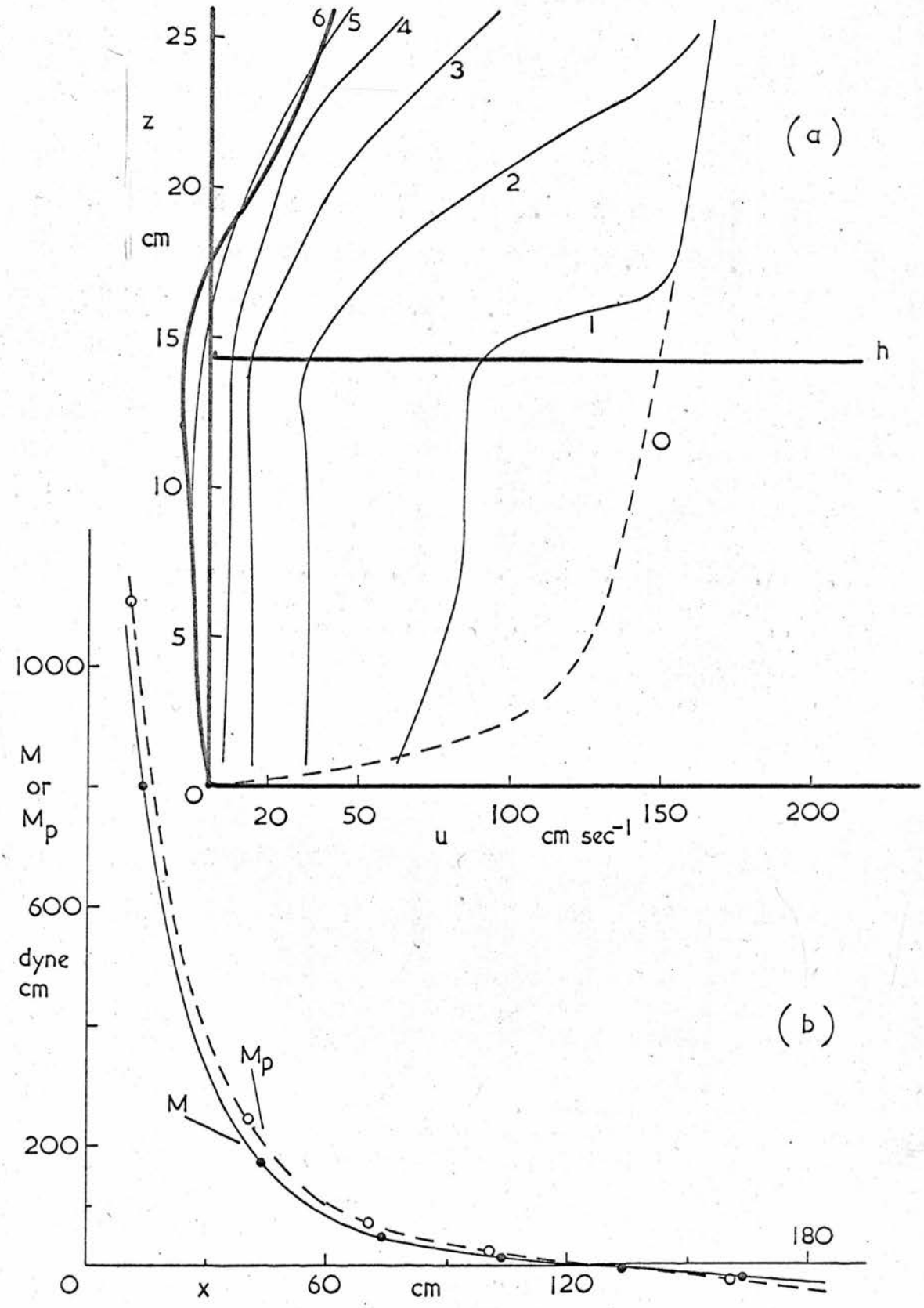

FIGURE 3.5 b = 0 cm. See Table 3.1, and page 56.

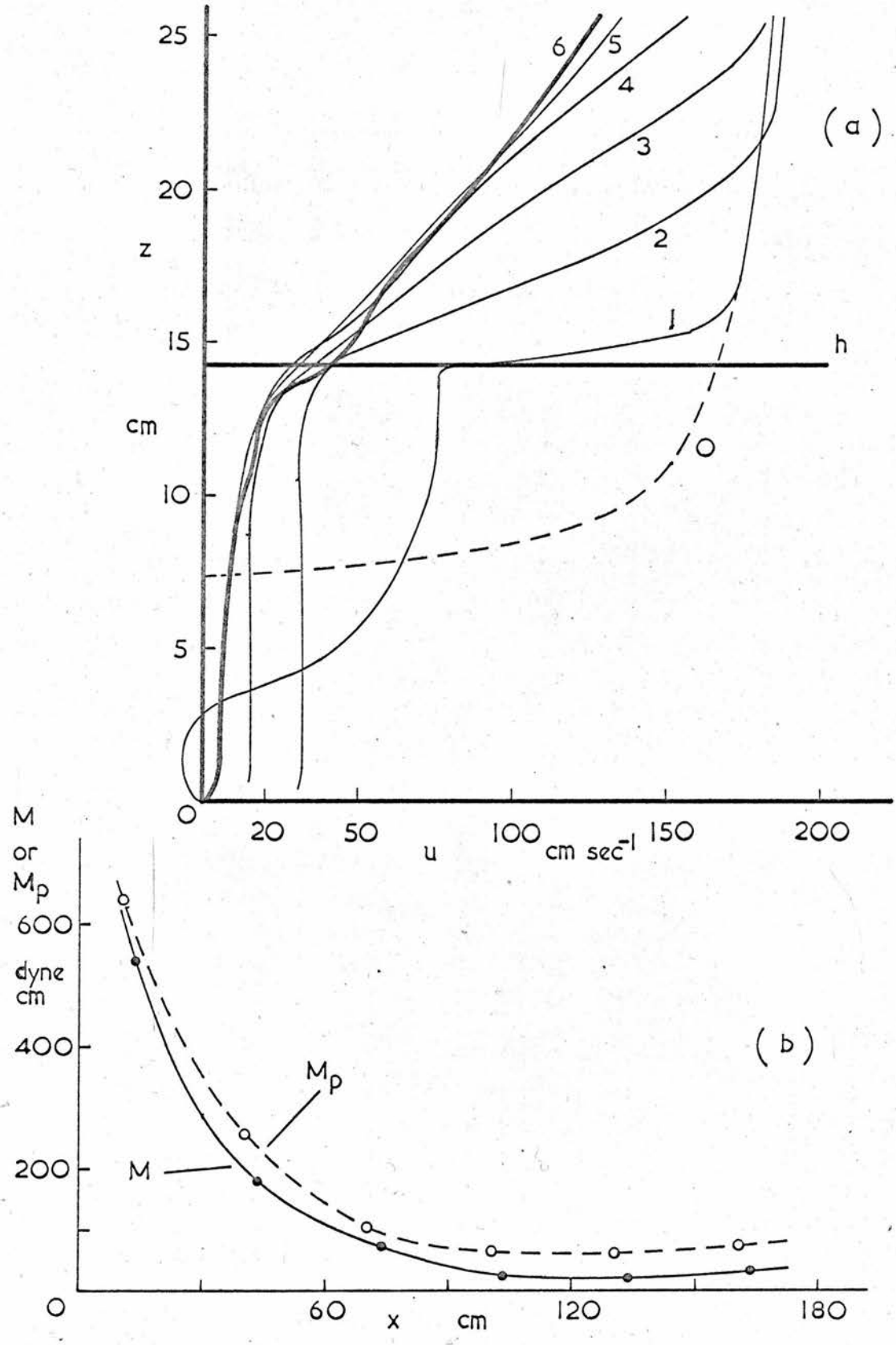

FIGURE 3.6 b = 7.4 cm. See Table 3.2, and page 56.

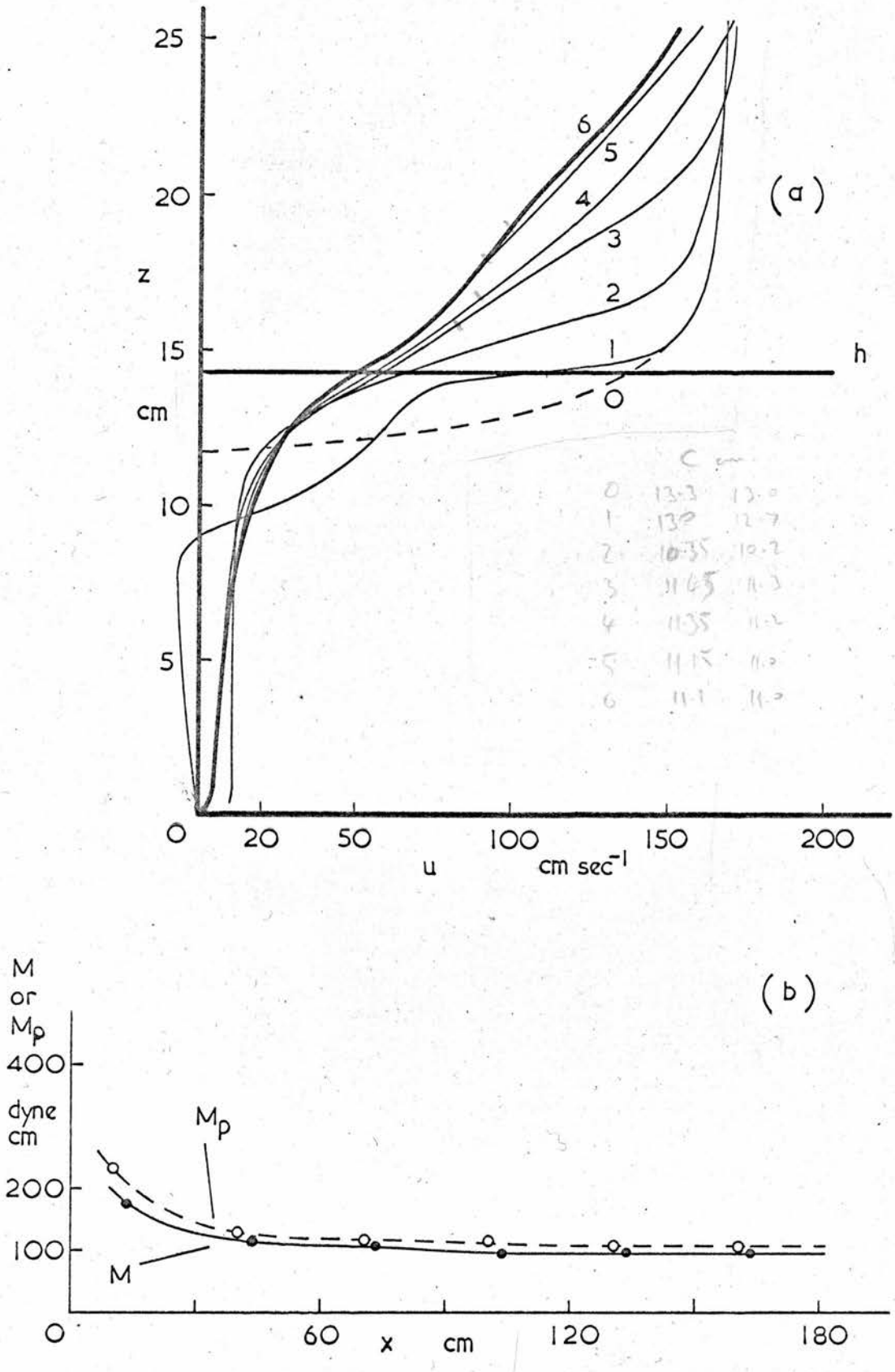

FIGURE 3.7 b = 11.7 cm. See Table 3.3, and page 56.

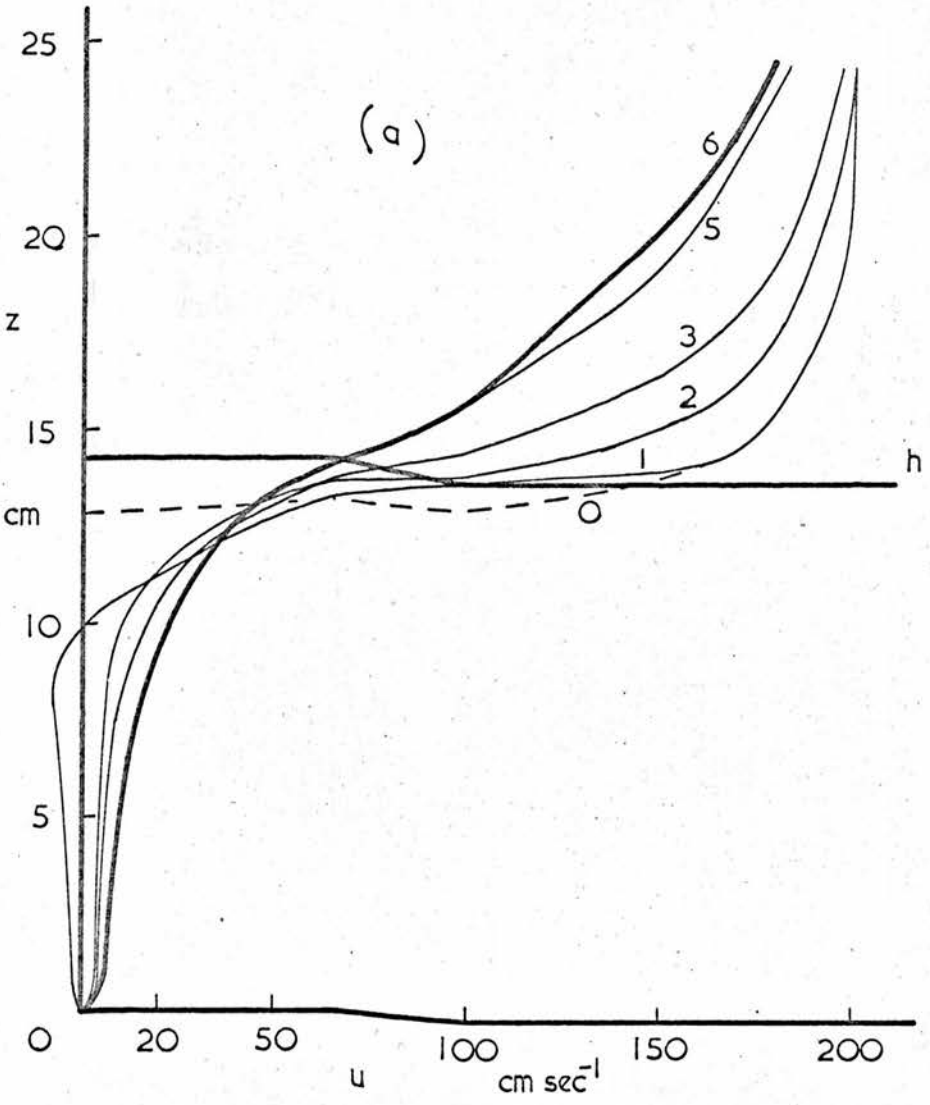

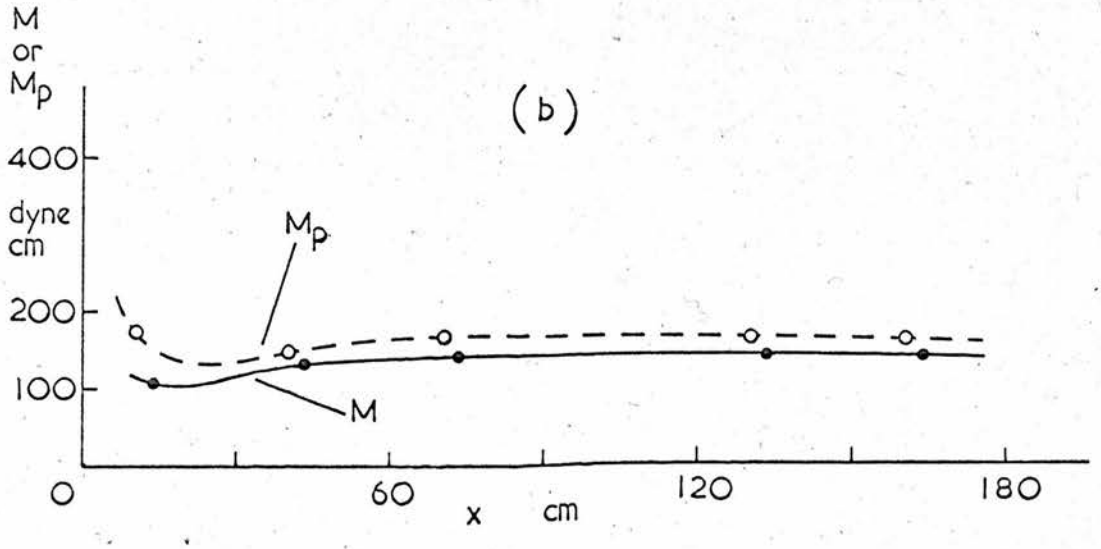

FIGURE 3.8 b = 12.9 cm. See Table 3.4, and page 56.

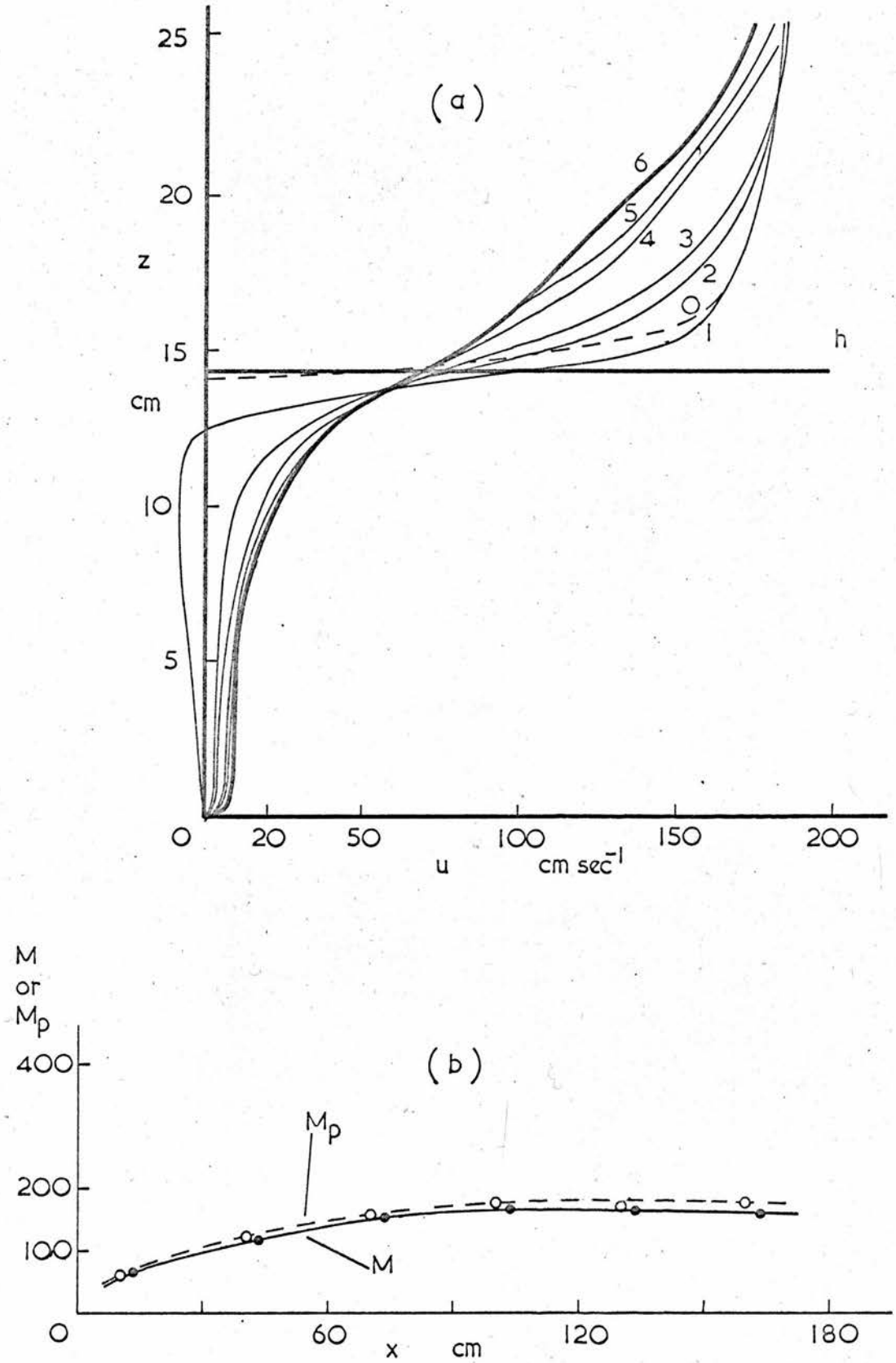

FIGURE 3.9 b = 14.1 cm. See Table 3.5, and page 56.

the leading edge of the crop spread downwards into the crop and streamlines above the crop are practically horizontal. These photographs were taken through a sheet of plate glass substituted temporarily for one wall of the wind-channel.

Disadvantages of using liquid nitrogen as a flow "tracer" are that the plume is short, and that the relatively high density of the air in the chilled plume can upset the flow pattern being investigated.

3.1(d) "Equilibrium" mass flow

Figs. 3.5 to 3.9 (inclusive) were prepared, in order, from the corresponding data in Tables 3.1 to 3.5. Each Figure shows (a), the development of the wind profile between x = 10.5 cm. (profile 1) and x = 160.5 (profile 6), and (b), the corresponding behaviour of the measured moment M. To give a clear and uninterrupted picture of the profiles, the experimental points are not shown: however, all points lie on, or very close to, the drawn curves, except those points representing wind speeds prefixed (z) in the Tables (see 3.1(b)). The (partly) estimated wind profile at x = 0 is shown by the broken curve in each Figure (a) (profile 0).

The most rapid development of an "equilibrium" profile of mean wind speed (i.e. a profile invariant with x) was obtained with b = 11.7 cm. (Fig. 3.7(a)). At this "optimum" value of b, the mass flow of air entering the

leading edge of the crop was nearly equal to the mass flow within the crop canopy at subsequent values of x. This can be inferred from the near equality of the values calculated for the "area",

$$A = \int_0^h u(z)\,dz \qquad (3.1)$$

of each of the profiles in Fig. 3.7(b); for the quantity

$$Q_1 = \rho \int_0^h u(z)\,dz = \rho A \qquad (3.2)$$

is the corresponding mass flow of air (per second) through a 1 cm. strip normal to the flow and extending between $z = 0$ and $z = h$.

When Q_1 is independent of x there can be no net transfer of air across the "surface" of the crop (i.e. across the plane $z = h$). This is a necessary condition for the development of an "equilibrium" wind profile both within and above the crop. The value of Q_1 at $x = 0$, called $(Q_1)_0$, depends on b : thus, if b is chosen so that

$$(Q_1)_0 = (Q_1)_E \qquad (3.3)$$

the "equilibrium" value of Q_1, then this "optimum" value of b permits the development of an "equilibrium" wind profile within the shortest possible distance from the leading edge of the crop.

3.1(e) Determination of the "optimum" value of b for an artificial crop

For any particular artificial crop, or any complex rough surface in general, the value of $(Q_1)_E$, Eq. (3.3), may neither be known nor easily estimated. However, it was possible to determine a quick method of finding the "optimum" value of b, by analysing the present extensive results collected for five values of b.

The mass flow Q_1 was estimated for each wind profile in Figs. 3.5 to 3.9, recorded in Table 3.6, and plotted against b, for constant x, in Fig. 3.10. This Figure shows that, for $x > 6h$, Q_1 is relatively insensitive to the choice of b, provided b is greater than h/2. If, in compliance with these limits of x and b, Q_1 is found experimentally to have a value $(Q_1)_{L1}$, then this value could be used as a first estimate for $(Q_1)_E$ in Eq. (3.3), and a value b_1, of b, determined. Using this value of b, a new value of $(Q_1)_L$, equal to $(Q_1)_{L2}$, could be found experimentally, and (if significantly different from $(Q_1)_{L1}$) a further adjustment of b, to b_2, could be made in such a way that $(Q_1)_0 = (Q_1)_{L2}$, a second and closer estimate of $(Q_1)_E$. It is unlikely that further repetition of this sequence would be required: b_2 if not b_1 should be close to the "optimum" value of b defined by Eq. (3.3).

The above method is recommended for determining the "optimum" value of b, a quantity of great importance to artificial crops of restricted downstream extent.

TABLE 3.6

b cm.	0	7.4	11.7	12.9	14.1
x cm.	$Q_1 = \int_0^h u(z)dz$ gm. sec.$^{-1}$ cm.$^{-1}$				
0	2.20	1.10	0.28	0.12	< 0.01
10.5	1.39	0.70	0.27	0.17	0.02
40.5	0.61	0.54	0.28	0.24	0.20
70.5	0.24	0.29	0.27	0.29	0.29
100.5	0.10	0.18	0.27	-	0.31
130.5	-0.05	0.18	0.26	0.32	0.34
160.5	-0.07	0.20	0.26	0.32	0.34

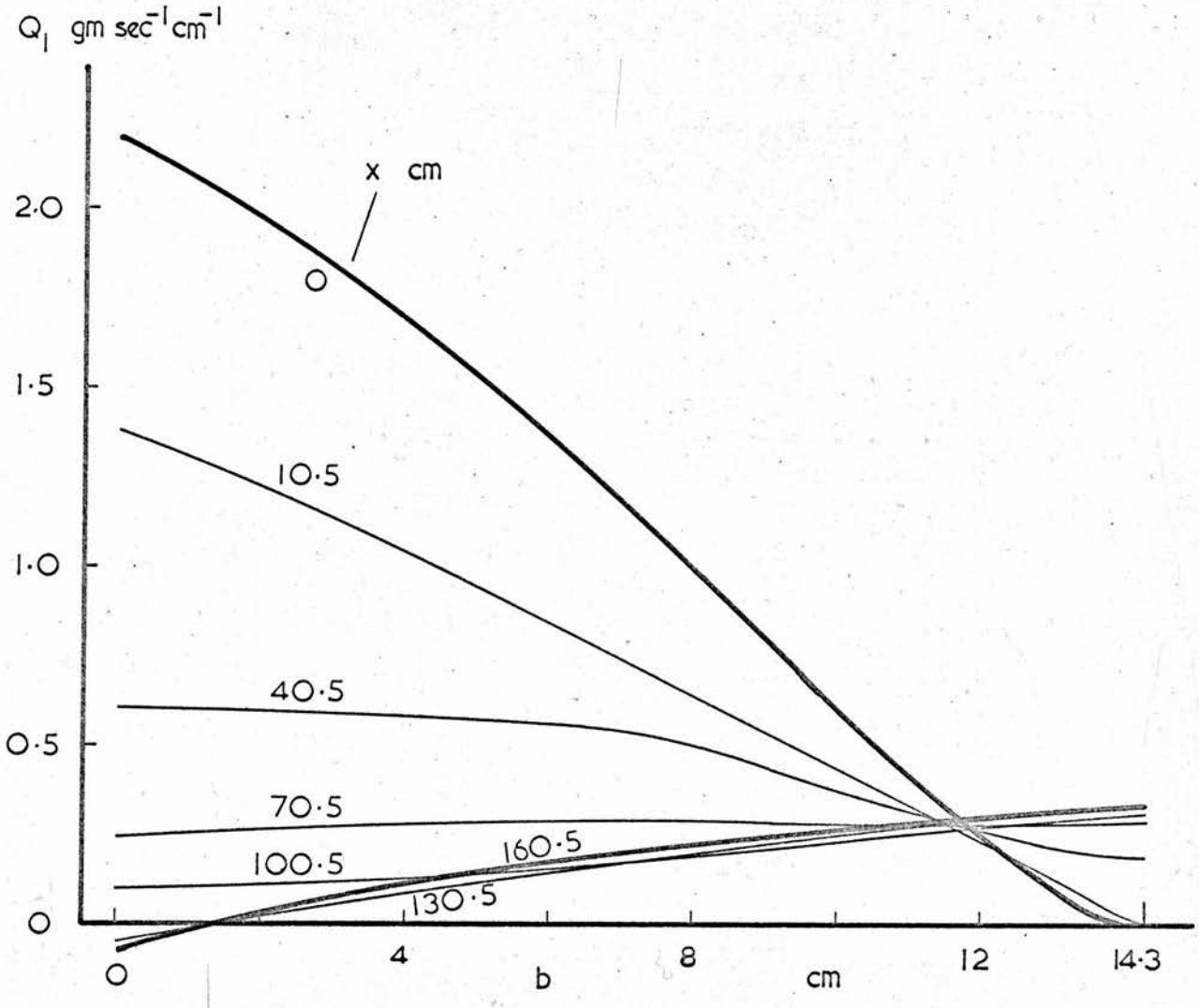

FIGURE 3.10 Q_1, the mass flow rate of air per cm. width of canopy, as a function b for each x; from Table 3.6.

3.2 Calculation of Moments from the Wind Profiles within the Crop

3.2(a) The centre of pressure c and the moment M_p.

Figure 3.11 shows the profile of mean wind speed within the crop at x = 160.5 cm. when b had the "optimum" value 11.7 cm. (see Table 3.3; also Fig. 3.7(a), profile 6): this profile is the mean of two separate determinations.

The values of u(z) at the nine chosen levels (i) in Table 3.7 were obtained from Fig. 3.11. The force $(f_i)_p$ on each incremental length $(\delta z)_i$ of a single crop element was calculated from the relation

$$(f_i)_p = \rho\, u_i^2\, C_d(u_i).d.(\delta z)_i \qquad (3.4)$$

where d is the diameter of the element and each $u_i^2 C_d(u_i)$ was derived from Fig. 2.1. The sum of these incremental forces gave the drag force f_p on a single crop element exposed to the wind profile shown in Fig. 3.11 - a force calculated on the assumption that the drag coefficient of an isolated element (C_d) can be applied to an element within the canopy (1.2(a), (i)).

The centre of aerodynamic pressure on the element was derived from the expression

$$c = \sum_{i=1}^{9} z_i(f_i)_p / f_p = \frac{(m_o)_p}{f_p} \qquad (3.5)$$

where $(m_o)_p$ is the moment, about z = 0, of the calculat-

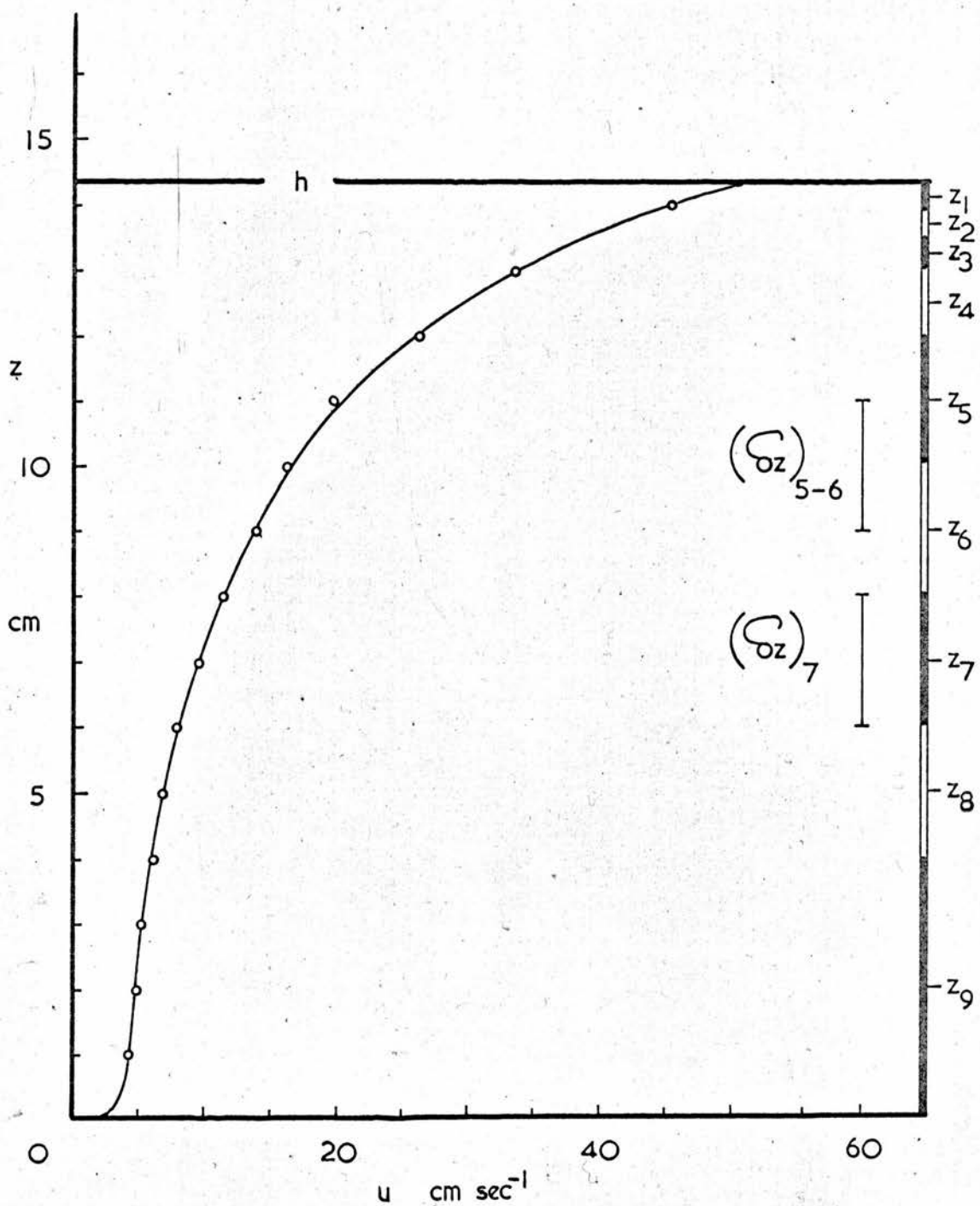

FIGURE 3.11 The wind profile within the canopy at x = 160.5 cm. for b = 11.7 cm.; from Table 3.3: also, each z_i and $(\delta z)_i$ used in Table 3.7.

TABLE 3.7

i	z_i cm.	$(\delta z)_i$ cm.	u_i cm. sec^{-1}	$u_i^2 C_d(u_i)$ cm^2 sec^{-2}	$(f_p)_i$ dyne	$z_i(f_p)_i$ dyne cm.
1	14.1	0.4	47.0	1950	0.094	1.325
2	13.7	0.4	41.4	1585	0.076	1.041
3	13.25	0.5	36.3	1290	0.078	1.033
4	12.5	1.0	29.5	950	0.114	1.425
5	11.0	2.0	20.5	560	0.134	1.472
6	9.0	2.0	13.7	320	0.077	0.693
7	7.0	2.0	9.5	182	0.044	0.308
8	5.0	2.0	6.8	110	0.026	0.130
9	2.0	4.0	4.7	66	0.032	0.064

f_p = 0.675 dynes

$(m_o)_p$ = 7.49 dyne cm.

c = 11.1 cm.

M_p = 107 dyne cm.

TABLE 3.8(a)

x cm.	0	10.5	40.5	70.5	100.5	130.5	160.5
b cm.				M_p dyne cm.			
0.0		1110	247	72	23	-	-27
7.4		640	258	104	66	63	74
11.7	-	231	128	113	114	106	107
12.9		177	150	170	-	170	167
14.1		59	118	154	175	169	176
0.0	(8.5)	7.8	7.05	6.95	7.55	-	9.05
7.4	(11.5)	10.0	7.5	7.9	10.0	10.2	10.6
11.7	(13.3)	13.0	10.35	11.45	11.35	11.15	11.1
12.9	(13.8)	13.9	12.4	11.85	-	11.15	11.1
14.1	(14.2)	15.8	12.4	11.75	11.35	11.1	10.85
b cm.				c cm.			

TABLE 3.8(b)

x cm.	0	14	44	74	104	134	164
b cm.				$M_{p/M}$			
0.0		1.18	1.23	1.31	1.43	-	1.27
7.4		1.07	1.31	1.30	2.56	2.82	2.23
11.7		1.17	1.13	1.10	1.16	1.13	1.13
12.9		1.39	1.15	1.18	(1.16)	1.16	1.14
14.1		1.02	1.05	1.05	1.09	1.10	1.09
0.0	(14.5)	5.90	1.32	0.37	0.10	-	-0.16
7.4	(9.7)	3.63	1.34	0.53	0.16	0.14	0.22
11.7	(3.4)	1.03	0.74	0.65	0.59	0.60	0.59
12.9	(1.2)	0.61	0.79	0.87	-	0.92	0.91
14.1	(0.02)	0.35	0.69	0.93	1.01	1.01	1.00
b cm.				f dyne			

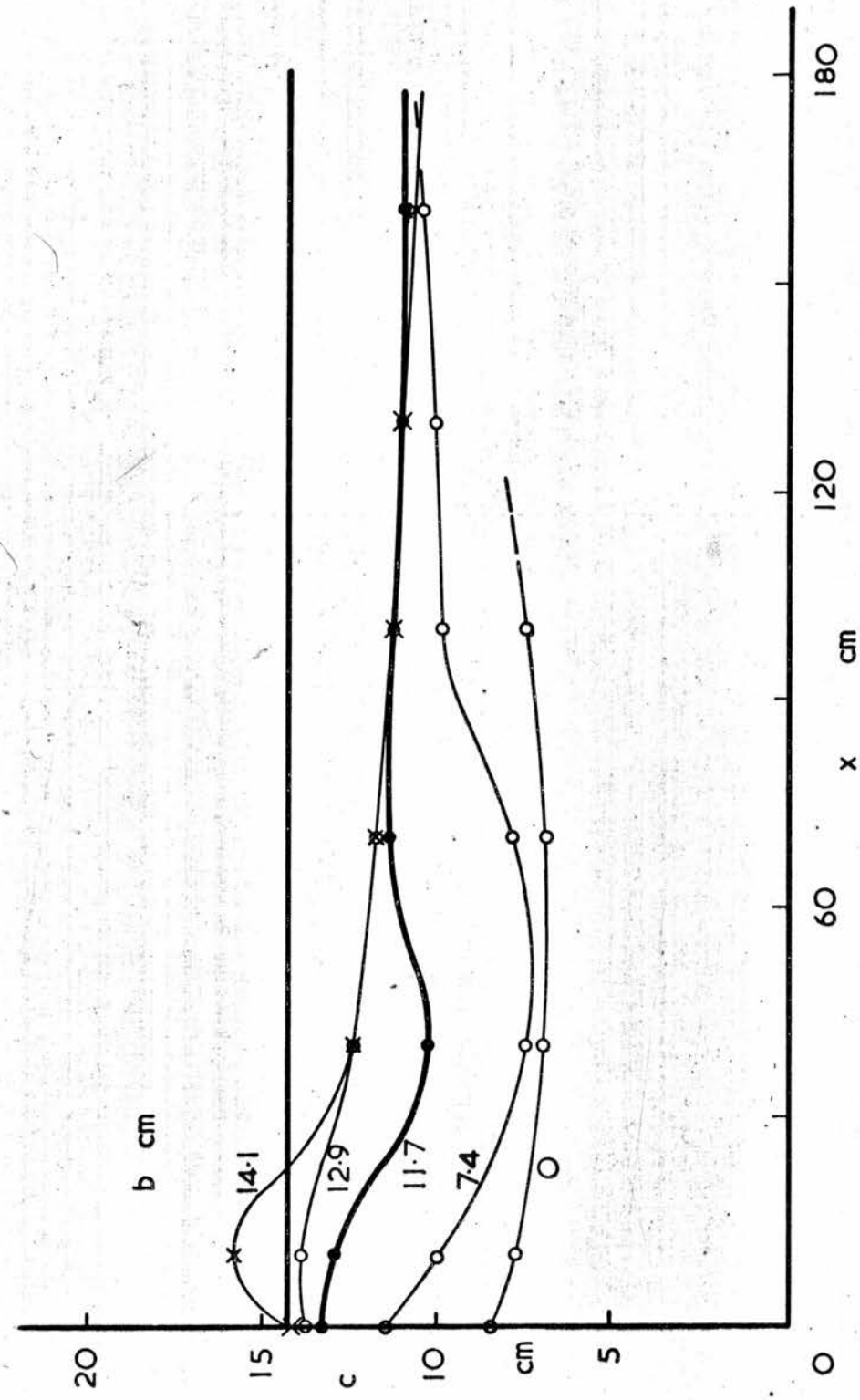

FIGURE 3.12 The centre of pressure c as a function of x for each b .

ed force f_p. As the measured moment M referred to the drag on seven crop elements about a point 11.7 cm. below z = 0, the corresponding calculated moment M_p, equal to $7.(m_o)_p.(11.7 + c)/c$, was derived. The value 107 dyne cm. was calculated for M_p, in comparison with the measured value M = 94 dyne cm. (at x = 164 cm.). This discrepancy is investigated in the following Section.

3.2(b) "Equilibrium" values of c and M_p/M: C_d within the canopy

Using the techniques of Section 3.2(a), but choosing different z_i and $(\delta z)_i$ where appropriate, the values of c and M_p for each profile in Figs. 3.5(a) to 3.9(a) were determined, and recorded in Table 3.8(a). The variation of M_p with x is shown by the broken curve in each of Figs. 3.5(b) to 3.9(b), inclusive. The corresponding behaviour of c is shown in Fig. 3.12 for each chosen value of b. (Values of c at x = 0 are estimated.)

Table 3.8(b) gives the value of the ratio M_p/M at each b and each x, together with the corresponding value of f, equal to the measured moment M divided by 7.(11.7 + c) and defined as the measured force on a single crop element. (Estimates of f are given for x = 0.)

Fig. 3.12 shows that, when b has the "optimum" value 11.7 cm., c quickly approaches the value 11.1 cm.

This "equilibrium" value of c can be asserted with confidence to be the value to which c would tend at a large enough value of x, no matter what value was given to b. Where both c and Q_1 are invariant with x, the wind profile within the canopy must be invariant with x (and vice-versa), and "equilibrium" conditions of truly horizontal mean flow must exist within the canopy.

Table 3.8(a) shows that the calculated moment M_p was always greater than the measured moment M. For the "equilibrium" conditions of flow described above (i.e. in regions of constant c and constant Q_1), M_p was some 13 per cent greater than M. This discrepancy could be explained in terms of a 6.5 per cent discrepancy in each u_i, Eq. (3.4), or a 13 per cent discrepancy in each $C_d(u_i)$. Although it is possible that the ("truly horizontal") mean wind speed was over-estimated by 6.5 per cent due to turbulence in the highly sheared flow, it is certain that end effects must reduce the effective value of C_d at the top of each crop element. However, on consulting Goldstein's treatise, it was decided that reasonable allowance for end effects could be made by neglecting the drag on the top-most 1 mm. of element (i.e. on a length of the circular cylinder equal to its diameter): this reduced the calculated moments by about 5 per cent. The remaining 8 per cent discrepancy was attributed to a consistent 4 per cent over-estimation, by the anemometer, of the mean horizontal wind speed, owing to vertical components of turbulence in the flow.

TABLE 3.9

	x cm.		0	14	44	74	104	134	164
b cm.	U_r cm.sec.$^{-1}$	N			f_n dyne.				
0	165	1.05	(15.2)	6.30	1.39	0.39	0.11	~0	0.17
7.4	185	0.87	(8.5)	3.16	1.17	0.46	0.14	0.12	0.19
11.7	170	1.00	(3.4)	1.03	0.74	0.65	0.59	0.60	0.59
12.9	200	0.76	(0.9)	0.46	0.60	0.66	-	0.70	0.69
14.1	185	0.87	(0.02)	0.30	0.60	0.81	0.88	0.88	0.87

FIGURE 3.13 The normalised force f_n on a single crop element as a function of x for each b; from Table 3.9.

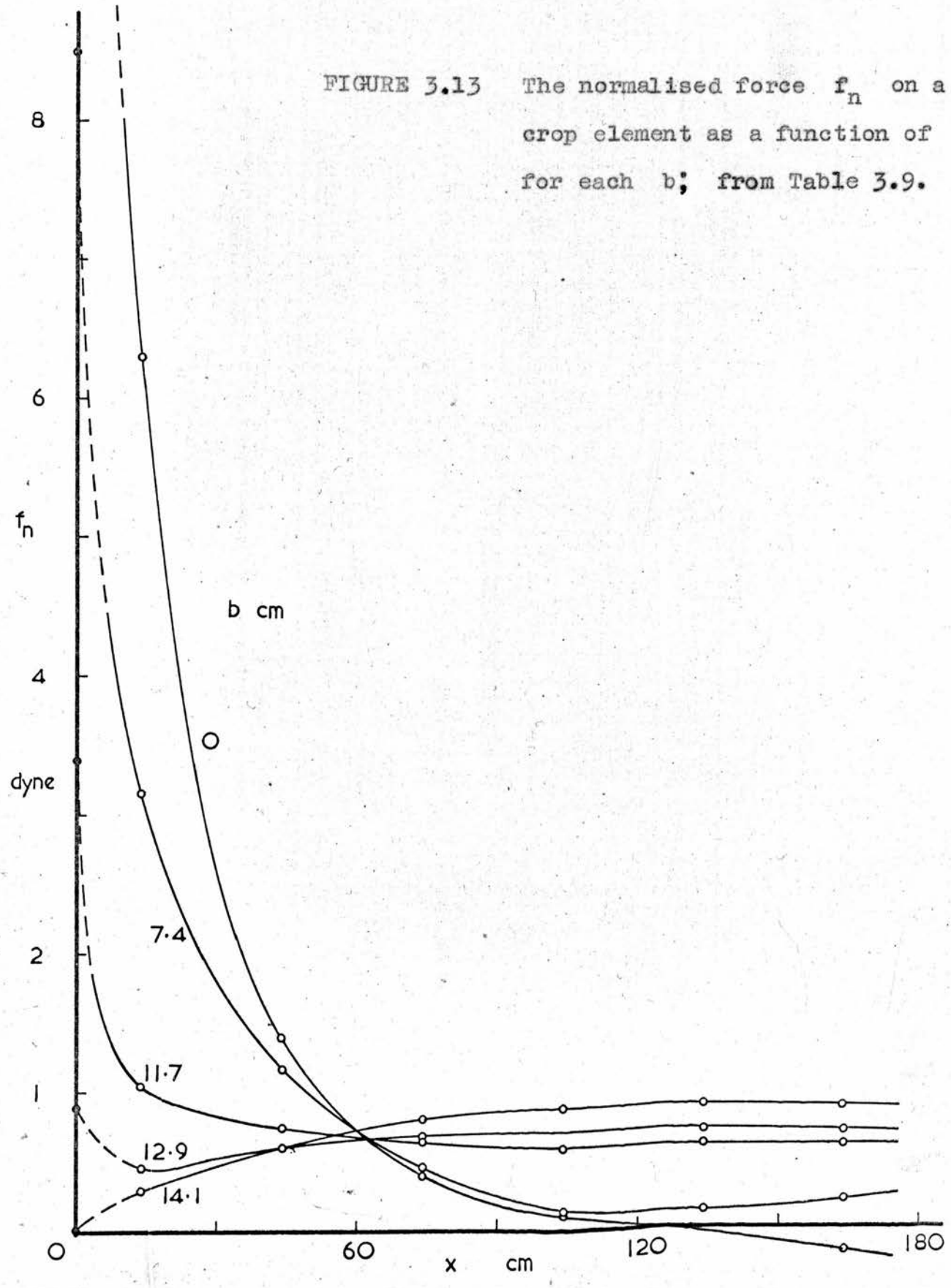

It has therefore been shown, within the limits of this analysis (which are about ± 10 per cent on the ratio M_p/M), that the drag coefficient C_d of an isolated crop element in a uniform laminar flow can be used, as in Eq. (3.4), to calculate the drag on an identical element exposed to the highly sheared and turbulent mean flow which exists within a crop canopy (1.2(a)).

3.2(c) The "equilibrium" value of the force f

Before making direct comparison between the values of f measured for the different values of b (Table 3.8(b)), it was recognised that each graded approach to the crop (Fig. 3.1) modified the "large scale" airflow over the crop in a characteristic way; so that, although the tunnel drive speed was always the same (T = 200 units), a reference speed representative of conditions above the crop such as U_r, equal to u at (z = 25 cm; x = 10.5 cm.), was not in practice constant. These values of U_r are recorded in Table 3.9, together with corresponding values of f (from Table 3.8(b)) normalised to f_n at U_r = 170 cm. sec.$^{-1}$, by the factor N equal to $((170)^2 C_d(170))/(U_r^2 C_d(U_r))$.

Fig. 3.13 shows f_n plotted against x for each b. It is likely that, for U_r = 170 cm. sec.$^{-1}$, f would tend to the same "equilibrium" value, close to 0.60 dynes, at a large enough value of x no matter what value was given to b.

3.3 Properties Determined from the Developed Wind Profile above the Crop

3.3(a) A value for d_o

Profiles 5 and 6 in Fig. 3.7(a), or Fig. 3.8(a), show that, when b was equal to, or close to, the "optimum" value defined by Eq.(3.3) (and here equal to 11.7 cm.), the wind profile was invariant with x (within experimental limits) up to a level exceeding z = h by an amount close to x/35. Eq. (1.13) could therefore be employed to describe profile 6 between z = h and z = (about) 19 cm.

To determine an appropriate value for d_o, profile 6 (Fig. 3.7(a)) was plotted against $\ell n(z - d_o)$ for each of d_o equal to 10, 11, and 12 cm: - Fig. 3.14. The "best straight line" was given by d_o = 11 cm.: the proximity of this displacement level to the corresponding centre of pressure c, equal to 11.1 cm., was noted with interest, and the proposition made that d_o should equal c (see 3.3(f)).

This value of d_o, i.e. 11.1 cm., was confirmed objectively, as follows:- The force f on a single crop element was known, by direct measurement; so that the shearing stress τ in the fully developed part (z less than 19 cm.) of the boundary layer above the crop could be determined: with n equal to unity, τ was numerically equal to f. Thus Eq. (1.2) could be written (with f in units of dyne cm.$^{-2}$) in the form

TABLE 3.10

d_o cm.	10.0	11.0	11.1	12.0
Z cm.		$\ell n(z - d_o)$		
25	2.707	2.636	2.629	2.565
24	2.636	2.565	2.557	2.485
23	2.565	2.485	2.476	2.398
22	2.485	2.398	2.390	2.300
21	2.398	2.300	2.292	2.196
20	2.300	2.196	2.186	2.080
19	2.196	2.080	2.065	1.946
18	2.080	1.946	1.930	1.791
17	1.946	1.791	1.774	1.608
16	1.791	1.608	1.589	1.386
15	1.608	1.386	1.360	1.098
14.3	1.457	1.193	1.163	0.832
14	1.386	1.098	1.064	0.693

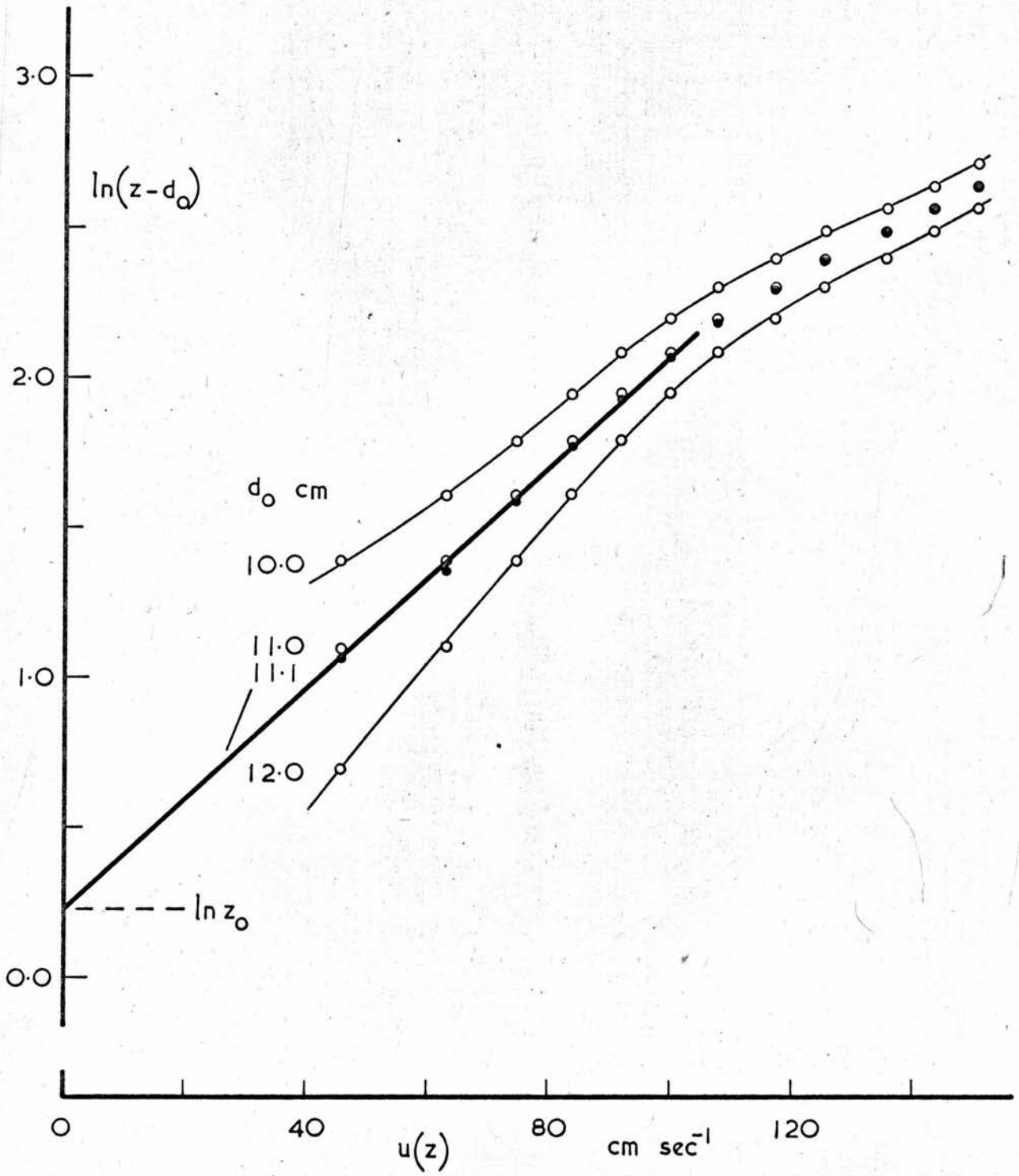

FIGURE 3.14 ($\ell n(z - d_o)$ versus $u(z)$: x = 160.5 cm., b = 11.7 cm., $z \geqslant h$; from Table 3.3. ($\ell n(z - d_o)$ from Table 3.10).

$$u_* = (f/\rho)^{\frac{1}{2}} \qquad (3.6)$$

According to Eq. (1.13), the gradient G of the "best straight line" in Fig. 3.14 should be given by

$$G = \frac{\partial u}{\partial(\ell n(z - d_o))} = \frac{u_*}{k} \qquad (3.7)$$

Using the appropriate measured value of f , namely 0.59 dyne ($cm.^{-2}$), and the accepted value 0.40 for k, the gradient G was found to be 55 $cm.\ sec.^{-1}$, close to the value 54 $cm.\ sec.^{-1}$ measured for the gradient of the line ruled through the points on Fig. 3.14 corresponding to d_o = 11.1 cm. (Values of $\ell n(z - d_o)$ for appropriate z and d_o are given in Table 3.10).

3.3(b) A value for z_o

Accepting that d_o = 11.1 cm., Fig. 3.14 shows that (when u_* = 22 $cm.\ sec.^{-1}$) the roughness length z_o of the crop is close to 1.3 cm. This can be compared with the value obtained from the empirical relation,

$$\log z_o = \log h - 0.88 \qquad (3.8)$$

due to Tanner and Pelton (1960), with h = 14.3 cm.: namely z_o = 1.9 cm. Eq. (3.8) is a useful correlation between measured values of z_o and h for various vegetated surfaces.

However, for tall crops, it is likely that z_o correlates more strongly with $(h - d_o)$ than with h itself. The length $(h - d_o)$ is a function of the mean spacing of the crop elements and must be less for a densely planted crop than for a sparsely planted crop of the same height. The denser crop must likewise present a smoother aspect to a given airflow, and have the smaller value of z_o. The empirical relation

$$z_o = k(h - d_o) \qquad (3.9)$$

is proposed, where k is von Karman's constant: this relation defines z_o as the Prandtl mixing length at $z = h$, the "surface" of the crop. For this artificial crop, $h = 14.3$ cm. and $d_o = 11.1$ cm., from which Eq. (3.9) gives $z_o = 1.28$ cm., close to the measured value (1.3 cm.). For the artificial grass used by Chamberlain (1966), $h = 7.5$ cm. and $d_o = 5.0$ cm., from which Eq. (3.9) gives $z_o = 1.0$ cm., equal to the measured value.

3.3(c) Measured wind profiles at several values of u_*

To investigate the dependence of z_o on wind speed (2.1(a), (v)), profiles were measured at $x = 160.5$ cm. for $T = 125$, 150, 175, and 225 units with $b = 11.7$ cm., and for $T = 150$ units with $b = 12.9$ cm. These profiles are recorded in Table 3.11, together with the appropriate profiles from Tables 3.3 and 3.4 ($T = 200$ units). The corresponding values of c and M_p (calculated as in

3.2(a) are included in Table 3.11, along with each measured moment M and the ratio M_p/M.

Both c and M_p/M were expected to be almost independent of wind speed, and equal to their respective "equilibrium" values at T = 200 units; namely 11.1 cm. and 1.13. However, the relatively low values of c and high values of M_p/M found at low wind speeds (Table 3.11) can be explained by a progressive over-estimation of the wind speed u as u decreases below a threshold value of about 7 cm. sec.$^{-1}$. (This is plausible owing to the tentative nature, at these low wind speeds, of the "horizontal" calibration of the anemometer: see 2.3(b)).

The centre of pressure c was assumed to be independent of wind speed, and equal to 11.1 cm. This value was used, together with the (measured) moments M, to calculate values for the force f. The friction velocity u_* (in Table 3.12) was then calculated, for each profile, using Eq. (3.6).†

3.3(d) Measured change in z_o with u_*

Although the roughness Reynolds' number (Eq. (1.7)) of the flow over the crop was close to 200, for $u_* = 22$ cm. sec.$^{-1}$, it can be shown (as for vegetation in 1.1(b)) that the critical value of R_o for the crop (i.e. the limit of "fully rough" flow regime over the crop) is around 1000. Thus, within the wind speed range covered by the experiment,

† See Appendix

z_o can be expected to be a decreasing function of u_*. (Note: the equivalent sand roughness of the crop is an unrealistic 39 cm.)

Table 3.12 gives the value of the ratio $u(z)/u_*$ at several values of z for each profile in Table 3.11. Fig. 3.15 shows that $u(z)/u_*$ increases with u_* at each chosen value of z, provided that $u(z)$ itself is above the threshold value of 7 cm. sec.$^{-1}$ (3.3(c)). Within the crop canopy, increase in the ratio $u(z)/u_*$ with wind speed is a manifestation of the decrease with wind speed of the drag coefficient $C_d(u)$ of each individual crop element (Fig. 2.1); whereas above the crop it is a measure of the decrease with wind speed of the corresponding drag coefficient of the surface as a whole, namely $C_D(z)$ (see Eq. (1.6)). The roughness length z_o is related to $u(z)/u_*$ by Eq. (1.13), so that this measured increase in $u(z)/u_*$ could indicate a decrease in either z_o or d_o with wind speed. However, by plotting each wind speed profile in Table 3.11 against $\ell n(z - 11.1 \text{ cm.})$, it can be shown that the constant value $d_o = 11.1$ cm. is equally consistent with each set of wind speed measurements; i.e. no trend in d_o with u_* could be detected experimentally. On this evidence, d_o was assumed to be independent of wind speed and the results for $u(z)/u_*$ analysed accordingly, as follows.

For each value of z, $\geqslant h$, the ratio $u(z)/u_*$ was regressed against u_* to determine a gradient m_1 cm. sec.$^{-1}$,

TABLE 3.11 — x = 160.5 or 164 cm.

T units	125	150	175	200	225	150	200
b cm.			11.7			12.9	
z cm.			u cm. sec.$^{-1}$				
25	-	99	-	~~162~~ 150	162	121	177
23	-	86.3	110	~~152~~ 135	152	113	166
21	-	76.9	97	117	137	95	151
20	54.3	73.3	89.4	107	127	88.5	139
19	47.6	65.5	83.0	100	117	82.8	130
18	44.5	61.6	77.4	91.6	108	78.5	118
17	39.2	56.0	70.8	83.6	98	71.6	102
16	35.5	47.6	62.6	74.4	86.3	62.9	95
15	29.7	41.7	51.6	63.0	74.4	52.0	78.5
14	21.9	31.0	39.7	45.5	57.6	38.5	61.0
13	14.4	21.7	27.9	33.6	41.7	27.6	44.1
12	11.5	18.0	22.1	26.3	33.3	19.5	34.8
11	8.3	13.6	16.8	19.7	25.4	15.8	26.0
10	6.8	11.1	13.5	16.1	19.2	13.9	22.9
9	-	9.1	10.0	13.8	16.0	11.3	18.6
8	5.4	-	-	11.4	14.6	9.0	15.1
7	-	6.8	8.2	9.5	12.0	7.0	12.3
6	4.8	-	-	7.8	10.2	6.6	-
5	-	5.5	6.2	6.8	8.8	6.4	9.6
4	4.3	-	-	6.1	8.2	5.8	-
3	-	4.6	4.8	5.2	6.7	5.5	7.1
2	3.9	-	-	4.8	6.2	-	-
1	3.6	3.8	4.0	4.2	5.6	4.7	7.0
M dyne cm.	24	44	71	94	137	67	145
M_p dyne cm.	35	61	83	107	154	83	167
c cm.	10.5	10.75	11.0	11.1	11.1	10.9	11.1
M_p/M	1.46	1.38	1.17	1.13	1.12	1.24	1.15

TABLE 3.12 †

u_* cm/sec.	11.0	15.0	18.5	19.1	22.0	26.5	27.3
z cm.				u/u_*			
19	4.30	4.45	4.53	4.40	4.53	4.42	4.73
17	3.66	3.69	3.87	3.71	3.79	3.71	3.92
16	3.21	3.25	3.40	3.27	3.35	3.28	3.54
15	2.67	2.72	2.81	2.75	2.81	2.83	2.93
14.3	2.13	2.19	2.33	2.25	2.29	2.39	2.45
13.25	1.47	1.60	1.62	1.60	1.65	1.76	1.76
11.1	0.79	0.93	0.90	0.90	0.94	1.00	1.00
8	0.50	0.53	0.51	0.50	0.51	0.51	0.55
4	0.36	0.33	0.31	0.28	0.27	0.29	0.30
b cm.	11.7	11.7	12.9	11.7	11.7	11.7	12.9
T units	125	150	150	175	200	225	200

† See Appendix

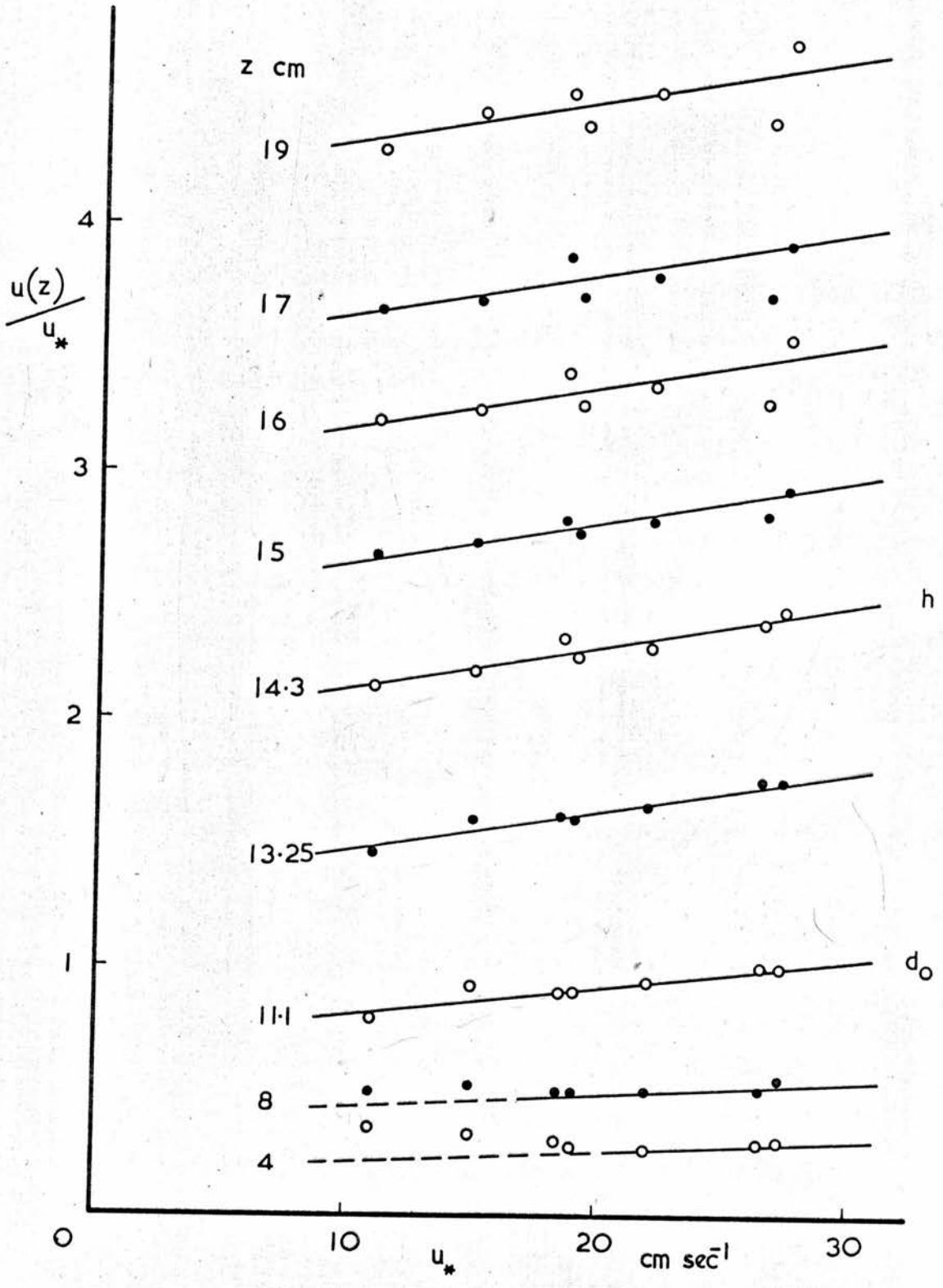

FIGURE † 3.15 $u(z)/u_*$ versus u_* for several chosen values of z; from Table 3.12.

† See Appendix

TABLE 3.13

z cm.	$\left(\frac{\overline{u(z)}}{u_*}\right)$	m_1 cm. sec.$^{-1}$	m_2 cm. sec.$^{-1}$	$\frac{m_1 + m_2}{2}$ cm. sec.$^{-1}$	r
19	4.486	0.0159	0.0570	(0.0365)	(0.53)
17	3.769	0.0099	0.0283	0.0191	0.59
16	3.334	0.0129	0.0283	0.0206	0.67
15	2.791	0.0131	0.0156	0.0144	0.92
14.3	2.290	0.0175	0.0211	0.0193	0.91

$$\bar{u}_* = 20.2 \text{ cm. sec.}^{-1}$$

$$\bar{m} = \frac{\Sigma r^2 \left(\frac{m_1 + m_2}{2}\right)}{\Sigma r^2} = 0.017 \text{ cm. sec.}^{-1}$$

TABLE 3.14†

u_* cm. sec.$^{-1}$	10	20	30
$\frac{u(h)}{u_*}$	2.11	2.28	2.45
z_o cm.	1.37	1.28	1.20
$C_D(h)$	0.224	0.193	0.167
$\overline{C}_d = C_d(u(d_o))$	2.15	1.44	1.05

† See Appendix

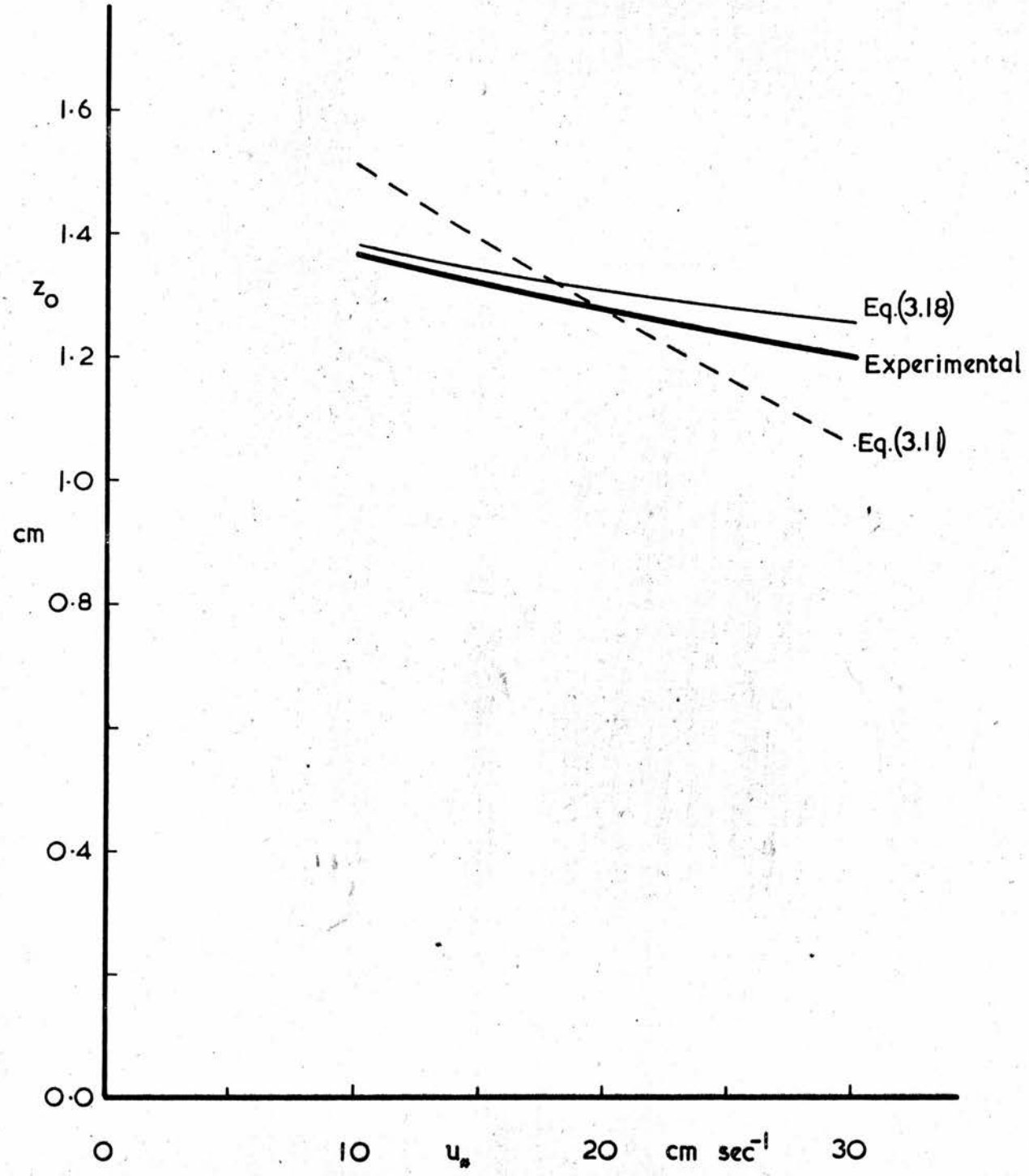

FIGURE 3.16† Measured and predicted behaviour of z_o over a range in u_*.

† See Appendix

and the friction velocity u_* was regressed against $u(z)/u_*$ to obtain a gradient m_2 cm. sec.$^{-1}$. Table 3.13 gives (the mean value) $\overline{u_*}$ and the value for each z of (the mean) $(\overline{u(z)/u_*})$, m_1, m_2, $(m_1+m_2)/2$, and r, the last being the correlation coefficient between $u(z)/u_*$ and u_*. The line of gradient $(m_1+m_2)/2$, passing through the point $(\overline{u_*}, (\overline{u(z)/u_*}))$, would be the best line through the experimental points at each z. However, the true gradient of each line must be given by

$$\left(\frac{\partial(u(z)/u_*)}{\partial u_*}\right)_z = -\frac{1}{k}\frac{\partial(\ell n\, z_o)}{\partial u_*} \qquad (3.10)$$

which is independent of z; so that each measured gradient $((m_1 + m_2)/2)$ can be treated as an independent determination of the true gradient. The mean measured gradient $\bar{m}$ was therefore defined, equal to the mean of $(m_1+m_2)/2$ weighted by the square of the correlation coefficient r, and calculated to be 0.017 cm. sec.$^{-1}$. (Results for z = 19 cm. were not included in this calculation.) A line of gradient $\bar{m}$ is drawn appropriately through each set of experimental points on Fig. 3.15 (for which $z \geqslant h$).

Table 3.14 records the values of $u(h)/u_*$, at u_* = 10, 20 and 30 cm. sec.$^{-1}$, obtained from Fig. 3.15, together with the corresponding values of z_o calculated from Eq. (1.13) with d_o = 11.1 cm. and k = 0.40: also included are $C_D(h)$ equal to $(u_*/u(h))^2$, and $\bar{C}_d$, a representative mean value of $C_d(u)$ within the canopy, equated conveniently (see 3.4(b)) to $C_d(u(d_o))$ and found

from Fig. 2.1. Fig. 3.16 shows the measured change in z_o with u_* to be a much smaller change than that predicted by the plausible expression

$$C_D(h) \propto \bar{C}_d \qquad (3.11)$$ †

However, writing Eq. (1.29) in the form

$$\frac{1}{C_D(h)} = u(h)\,\bar{R}_D + \frac{u(h)}{\bar{u}\,\bar{C}_d\,S_d} \qquad (3.12)$$ †

shows that Eq. (3.11) can be true only when $\bar{R}_D$ is negligible in comparison with $\bar{r}_d/S_d$ or $u(h) \propto \bar{u}$. † Thus, for this artificial crop, the canopy resistance $\bar{R}_D$ must compare in magnitude with $\bar{r}_d/S_d$, the resistance of the elements themselves (see 1.3(d); also 3.4(b), (c), (d) and (e) and 5.3(b)).

Thus, the roughness length of the artificial crop decreases only slightly with increase in wind speed, despite a relatively large simultaneous decrease in the drag coefficient of the indidivual crop elements. It is suggested, for crops in general, that z_o can be taken to be independent of wind speed unless C_d decreases markedly with wind speed either absolutely (i.e. at constant ϕ) or due to streamlining effects. †

† See Appendix

3.3(e) Confirmation of the value of von Karman's constant

Sheppard (1947) has shown that the laboratory value of k, equal to 0.40, can be used to calculate the wind drag on (a relatively smooth part of) the earth's surface; while later workers, such as Rider (1954), have demonstrated that this value of k is consistent with the eddy transport properties of the turbulent boundary layer over a natural rough surface. The results of this present experiment were nevertheless analysed to determine the value of k in the boundary layer above the artificial crop.

The mean normalised wind speed recorded in Table 3.13, namely $(u(z)/u_*)$, was plotted against $\ell n(z - d_o)$ on Fig. 3.17 for d_o = 10, 11.1, and 12 cm. This Figure shows d_o = 11.1 cm. to be consistent with the mean of all the measured wind speed profiles. The gradient of the straight line passing through the points for d_o = 11.1 cm. gives k = 0.41 (see Eq. (3.7)). The average gradients of the curves for d_o = 12 cm. give k = 0.34 and k = 0.51, respectively. However, accepting that Fig. 3.17 defines d_o as 11.1 cm. within limits of $\pm$ 0.3 cm., the experimental result for k is (0.41 ± 0.03).

Determination of k close to the accepted neutral stability value, 0.40, shows that there can have been little or no vertical temperature gradient, on the average, across the boundary layer. In practice, direct (thermocouple) measurement between z = 14 cm. and z = 18 cm. showed that such a temperature gradient was always negligible.

3.3(f) The coincidence between d_o and c.

It has been found, for this particular (artificial) crop, that the zero plane displacement d_o is given closely by the calculated value of c, the centre of pressure, or level of action of the wind drag, on an individual crop element.

In the limits of zero and maximum density of spacing of crop elements, both d_o and c must tend to zero and h respectively. In terms of Eq. (1.13), the plane $z = d_o$ defines the level at which a virtual surface could be placed to duplicate the aerodynamic characteristics of the real surface. Similarly, the plane $z = c$ defines the level at which the drag on the real surface acts, or at which the drag on a coincident virtual surface would act. It is not physically unreasonable to propose that these two virtual surfaces are identical, and that the empirical relation

$$d_o = c \qquad (3.13)$$

is true in general.

Chamberlain (1966) quotes $d_o = 5.0$ cm. for an artificial grass surface, with $h = 7.5$ cm. It can be shown, from the shape of the measured wind profile within the "grass" canopy, that c is approximately 4.5 cm.

Plate and Quraishi (1965) used $d_o = h$ in an analysis of the flow above an artificial crop consisting of an array of 4 in. high spills. They find the plot of

$\ell n(z - h)$ against $u(z)$ to be linear for z above $2h$ only: i.e. $d_o = h$ is a useful approximation to the true value of d_o, provided z is large enough. However, in using Eq. (1.13) to describe the flow between $z = h$ and $z = 2h$ a closer approximation (than h) to d_o is required. It can be shown from the data of Plate and Quraishi that c (for their crop) is close to $0.7h$, and that the subsequent plot of $\ell n(z - 0.7h)$ versus $u(z)$ is linear down to $z = h$.

The above examples show that the value of c can provide a useful estimate of the value of d_o, at least for artificial crops. Eq. (3.13) is applied to a field crop in Section 5.3(d).

3.4. The Resistance of the Crop to Momentum Transfer

In writing Eq. (1.29) it was assumed that the total resistance $r_D(h)$ of a crop can be separated into two (suitably defined) mean resistances $\bar{R}_D$ and $\bar{r}_d/S_d$, where $\bar{R}_D$ is a measure of the turbulent resistance of the canopy and depends on K_M within the canopy, and where $\bar{r}_d/S_d$ is a measure of the resistance of the crop elements themselves. In this Section, values of $\bar{R}_D$ and $\bar{r}_d/S_d$ are derived for the crop; values appropriate to the "equilibrium" wind speed profile shown in Fig. 3.11, for which $r_D(h)$ is equal to 0.104 sec. cm.$^{-1}$ (Eq. (1.22), with $u(h) = 50.3$ cm. sec.$^{-1}$; $u_* = 22.0$ cm. sec.$^{-1}$.)

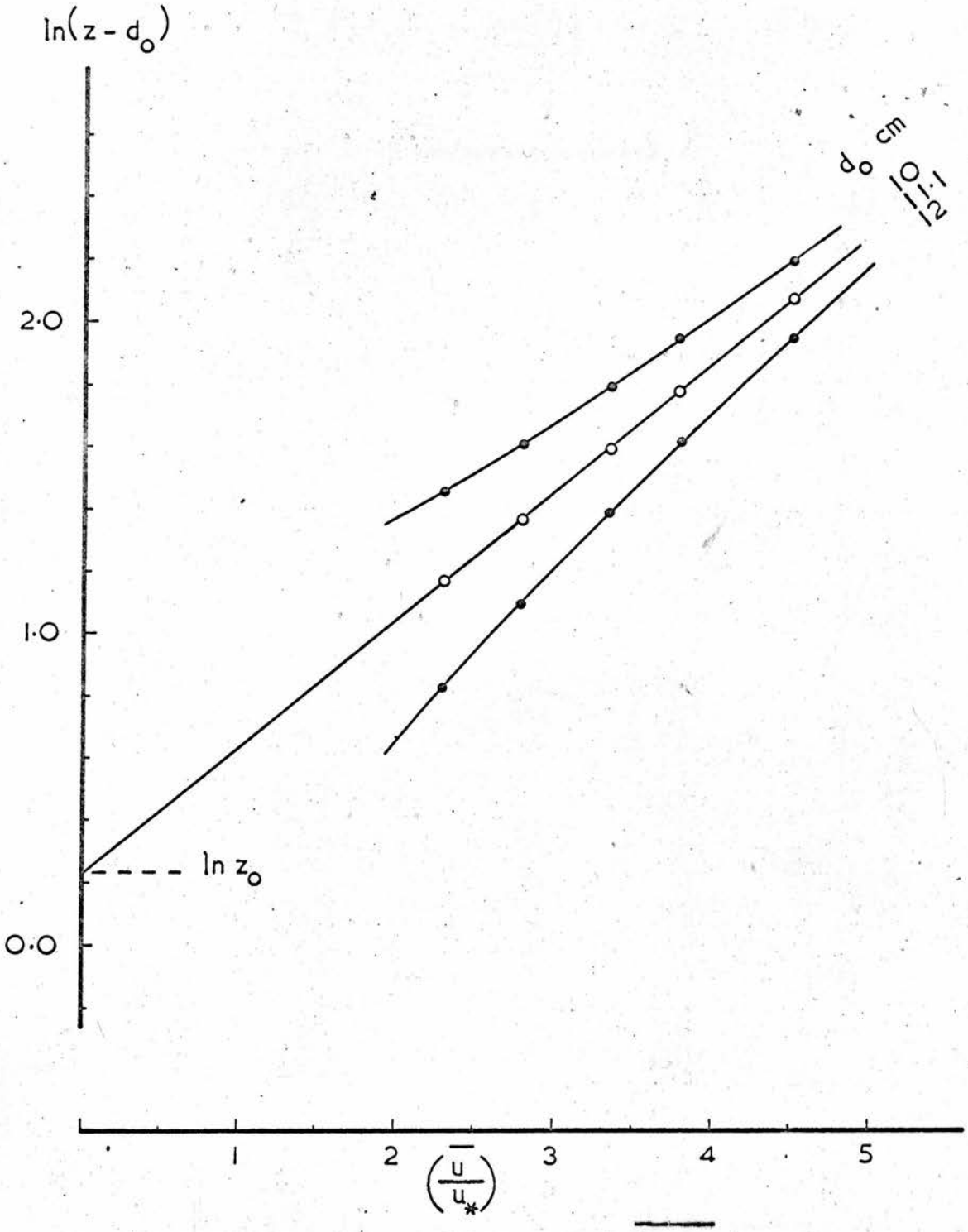

FIGURE 3.17 $\ell n(z - d_o)$ versus $(\overline{u(z)/u_*})$; from Table 3.13 ($\ell n(z - d_o)$ from Table 3.10).

TABLE 3.15

z cm.	i	$(\delta z)_i$ cm.	$u(z)$ cm. sec.$^{-1}$	f_i dyne(cm.$^{-2}$)	$\tau(z)$ dyne cm.$^{-2}$	$\frac{\partial u(z)}{\partial z}$ sec.$^{-1}$	$K_M(z)$ cm.^{2} sec.$^{-1}$	$\frac{K_M(z)}{u_*}$ cm.
14.3			50.3		0.590	17.2	28.1	1.28
14.1	1	0.4	47.0	0.065	0.555	16.5	27.6	1.25
13.9			43.7		0.525	14.0	30.7	1.40
13.7	2	0.4	41.4	0.069	0.490	12.2	33.0	1.50
13.5			38.8		0.456	11.2	33.4	1.51
13.25	3	0.5	36.3	0.071	0.417	10.0	34.1	1.55
13.0			33.8		0.385	9.0	35.0	1.59
12.5	4	1.0	29.5	0.105	0.327	7.7	34.8	1.58
12.0			26.1		0.280	6.4	35.9	1.63
11.0	5	2.0	20.5	0.120	0.208	4.7	36.3	1.65
10.0			16.6		0.160	3.6	36.5	1.66
9.0	6	2.0	13.7	0.067	0.121	2.6	38.1	1.73
8.0			11.4		0.093	2.1	36.3	1.65
7.0	7	2.0	9.5	0.041	0.070	1.7	33.7	1.53
6.0			8.0		0.052	1.2	35.5	1.61
5.0	8	2.0	6.8	0.024	0.038	1.0	31.2	1.42
4.0			5.9		0.028	0.8	28.7	1.30
2.0	9	4.0	4.7	0.028	0.013	0.8	13.3	0.60
0.0			0.0		0.000	-	-	-

-96-

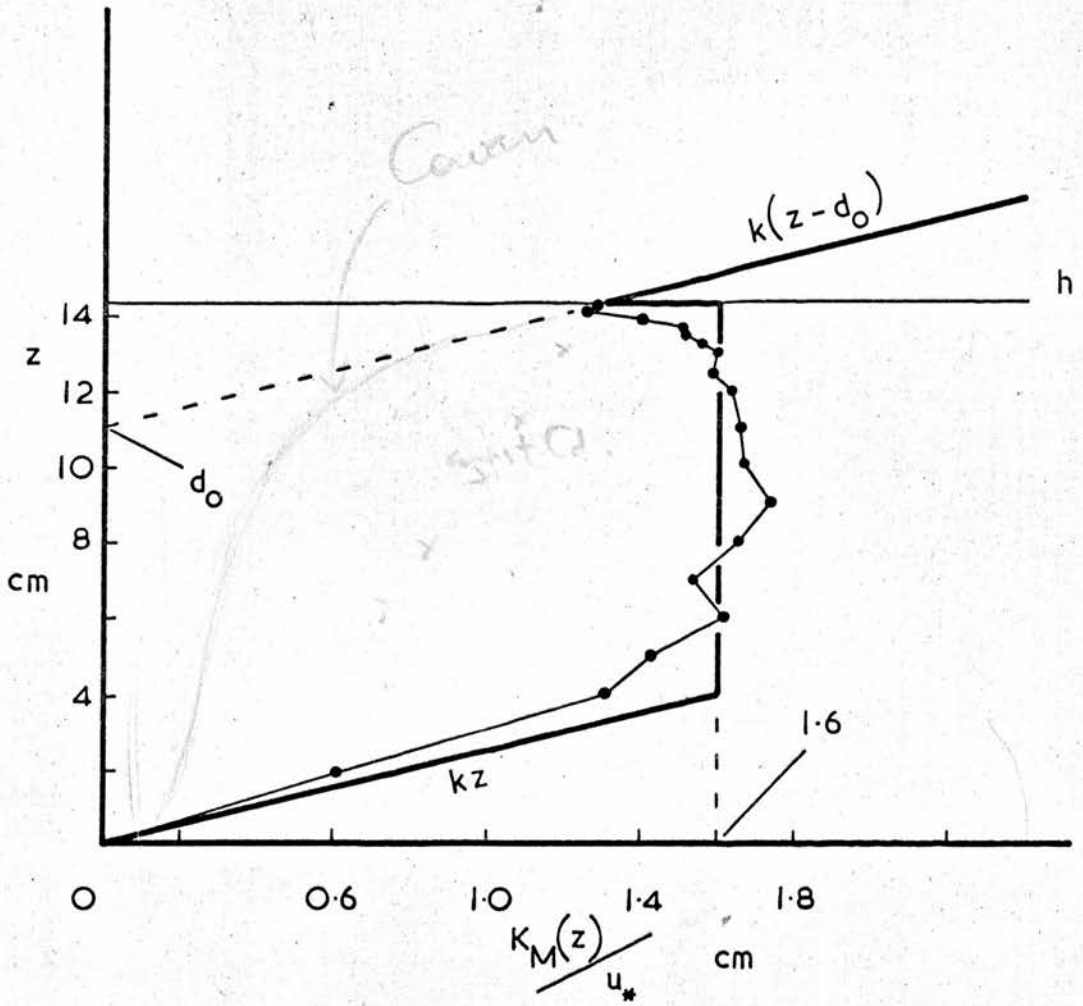

FIGURE 3.18 Measured values of $K_M(z)/u_*$ within the canopy; from Table 3.15. (Down to z = h, Eq. (1.15) applies).

3.4(a) K_M within the canopy

The calculated force $(f_i)_p$ on each incremental length $(\delta z)_i$ of element is recorded for the chosen profile in Table 3.7. The sum f_p is some 13 per cent greater than the measured force f, which is equal to τ, i.e. to $\tau(h)$. Thus, before Eq. (1.18) could be used (in finite difference form) to determine $\tau(z)$ within the canopy (or rather each τ_i equal to $\tau(z_i)$), each $(f_i)_p$ had to be reduced in such a way that the sum f_p was equal to τ. In accordance with Section 3.2(b), each $(f_i)_p$ was reduced by 8 per cent of its original value, while $(f_1)_p$, the calculated force on the topmost section, was reduced by a further 25 per cent. These modified force increments, redefined as f_i, are included in Table 3.15, together with the resulting values of $\tau(z)$: each $u(z)$ was obtained from Fig. 3.11, from which Figure the corresponding values of $\partial u(z)/\partial z$ were derived. These values of $\tau(z)$ and $\partial u(z)/\partial z$ were used in Eq. (1.19), with $\rho = 1.22 \times 10^{-3}$ gm. cm.$^{-3}$, to determine the values of $K_M(z)$ recorded in Table 3.15.

Fig. 3.18 shows the measured value of $K_M(z)/u_*$ to be approximately constant between h and about h/4, and to be about 25 per cent greater, over the same range, than the corresponding value of $K_M(h)/u_*$ derived from Eq. (1.15). Below h/4, $K_M(z)/u_*$ is conveniently (but in no way rigorously) represented by the function kz.

The relatively high value found for K_M within the

canopy is a manifestation of the conductivity introduced into the mean flow by the turbulent mixing in the wake of each crop element.

3.4(b) Determination from K_M of the canopy resistance $\bar{R}_D$

In Eq. (1.31), R_D is written for convenience as the integral between $z = h$ and some mean level $\bar{z}_D$ of the specific turbulent resistance $1/K_M(z)$.

However, in Table 3.16, each $(R_D)_i$ is the integral of $1/K_M(z)$ (deduced from Fig. 3.18) between h and the level z_i; and $\bar{R}_D$ is equated to the mean resistance derived by weighting each $(R_D)_i$ with the corresponding value of f_i (from Table 3.15); i.e. $\bar{R}_D$ = 0.094 sec. $cm.^{-1}$, a substantial fraction of $r_D(h)$. (Note: this is the value of $\bar{R}_D$ given by Eq. (1.31) if $\bar{z}_D$ has the value 11.0 cm., which is close to d_o.)

This method of obtaining $\bar{R}_D$, although providing a useful estimate of its size in relation to $r_D(h)$, is sensitive to $K_M(z)$ at all levels in the canopy, including those lowest levels (below h/4) where $K_M(z)$ itself is most difficult to measure. However, $\bar{R}_D$ can be found, without recourse to measured values of K_M, by the following analytical method.

3.4(c) Indirect determination of $\bar{R}_D$.

Consider the total resistance of the crop $r_D(h)$ composed partly of the canopy resistance $\bar{R}_D$: if, hypothetically, $\bar{R}_D$ were zero, but u_* remained unchanged, $r_D(h)$ would assume a minimum value $(r_D(h))_m$ such that

$$r_D(h) - (r_D(h))_m = \bar{R}_D = \frac{u(h) - (u(h))_m}{u_*^2} \quad (3.14)$$

and a knowledge of $(u(h))_m$, the corresponding minimum value of $u(h)$, would determine the original value of $\bar{R}_D$.

The hypothesis $\bar{R}_D = 0$ requires (via Eqs. (1.19) and (1.31)) that $\partial u(z)/\partial z = 0$ for $0 < z \leqslant h$, so that over the same range of z, $u(z)$ must equal the constant value $(u(h))_m$. This uniform wind speed, re-written simply as u_m, can be determined by writing Eq. (1.17) in the form

$$f = \rho u_m^2 . A . C_d(u_m) . h \quad (3.15)$$

which, in combination with Eq. (3.6) and substitution of S_d for the product Ah, leads to the relationship

$$u_m^2 C_d(u_m) = \frac{u_*^2}{S_d} \quad (3.16)$$

With $u_* = 22.0$ cm. sec.$^{-1}$ and $S_d = 1.43$, Eq. (3.16) gives $u_m^2 C_d(u_m)$ equal to 338 cm.^{2} sec.$^{-2}$ which, from Fig. 2.1, yields $u_m = 14.4$ cm. sec.$^{-1}$, in comparison

with $u(h) = 50.3$ cm. sec.$^{-1}$. The canopy resistance $\bar{R}_D$ is therefore determined from Eq. (3.14) to be 0.074 sec. cm.$^{-1}$, in comparison with a total resistance $r_D(h)$ of 0.104 sec. cm.$^{-1}$.

3.4(d) Calculation of $\bar{r}_d/S_d$

Table 3.17 includes each u_i and f_i from Table 3.15, and records the corresponding values of $r_d(u_i)$ deduced from Fig. 2.1. The resistance $\bar{r}_d$ is equated to the mean resistance derived by weighting each $r_d(u_i)$ with the corresponding value of f_i; so that $\bar{r}_d = 0.036(6)$ sec. cm.$^{-1}$ (Note: this is close to the value of $\bar{r}_d$ given by $r_d(\bar{u})$, where $\bar{u} = u(\bar{z}_D)$, if $\bar{z}_D = d_o$; see 1.3(d), and also $\bar{C}_d$ in 3.3(d)).

The part of $r_D(h)$ contributed by the resistance of the crop elements themselves is $\bar{r}_d/S_d$, where S_d is the total area of element per unit area of horizontal surface - to which latter area all $r(z)$, including $r_D(h)$, refer. As $S_d = 1.43$, ($h = 14.3$ cm., $d = 1$ mm, $n = 1$), the resistance $\bar{r}_d/S_d$ is equal to 0.026 sec. cm.$^{-1}$. This agrees well with the result which can be deduced from the preceding analytical determination of $\bar{R}_D$, namely $\bar{r}_d/S_d = u_m/u_*^2 = 0.030$ sec. cm.$^{-1}$.

TABLE 3.16

i	z_i cm.	$(R_D)_i = R_D(h \leftrightarrow z_i)$ sec. cm.$^{-1}$	f_i dyne
1	14.1	0.006	0.065
2	13.7	0.017	0.069
3	13.25	0.030	0.071
4	12.5	0.051	0.105
5	11.0	0.094	0.120
6	9.0	0.150	0.067
7	7.0	0.207	0.041
8	5.0	0.264	0.024
9	2.0	0.368	0.028

$$\bar{R}_D = \left(\sum_i f_i (R_D)_i \right) / f = 0.094 \text{ sec. cm.}^{-1}$$

TABLE 3.17

i	u_i cm. sec.$^{-1}$	f_i dyne	$r_d(u_i)$ sec. cm.$^{-1}$
1	47.0	0.065	0.0243
2	41.4	0.069	0.0261
3	36.3	0.071	0.0285
4	29.5	0.105	0.0314
5	20.5	0.120	0.0363
6	13.7	0.067	0.0442
7	9.5	0.041	0.052
8	6.8	0.024	0.06
9	4.7	0.028	0.07

$$\bar{r}_d = \frac{\sum_i f_i \, r_d(u_i)}{f} = 0.0366 \text{ sec. cm.}^{-1},$$

so that $\bar{r}_d / s_d = 0.026$ sec. cm.$^{-1}$.

TABLE 3.18

u_* cm. sec.$^{-1}$	10	20	30
$u(d_o)$ cm. sec.$^{-1}$	8.4	18.6	30.6
$r_d(u(d_o))$ sec. cm.$^{-1}$	0.053	0.038	0.030
$u_* r_d(u(d_o))/S_\lambda$	0.39	0.53	0.63
$u_* \bar{R}_D$	1.70	1.70	1.70
$u(h)/u_*$	2.09	2.23	2.33
z_o cm.	1.38	1.31	1.26

3.4(e) An expression for $u(h)/u_*$, and the predicted variation in z_o with u_*

If the resistance equation (Eq. (1.29)) is multiplied throughout by u_*, it takes the non-dimensional form

$$\frac{u(h)}{u_*} = u_* \bar{R}_D + \frac{u_* \bar{r}_d}{S_d} \qquad (3.17)$$

in which the product $u_* \bar{R}_D$ can reasonably be assumed to † be independent of u_* (as indeed is the product $u_* \int_{z_1}^{z_2} dz/K_M$ above the crop). Accepting the calculated value 0.026 sec. cm.$^{-1}$ for $\bar{r}_d/S_d$ gives $\bar{R}_D = 0.078$ sec. cm.$^{-1}$; and $u_* = 22.0$ cm. sec.$^{-1}$, so that Eq. (3.17) can be written, for this artificial crop, as

$$\frac{u(h)}{u_*} = 1.70 + \frac{u_* \, r_d(u(d_o))}{S_d} \qquad (3.18) \; \dagger$$

in which $\bar{r}_d$ has been replaced, for convenience (but see 3.4(d)), by $r_d(u(d_o))$. In combination with Eq. (1.13), this last equation relates directly, for the first time, the roughness length z_o of a rough surface to the drag coefficient C_d, (equal to $(u \, r_d)^{-1}$), of individual roughness elements of the surface.

Table 3.18 records the values of $u(h)/u_*$ predicted by Eq. (3.18) for $u_* = 10$, 20 and 30 cm. sec.$^{-1}$. Each $u(d_o)$ was obtained from Fig. 3.15 and the corresponding values of r_d deduced from Fig. 2.1. Fig. 3.16 demonstrates that Eq. (3.18) provides a good measure of the

† See Appendix

experimentally determined rate of decrease in z_o with u_*.

In general, therefore, the contribution made to the total resistance of a crop by the turbulent resistance of its canopy leads to a smaller variation in roughness length of the crop with wind speed than that suggested by a simple empirical proportionality between the drag coefficient $C_D(h)$ of the crop as a whole and the drag coefficient C_d of the individual crop elements (as Eq. (3.11)).

3.4(f) An electrical analogue to the crop as a momentum sink

Fig. 3.11 shows the crop divided into nine strata, corresponding to the nine $(\delta z)_i$ chosen to facilitate calculations in finite difference form, such as those in Table 3.7. Fig. 3.19 demonstrates a corresponding electrical analogue to the crop, in which the nine momentum sinks are at earth potential (i.e. u = 0). The sinks are connected in parallel, each through a resistance $(r_d)_i/(\delta S)_i$, to appropriate points on a vertical potentiometer of specific resistance $1/K_M(z)$ sec. cm.$^{-1}$ per cm. The resistance between any two adjacent levels is given by

$$R_{D\ i\ i+1} = \int_{z_i}^{z_i+1} dz/K_M(z) \qquad (3.19)$$

appropriate values of which were deduced from Fig. 3.18

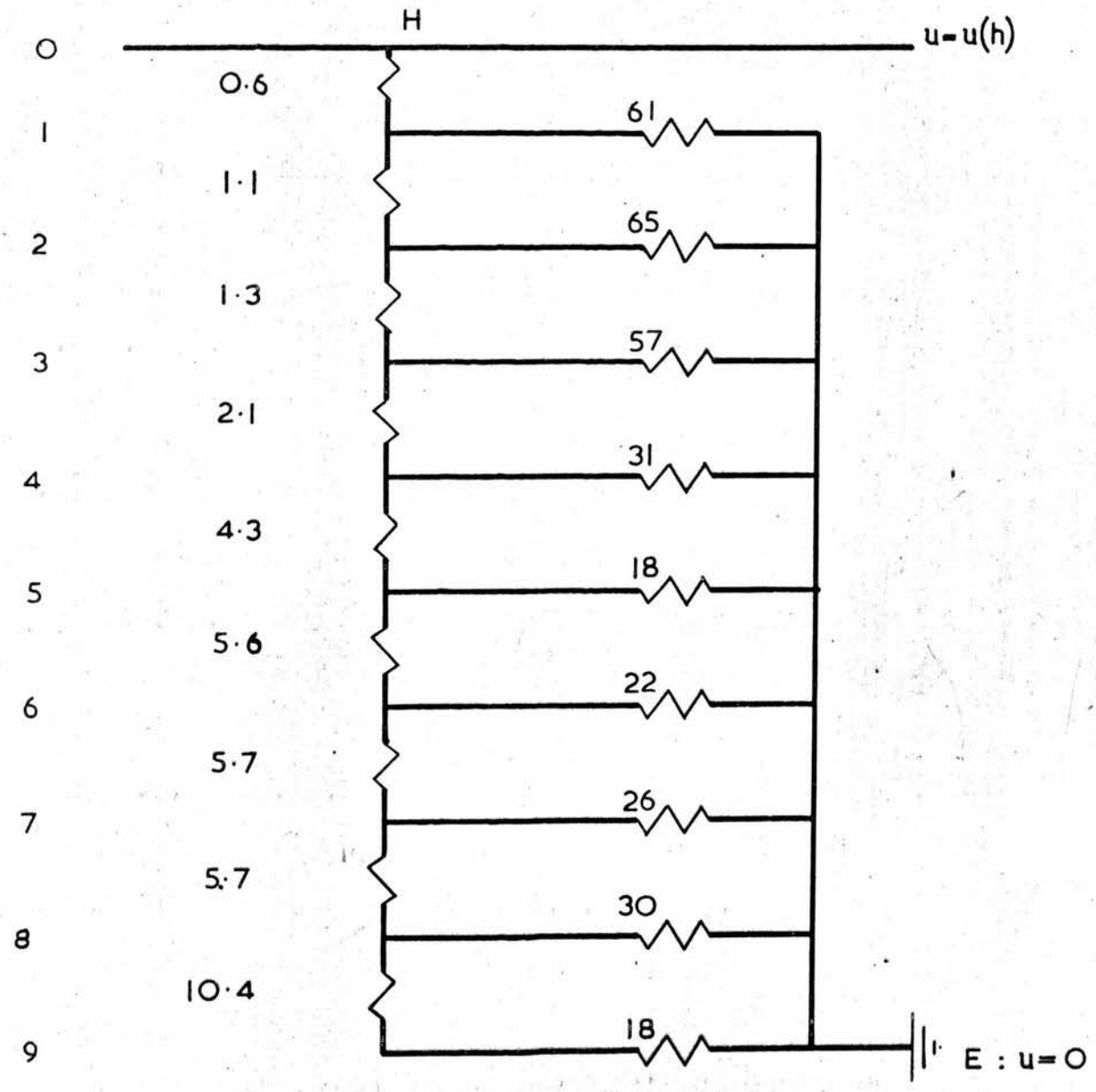

FIGURE

TABLE 3.19 Electrical analogue to the crop: potential = wind speed. See text, Section 3.4(f).

via Table 3.16. Each $(\delta S)_i$ is the area of the corresponding incremental length $(\delta z)_i$ of element per unit area of horizontal surface (to which latter area all R_D refer, by definition).

The resistance between the points H and E on the analogue corresponds to the total resistance $r_D(h)$ of the crop, and can be shown by calculation to be 0.093 sec. cm.$^{-1}$. This is close enough to the measured value of $r_D(h)$, equal to 0.104 sec. cm.$^{-1}$, to support the physical assumptions embodied in the analogue: namely, that (at least in terms of a multi-layered "model") the integral of $dz/K_M(z)$ within a region of momentum sinks does in fact define a resistance; and, that momentum can be considered to diffuse vertically downwards into a crop and then transfer horizontally to the crop elements. These conclusions, in turn, lend support to equations of the form (1.31) and (1.29).

CHAPTER 4*

THE ARTIFICIAL LEAF EXPERIMENT

4.1 Coefficients for the Transfer of Momentum, Mass and Heat between a Single Leaf and a Uniform Airflow

The effectiveness of transfer of any property between a single leaf of area a (total surface area 2a) and air flowing past with speed u can be represented by a dimensionless transfer coefficient C defined by

$$Q = C\,u\,a\,\delta\chi \qquad (4.1)$$

(similar in form to Eq. 1.20). Q is the rate of transfer of the property and $\delta\chi$ the difference in concentration of the property between the leaf surface, where its average concentration is χ_L, and the undisturbed airflow where its concentration is χ. The corresponding transfer resistance is

$$r = (u\,C)^{-1} \qquad (4.2)$$

for the transfer of momentum to the leaf, $\chi = \rho u$ and χ_L is zero. When F is the total force on the leaf, in the direction of the incident airflow,

$$C_d = \frac{1}{\rho a} \cdot \frac{F}{u^2} \qquad (4.3)$$

and is the total drag coefficient of the leaf in air of

---

* A curtailed version of this Chapter is in publication with the Royal Meteorological Society (Thom, 1968).

density ρ. If F is separated into a force F_b due to differences in normal pressure over the surface of the leaf, and a force F_f due to tangential skin friction on the surface of the leaf, then the "bluff-body" drag coefficient is defined by

$$C_b = \frac{1}{\rho a} \cdot \frac{F_b}{u^2} \qquad (4.4)$$

and the skin friction drag coefficient by

$$C_f = \frac{1}{\rho a} \cdot \frac{F_f}{u^2} \qquad (4.5)$$

When E is the rate of evaporation from the leaf of a volatile liquid whose vapour pressure in the free stream is e and at the leaf surface is e_L, equal to $(e + \delta e)$, then C is a mass transfer coefficient defined by

$$C_v = \frac{p - e_L}{\rho\, a\, \varepsilon} \cdot \frac{E}{u\, \delta e} \qquad (4.6)$$

where p is total atmospheric pressure and ε is the ratio of the molecular weight of the vapour to the effective molecular weight of air.

Finally, the coefficient of sensible heat transfer can be defined by

$$C_h = \frac{1}{\rho a\, c_p} \cdot \frac{H}{u \delta T} \qquad (4.7)$$

where H is the rate of sensible heat exchange between the air-stream at temperature T and the leaf whose surface is at a uniform temperature T_L, equal to $(T+\delta T)$.

c_p is the specific heat of air at constant pressure.

Values of C_d, C_v, and C_h measured for the leaf can in general be expected to be functions of wind speed and of ϕ, the angle between the leaf and the incident airflow. Differences in the measured values of $C(u,\phi)$ for various properties can be related to differences in molecular diffusivity or to differences in transfer process.

4.2 Experimental Technique

4.2(a) Measurement of C_d

A rigid artificial leaf was made from thin aluminium sheet. Its shape and size, Fig. 4.1, were chosen to be typical of a leaf of the bean plant Vicia faba. This was to allow direct application of the results to a bean crop (Chapter 5), but should detract little from the generality of the experimental conclusions. The angle ϕ and the standard dimension d are each defined in Fig. 4.1.

The leaf was mounted on a thin steel rod attached to the moment balance (see 2.5) and held within the Rothamsted wind-tunnel, as sketched in Fig. 4.2. The fan is driven by a constant speed electric motor, but a differential pulley system allows several fan speeds to be selected. Further variation of the wind speed in the working section was obtained by fixing various perforated

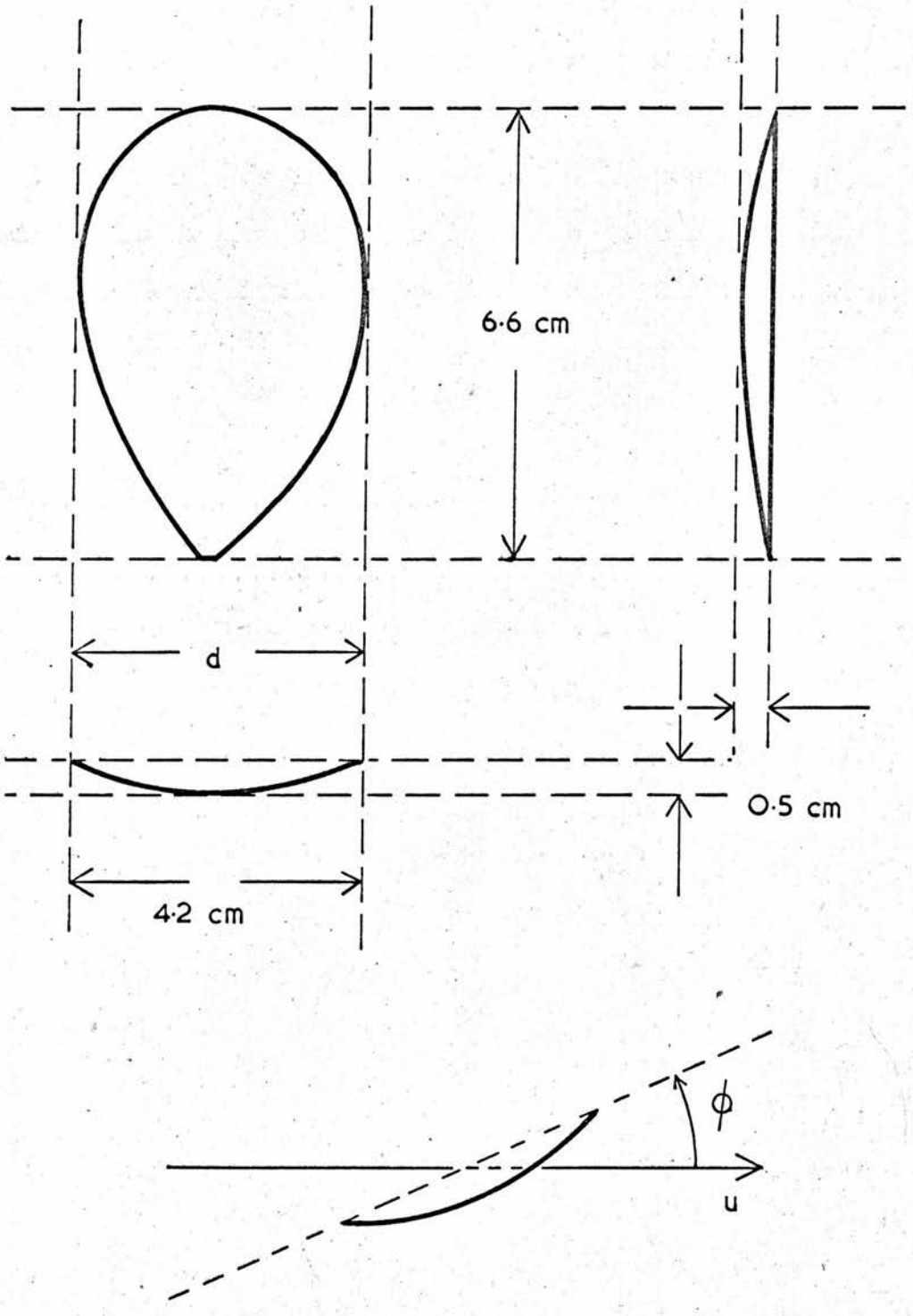

FIGURE 4.1 Dimensions of the artificial bean leaf: definition of the angle of incidence ϕ.

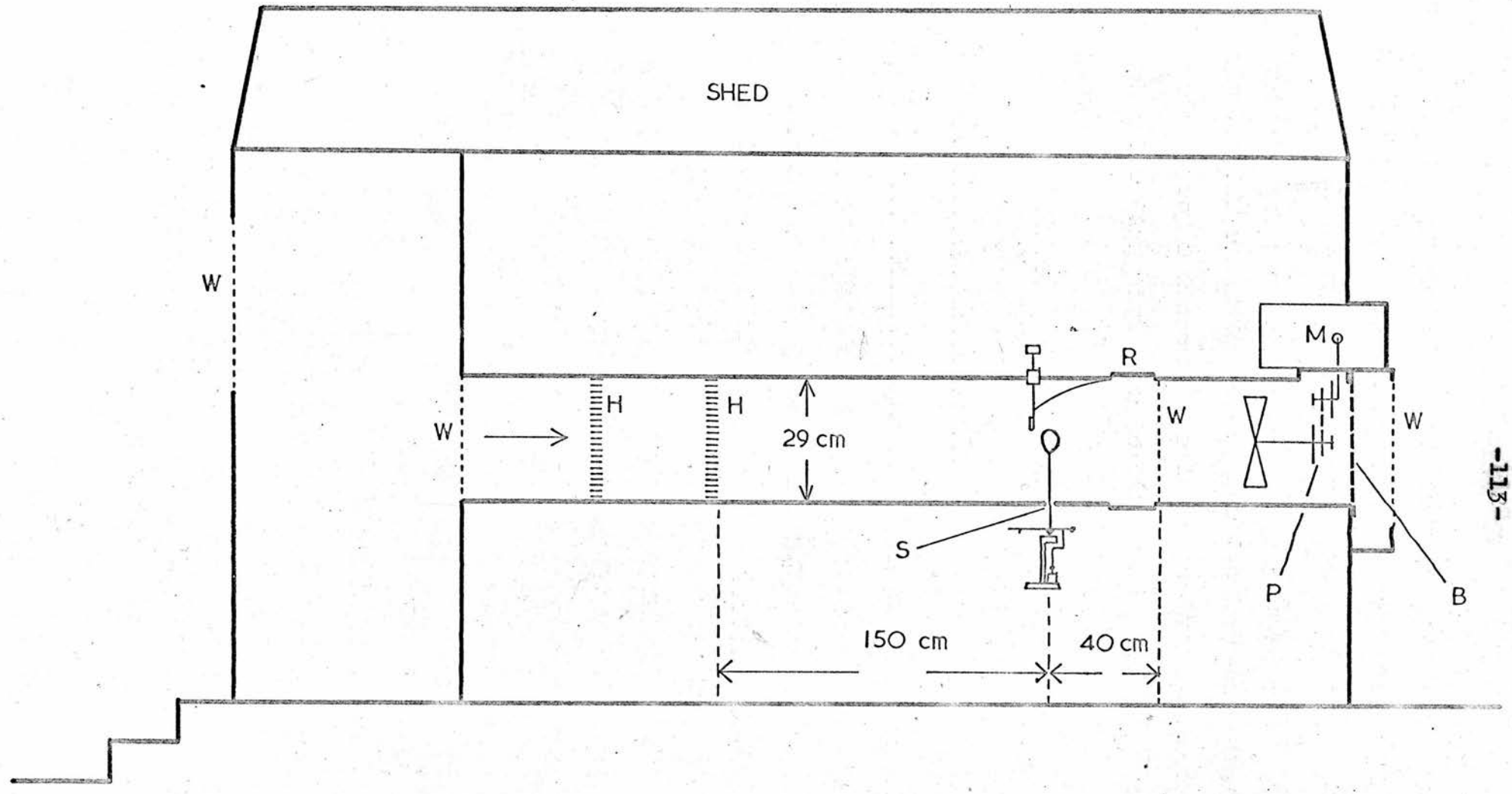

FIGURE 4.2 Sketch of Rothamsted wind-tunnel: leaf mounted for drag measurement.
B : perforated plywood sheets (interchangeable).
H : Honeycombs. M : electric motor. P : pulley system.
R : removeable section. S : access slit. W : wire mesh.

plywood sheets against the exit of the tunnel. This reduced the intake to the tunnel (at a given fan speed) without dropping farther the pressure in the working section, thus keeping to a minimum the leakage of air into the working section through the slit provided for the rod holding the leaf. The slit, centrally placed in the floor of the tunnel, was 5 mm. long and 2 mm. wide to accommodate any likely motion of the 1 mm. thick rod.

The Simmons anemometer (see 2.3) was used to determine the wind speed u, which was in the range 20 to 150 cm. sec.$^{-1}$. The total moment, m_t, on the leaf and supporting rod was measured for chosen values of u and ϕ, and the moment, m_s, on the supporting rod alone for several values of u. By plotting m_s against u, m_s was obtained as a function of u (see Fig. 4.5), so that the moment on the leaf was given by

$$m(u, \phi) = m_t(u, \phi) - m_s(u) \qquad (4.8)$$

The force, F, on the leaf was obtained by dividing the measured moment, m, by the vertical distance, L_z, between the knife-edge of the balance and the estimated point of action of F on the leaf. Values of C_d were than calculated from Eq. (4.3) using the value of ρ appropriate to air at 17°C and normal atmospheric pressure (i.e. $\rho = 1.21 \times 10^{-3}$ gm. cm.$^{-3}$).

4.2(b) Measurement of C_v

A filter paper covering was fixed securely to the leaf with Durofix adhesive. The leaf was mounted on the suspension of the balance in such a way that it had a moment arm L_x, due to gravity, about the knife-edge (see Fig. 4.3). When the filter paper had been saturated with a volatile liquid and a constant wind speed established in the tunnel, the rate of evaporation, E, from the leaf was determined by the rate at which a chosen rider weight had to be moved (outwards) along the moment arm in order to maintain the suspended system in balance: i.e. when a rider weight R gm. was moved ℓ_x cm. in T seconds then E was given, in gm. sec.$^{-1}$, by

$$E = \frac{\ell_x R}{L_x T} \qquad (4.9)$$

Use of the length L_x in Eq. (4.9) is rigorous only if the centre of gravity of the liquid on the leaf was always coincident with the centre of gravity of the leaf itself. This would be true if the filter paper held a uniform amount of liquid initially and if the subsequent forced evaporation took place at a uniform rate from all parts of the leaf's surface. It is likely that the former condition was satisfied but that non-fulfilment of the latter resulted in a small though progressive departure of the centre of gravity of the (evaporating) liquid from the centre of gravity of the leaf. However, this departure was neglected and Eq. (4.9) used without modification.

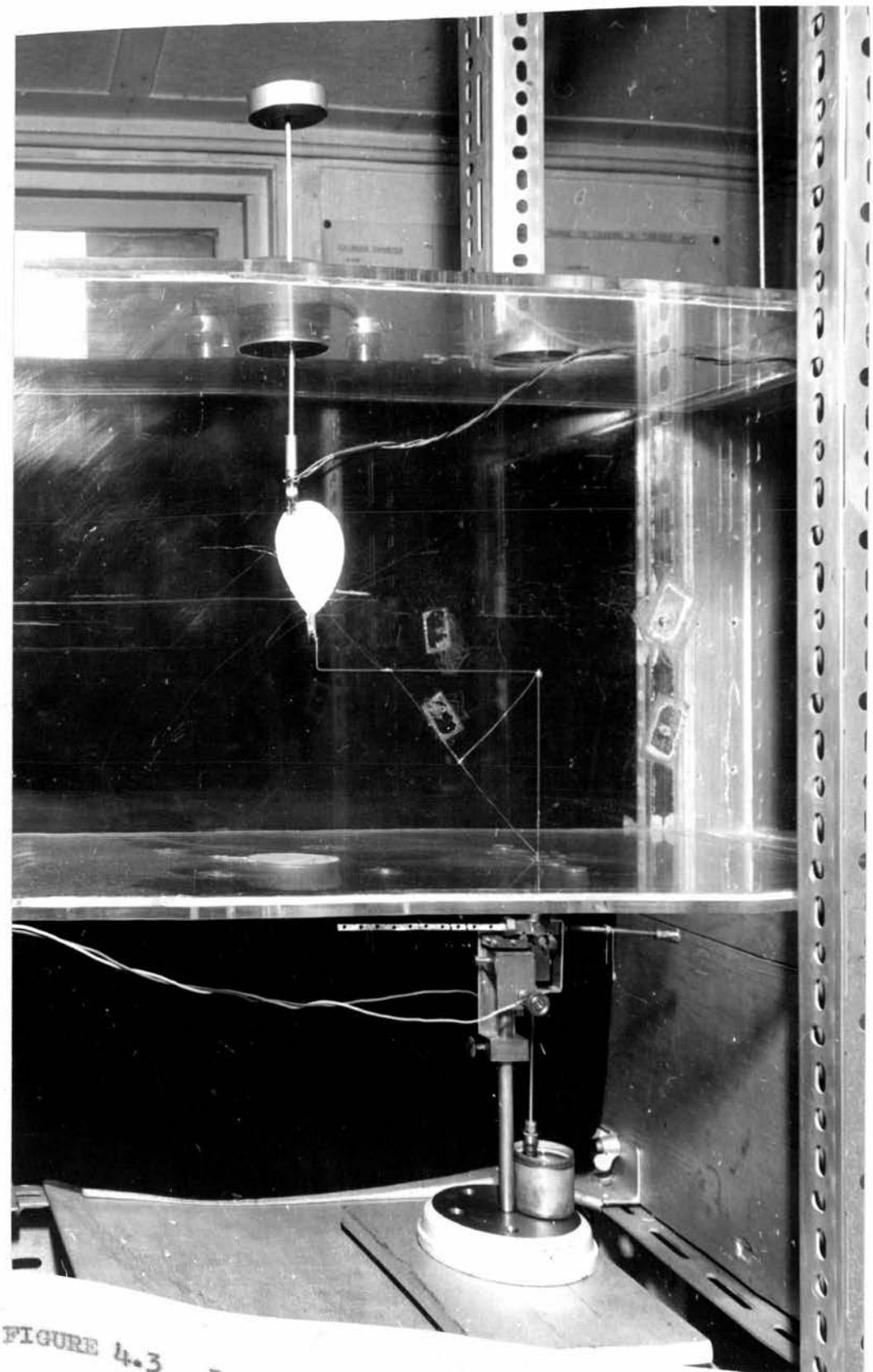

FIGURE 4.3 Leaf mounted for evaporation measurement.

In Eq. (4.6), δe represents $(e_L - e)$ where e_L is the partial pressure of the diffusing vapour at the surface of the leaf. Powell (1940) showed that evaporation from saturated filter-paper is similar to that from a free liquid surface, so that e_L can be equated to $e_s(T_L)$, the saturated vapour pressure at the temperature of the leaf. To find T_L, a copper-constantan thermocouple was made from 42 s.w.g. wire. One junction was exposed at right angles to the incident air-stream, whose temperature, T, it was assumed to acquire. The other junction was placed centrally against the metal chassis of the leaf and held securely in position by the filter-paper covering. This junction was assumed to reach a temperature representative enough of surface conditions over the whole leaf to make the thermo-couple output a measure of $(T - T_L)$, so that T_L could be calculated from an independent determination of T. The difference $(T - T_L)$ was found with a Scalamp galvanometer of known sensitivity. For the evaporation of a volatile organic liquid from the leaf, the vapour pressure e in the incident air-stream was zero and δe was equal to $e_s(T_L)$. When distilled water evaporated from the leaf, e was measured immediately before and immediately after a determination of the evaporation rate E by inserting the snout of an Assmann psychrometer into the tunnel to extract air from a region near the upwind side of the leaf. The value of e was then given by

$$e = e_s(T') - A(T - T') \qquad (4.10)$$

where T' and T were the wet and dry bulb temperatures registered by the instrument and A, equal to 0.66 mb. $^{o}C^{-1}$, is the standard Assmann psychrometer constant. The deficit δe was determined in the form

$$\delta e = A(T - T') + \Delta(T_L - T') \qquad (4.11)$$

where Δ is the slope of the saturated vapour pressure versus temperature curve for water between $T'^{o}C$ and $T^{o}C$. Values of C_v were then calculated from Eq. (4.6), with $\rho = 1.21$ gm. cm.$^{-3}$ as in 4.2(a). Appropriate mean values were assigned to the pressure difference $(p - e_L)$, namely 1000, 1010, and 1013 mb. for water vapour, bromobenzene and methyl salicylate respectively,

4.2(c) Measurement of C_h

The ratio C_h/C_v could have been derived by analysing the heat exchange of an evaporating leaf, but to determine C_h independently of C_v another similarly shaped leaf was made from two thin sheets of aluminium held together by a layer of Durofix adhesive. Within this layer was wound a length of resistance wire through which an electric current could be passed. When the leaf was mounted in the tunnel and a constant electrical power, W, dissipated within the leaf, its temperature remained above that of the incident airflow by an amount depending primarily on the speed of the airflow. To measure this

temperature excess, two thermo-couples were employed. Their hot junctions were embedded in the adhesive layer at central points on the leaf, and did not touch the heater wire. With their cold junctions at right angles to the incident airflow these thermo-couples gave closely similar values for the temperature difference $(\delta T)_i$ between the interior of the leaf and the air incident on the leaf. However, by tying back one of the thermo-couple cold junctions to the surface of the leaf at several points in turn, on either side of the leaf, it was found that δT was always less than $(\delta T)_i$. Fig. 4.4 shows measured values of $\delta T/(\delta T)_i$ for the convex and concave faces of the leaf ($\phi = 0^o$. $u = 127$ cm. sec.$^{-1}$). The smoothed isotherms drawn on the leaf demonstrate differential cooling of the leaf; heat transfer being most effective from the exposed parts of its surface. The average value of δT was deduced, from Fig. 4.4, to be

$$\delta T = 0.90\ (\delta T)_i\ (1 \pm 0.05) \qquad (4.12)$$

The power W, which was always close to 100 milli-watts (mW.), was determined from the voltage drop across the known resistance of the constantan heater wire (26.8 ohms.). The rate of convection of sensible heat from the leaf was then given by

$$H = W - R - K \qquad (4.13)$$

where R and K were the corresponding rates of heat

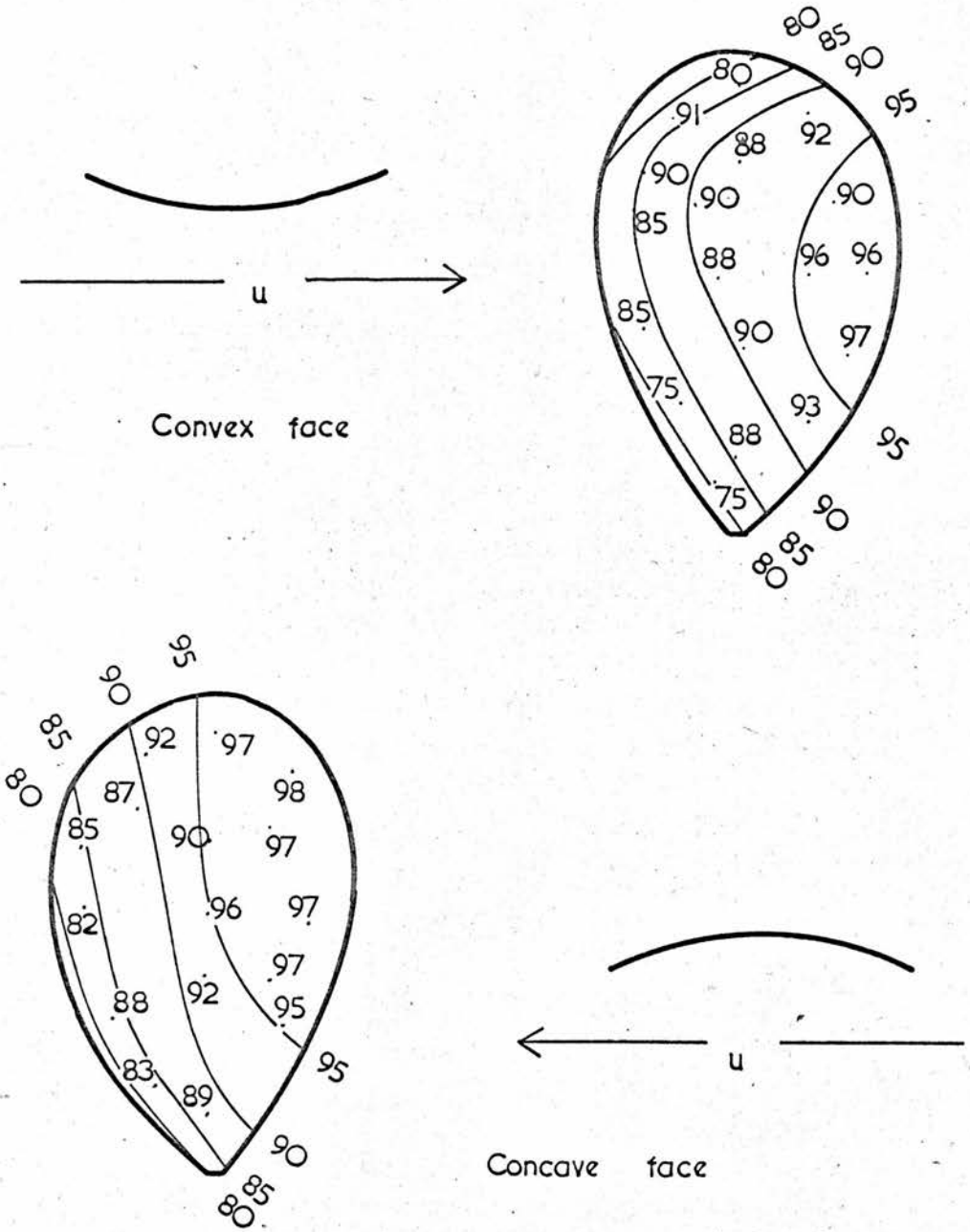

FIGURE 4.4 Distribution of temperature over the surface of the leaf ($\phi = 0^{\circ}$): the numerals represent the ratio $\partial T/(\partial T)_i$ in per cent. (The isotherms are smoothed).

loss by radiation and conduction respectively. K was separated into K_1, the rate at which heat was conducted away by the thermo-couple leads, and K_2, the rate of heat loss down the support holding the leaf in the tunnel, and an estimate of each was made, as follows.

Each thermo-couple wire entering or leaving an edge of the leaf was treated as a long circular cylinder of radius r, set in a surface $(\delta T)_w$ °C above the temperature of a uniform airflow incident normally on the cylinder. The rate of loss of heat from each wire could then be written

$$q_w = (2k)^{1/2} \pi r \left(\frac{k_a N_m}{2r}\right)^{1/2} (\delta T)_w \qquad (4.14)$$

where k and k_a are the thermal conductivities of the wire and of air, and N_m is the (diameter) Nusselt number of the wire. Appropriate values of N_m were obtained from Fig. 14.12 in Schlichting's (1955) treatise: for u = 127 cm. sec.$^{-1}$. Eq. (4.14) gave $q_w = 0.6(\delta T)_w$ mW. for one of the copper wires, and $q_w = 0.15\ (\delta T)_w$ mW. for a constantan wire. Assuming that $(\delta T)_w$ was close to 75 per cent of $(\delta T)_i$ and neglecting the loss through the constantan wires the corresponding value of K_1 was found to be 3.8 mW. ($(\delta T)_i \doteq 1.4$ °C at u = 127 cm. sec.$^{-1}$: each thermo-couple had two copper leads entering the bottom edge of the leaf, and one each of copper and constantan leaving the upper edge.) In the course of the experiment K_1 was halved by the removal of one of the thermo-couples.

To make K_2 negligibly small the leaf had been mounted on a narrow wooden dowal. However, assuming a thermal conductivity of 10^{-4} cal. cm.$^{-1}$ sec.$^{-1}$ $^{o}C^{-1}$ for the wood, K_2 was found to be of order 0.5 mW. Thus the total conducted loss, K, was about 4 per cent of the heat input W (close to 100 mW.).

The radiative loss R was more difficult to estimate, being dependent on the distribution of temperature over that (large) part of the interior surface of the wind-tunnel "visible" to the leaf. However, with the leaf mounted parallel to the sides of the tunnel (i.e. $\phi = 0$), a temperature, T_W, was determined which was the mean of the temperatures T_{W1} and T_{W2} (measured by thermo-couple) at two points, one on the inside of each wall of the tunnel immediately opposite the leaf. It was then assumed that R would be zero when T_W was equal to the temperature of the leaf surface T_L, so that (in mW.)

$$R = 18.3e \left(\frac{\overline{T}}{273}\right)^3 (T_L - T_W) \qquad (4.15)$$

where e is the effective emissivity of the leaf-tunnel system and $\overline{T}$ the mean of T_L and T_W. For chosen constant values of u and W, the difference $(T_L - T_W)$ depended partly on the size of $(T_W - T)$, and this latter difference varied slowly with changing temperature conditions in the wind-tunnel room. At a high enough value of u (such as 127 cm. sec.$^{-1}$) the difference $(T_L - T_W)$ assumed negative as well as positive values,

so that it was possible, having measured δT for each $(T_L - T_W)$, to find by graphical interpolation (see Fig. 4.12) the value of δT corresponding to $T_L = T_W$. This value of δT was then used in Eq. (4.7), together with $H = W - K$, to determine the value of C_h relevant to $u = 127$ cm. sec.$^{-1}$. The emissivity e was deduced from the rate of change of δT with $(T_L - T_W)$ (see 4.3(c)), and used to determine R, and hence C_h, at those (lower) values of wind speed for which $(T_L - T_W)$ was always positive.

4.3 Results

4.3(a) Measured values of C_d

Fig. 4.5 shows the moment, m_s, on the supporting rod alone: (a) for $L_z = 18.0$ cm., and (b) for $L_z = 21.6$ cm. Tables 4.1(a) and (b) give the values measured for the total moment, m_t, on the leaf and rod at several values of wind speed when $\phi = 0^\circ$. Also given are the corresponding values of m_s from Fig. 4.5, m from Eq. 4.8, F equal to m/L_z, and C_d from Eq. (4.3) ($a = 19.6$ cm.^{2}). Table 4.2 gives measured values of F and C_d at several values of wind speed for $\phi = +90^\circ, -90^\circ, +23^\circ$ and -23° (23° is most representative of ϕ in a crop canopy). Fig. 4.6 was drawn from the data in Tables 4.1 and 4.2 and shows the total drag coefficient, C_d, of the leaf as a function of wind speed for the five chosen values of ϕ. The coefficient C_d depends greatly on ϕ, but little on

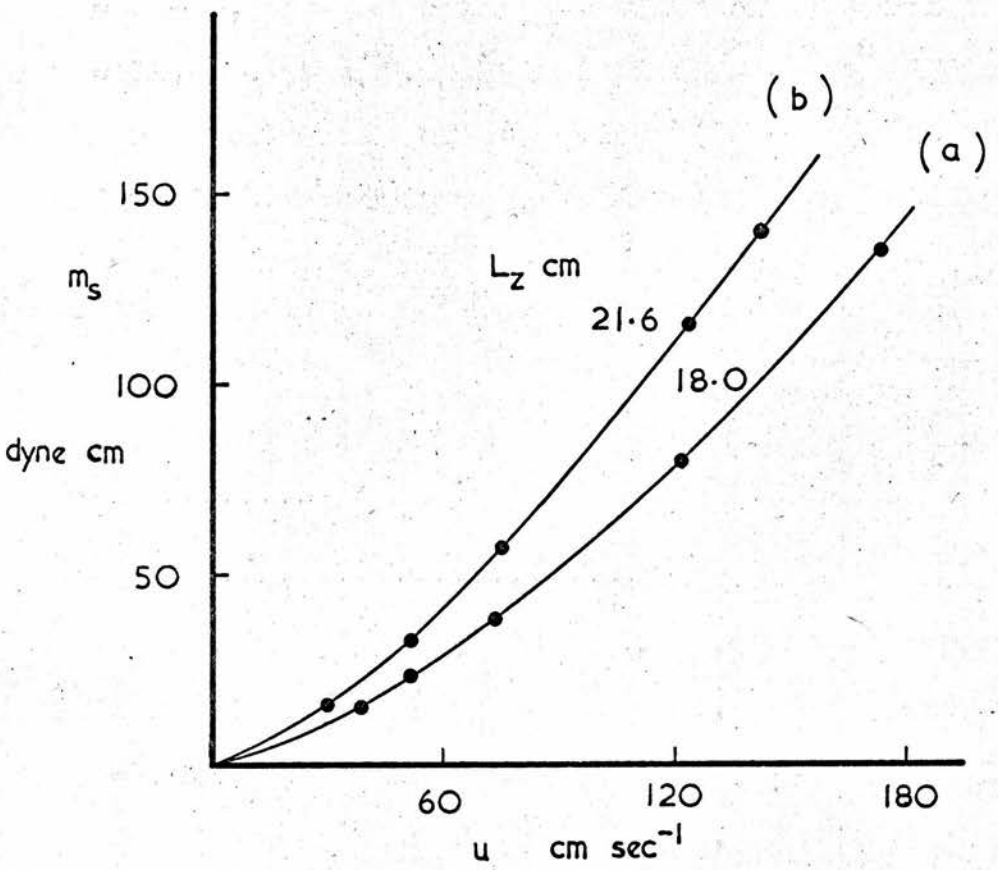

FIGURE 4.5 m_s, the moment on the (leaf) supporting rod, versus wind speed.

TABLE 4.1(a) $\phi = 0$ $L_z = 18.0$ cm.

u cm. sec.$^{-1}$	23.8	25.0	25.6	32.3	43.0	49.7	67.7	80.4	150.0
m_t dyne cm.	26	22	25	39	55	70	110	145	410
m_s dyne cm.	8	8	8	11	18	22	33	43	108
m dyne cm.	18	14	17	28	37	48	77	102	302
F dyne	1.00	0.78	0.95	1.55	2.05	2,67	4.28	5.66	16.76
C_d	0.074	0.053	0.061	0.063	0.047	0.046	0.040	0.037	0.031

TABLE 4.1(b) $\phi = 0$ $L_z = 21.6$ cm.

u cm. sec.$^{-1}$	22.5	30.9	41.8	46.7	61.2	75.6	124	127	145
m_t dyne cm.	27	46	78	75	130	170	410	430	510
m_s dyne cm.	11	16	25	27	41	57	116	121	144
m dyne cm.	16	30	53	48	89	113	294	309	366
F dyne	0.74	1.39	2.45	2.22	4.12	5.23	13.6	14.3	16.9
C_d	0.062	0.061	0.059	0.043	0.046	0.039	0.037	0.037	0.034

TABLE 4.2

L_z = 18.0 cm.

ϕ = +90°	u cm. sec.$^{-1}$	22.6	24.4	24.7	25.9	27.7	36.0
	F dyne	6.54	7.32	7.90	8.45	9.20	15.3
	C_d	0.537	0.515	0.539	0.523	0.503	0.496
	u cm. sec.$^{-1}$	41.2	40.6	60.2	60.6	61.2	62.6
	F dyne	20.7	18.5	41.8	41.7	43.9	45.1
	C_d	0.513	0.470	0.483	0.463	0.491	0.482
	u cm. sec.$^{-1}$	73.4	75.5	75.6	76.9	137.2	174.2
	F dyne	60.2	66.3	64.5	66.7	201	344
	C_d	0.467	0.487	0.467	0.467	0.460	0.470
ϕ = -90°	u cm. sec.$^{-1}$	24.1	41.2	66.6	79.3	148	
	F dyne	6.51	17.4	43.2	60.4	206	
	C_d	0.470	0.429	0.407	0.403	0.395	
ϕ = +23°	u cm. sec.$^{-1}$	20.0	26.8	42.4	65.6	79.3	142
	F dyne	1.81	3.06	6.96	14.45	21.9	63.8
	C_d	0.192	0.181	0.164	0.142	0.141	0.138
ϕ = -23°	u cm. sec.$^{-1}$	24.1	41.2	64.5	79.6	144	
	F dyne	2.13	5.37	11.77	18.2	53.1	
	C_d	0.143	0.130	0.115	0.118	0.105	

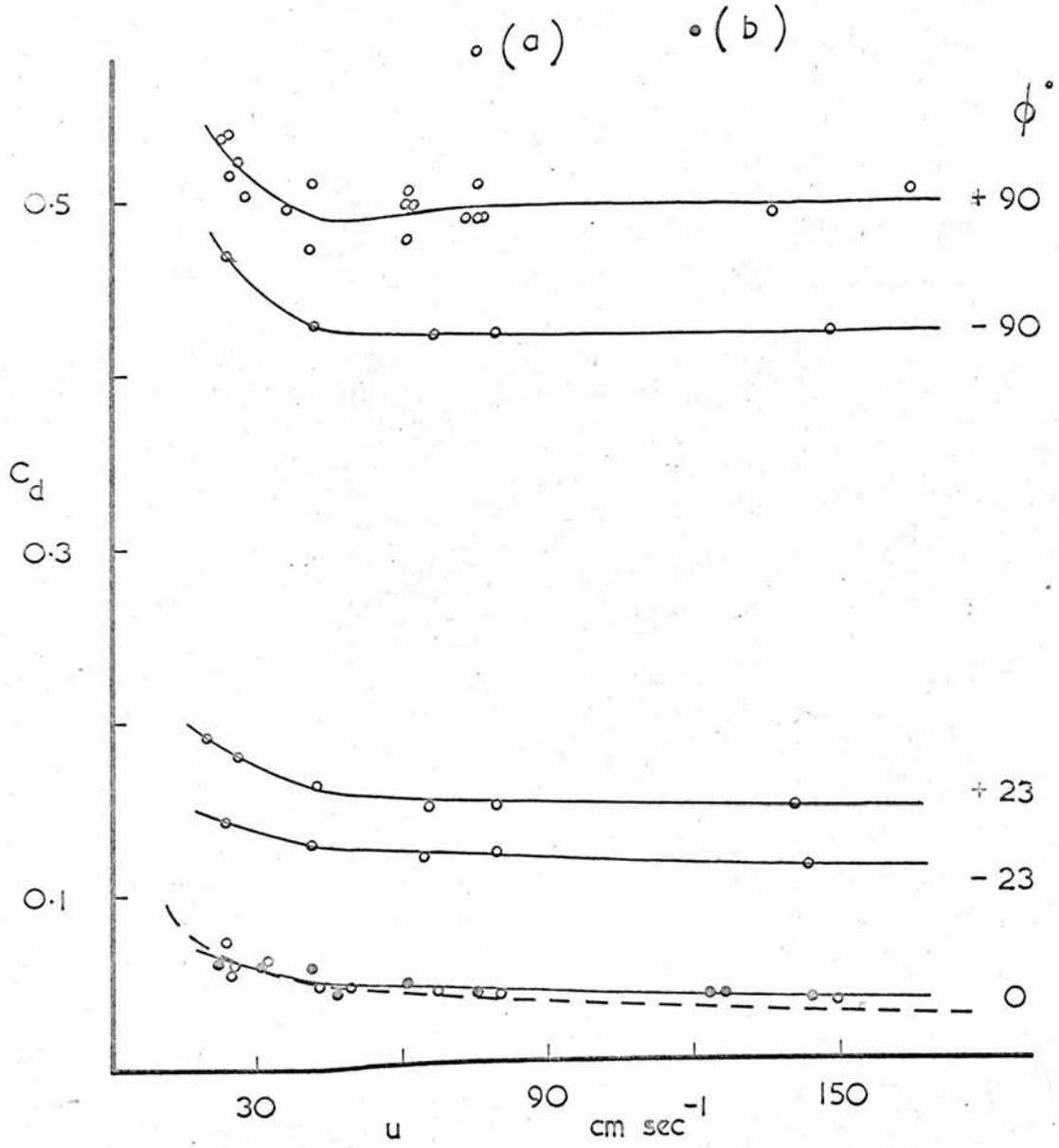

FIGURE 4.6 Drag coefficient of leaf versus wind speed for $\phi = -90^\circ, -23^\circ, 0^\circ, +23^\circ$ and $+90^\circ$; from Tables 4.1 and 4.2. (a): L_z = 18.0 cm. (b): L_z = 21.6 cm. (and filter paper covering on leaf). The broken curve is the Blasius skin friction drag coefficient for a thin flat leaf at $\phi = 0^\circ$.

wind speed.

For any value of u or ϕ, C_d must equal $(C_b + C_f)$, the sum of its "bluff-body" and skin friction components. Neither C_b nor C_f was measured separately, but the size of C_f was estimated by calculating the theoretical skin friction drag coefficient, C_f' (at $\phi=0^\circ$), of a thin flat plate with the same area and shape as the leaf. Blasius (1908) showed that the skin friction drag coefficient, c_f (at $\phi = 0^\circ$), of a thin flat plate with uniform chord, d, is given by

$$c_f = 1.328 \left(\frac{ud}{\nu}\right)^{-1/2} \qquad (4.16)$$

When d is the maximum chord of the leaf (Fig. 4.1) it can be shown that C_f' is close to $1.3c_f$. This value of C_f' is shown by the broken curve on Fig. 4.6 to be only slightly less than the value of C_d for $\phi = 0$, the only angle at which C_f is expected to be much larger than C_b. At other angles of incidence it is unlikely that the contribution to C_d from skin friction exceeds C_f'; for skin friction can not in the limit when $\phi = 90^\circ$ contribute to the drag on a thin flat plate. Thus, as ϕ is increased from zero, C_b should soon become much larger than C_f. Similarly, C_d should, and does, become less dependent on wind speed as ϕ increases, confirming that the then dominant pressure force F_b is nearly proportional to u^2 (see Eq. (4.4)). Thus, unless ϕ is very small, the transfer of stream-wise momentum to the leaf, i.e. to a typical element of a natural rough

surface, is greatly enhanced by normal pressure forces (1.3(c)).

4.3(b) Measured values of C_v

Table 4.3 gives measured values of C_w, the transfer coefficient for water vapour, at several values of wind speed for each of the previous values of ϕ, namely $\pm 90^\circ$, $\pm 23^\circ$ and 0°. Included for $\phi = 0^\circ$ only are the corresponding values of T, $(T - T')$, $(T_L - T')$ and E, together with each δe calculated from Eq. (4.11). The method used to determine E (see 4.2(b)) is demonstrated in Fig. 4.7 for $u = 127$ cm. sec.$^{-1}$, $\phi = 0^\circ$. The moment $\ell_x R$ is shown plotted against the corresponding time t, in minutes, at which the suspended system (Fig. 4.3) was observed to be exactly in balance. The rider weight R, equal to 500 mg., was moved a total of 6 cm. outward along the moment arm in about 22 minutes . Eq. (4.9) is used to calculate E from the gradient of the straight line drawn through the experimental points on the Figure.

Fig. 4.8 shows the curves obtained for the wind speed dependence of C_w at the chosen values of ϕ. The coefficient C_w, unlike C_d, depends little on ϕ, and is much smaller than C_d unless ϕ itself is small. The latter observation demonstrates the "bluff-body" effect (1.3(c)) for a typical element of a natural rough surface, while the former confirms Powell's (1940) observation that the rate of forced convection of water

TABLE 4.3

$\phi = 0^{\circ}$	u cm. sec.$^{-1}$	22.6	30.5	49.1	62.5	105	127	145	151
	$T^{\circ}C$	16.5	18.7	16.5	16.4	14.5	19.1	14.4	16.4
	$T-T'$ $^{\circ}C$	4.8	5.9	4.2	4.35	3.2	3.2	3.1	4.5
	T_L-T' $^{\circ}C$	0.20	0.25	0.18	0.19	0.24	0.30	0.22	0.31
	δe mb.	3.36	4.18	2.96	3.07	2.33	2.49	2.26	3.34
	$10^4 \times E$ gm/sec.	1.14	1.49	1.28	1.47	1.32	1.51	1.45	2.21
	C_w	0.102	0.080	0.060	0.052	0.036	0.032	0.030	0.0295
$\phi = +23^{\circ}$	u cm. sec.$^{-1}$	20.7		52.4		105			157
	C_w	0.120		0.059		0.040			0.032
$\phi = -23^{\circ}$	u cm. sec.$^{-1}$	20.7		55.2	66.7	92.4		149	
	C_w	0.103		0.051	0.048	0.041		0.030	
$\phi = +90^{\circ}$	u cm. sec.$^{-1}$	25.0		41.2	66.7	110		147	
	C_w	0.084		0.059	0.043	0.034		0.031	
$\phi = -90^{\circ}$	u cm. sec.$^{-1}$	19.8		45.2	66.7	108			163
	C_w	0.106		0.070	0.053	0.039			0.033

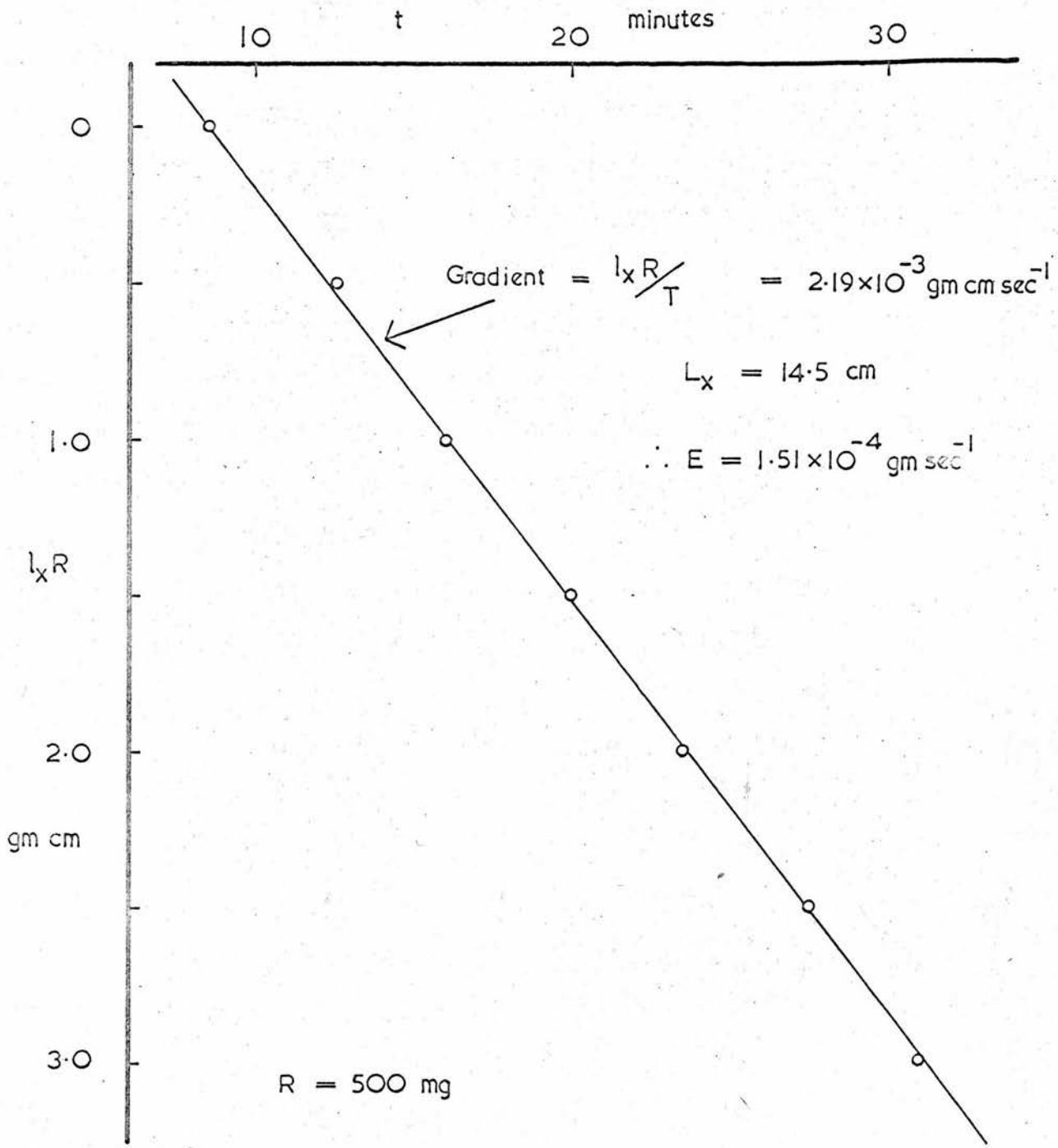

FIGURE 4.7 Determination of rate of evaporation from leaf.

Volatile liquid	:	water
Wind speed, u	:	127 cm. sec.$^{-1}$
Leaf angle, ϕ	:	0^{o}.

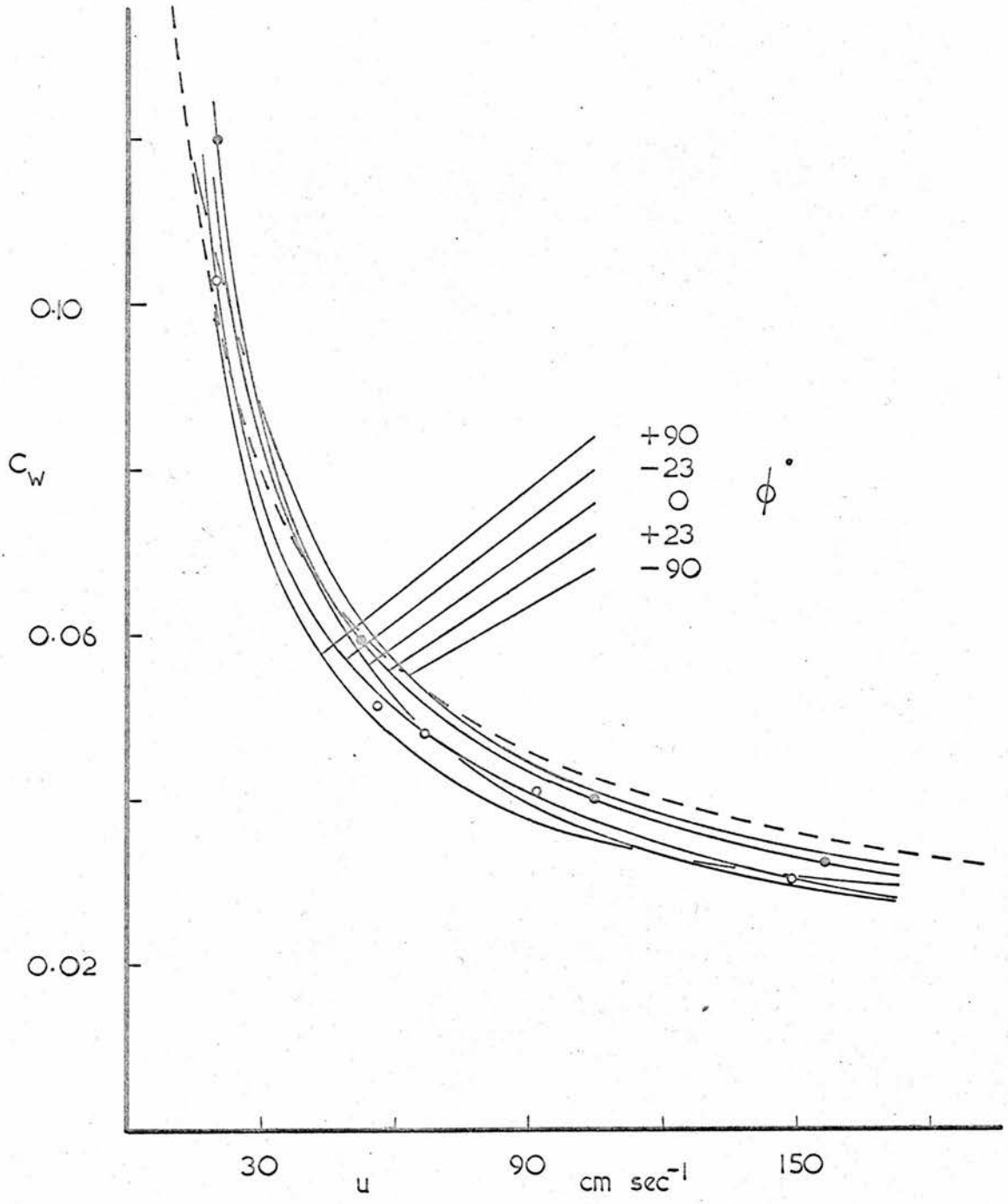

FIGURE 4.8 Transfer coefficient for water vapour versus wind speed for ϕ as in Fig. 4.6 (experimental points, from Table 4.3, shown for $\phi = -23^\circ$ and $\phi = +23^\circ$ only). The broken curve derives from Polhausen's theory and applies to the transfer of water vapour from a thin flat leaf at $\phi = 0^\circ$.

vapour from a flat disc is not sensitive to the angle between the disc and the airflow. The broken curve on Fig. 4.8 shows the theoretical water vapour transfer coefficient, C_w' (at $\phi = 0^o$) of the thin flat leaf (introduced in 4.3(a)). C_w' is 1.3 times the value of c_v (for a thin flat plate of chord d) obtained from the expression

$$c_v = 1.328 \left(\frac{ud}{\nu}\right)^{-1/2} \left(\frac{D}{\nu}\right)^{2/3} = c_f \left(\frac{D}{\nu}\right)^{2/3} \qquad (4.17)$$

when D equals the diffusivity of water vapour, 0.24 $cm.^2 sec.^{-1}$. This relation, which is due to Pohlhausen (1921), demonstrates a form of analogy between the coefficients c_v and c_f, exact only when $D = \nu$. That the power to which the diffusivity is raised is less than unity is consequent to a thickening of the diffusion boundary layer as D is increased (see, e.g. Davies (1966)). Fig. 4.8 shows that the theoretical curve, representing C_w', agrees well with the experimental curves for C_w, regardless of the value of ϕ.

The weak dependence of C_w (and therefore of C_v and C_h, in general) on ϕ was examined in terms of the relative exposures of the two sides of the leaf at different values of ϕ. The rate of evaporation from the leaf wetted on its concave (+) face only was measured, to determine a transfer coefficient C_w^+. The corresponding coefficient, C_w^-, was found for the leaf wetted on its convex (-) face only. Table 4.4 gives measured values of C_w^+ and C_w^- for several wind speeds at each

of the five previous values of ϕ. Fig. 4.9 shows the curves obtained for the wind speed dependence of C_w^+, C_w^- and their sum C_w^{+-}: the broken curves (from Fig. 4.8) give the corresponding values of C_w. The different values of C_w^+ and C_w^-, at each value of ϕ, demonstrate the influence of relative shelter or relative exposure on the effectiveness of transfer between a surface of the leaf and the passing airflow. Although the sum C_w^{+-} changes with wind speed like C_w, it is about 30 per cent greater than C_w for all values of u and ϕ: this is a new result. The smaller C_w values (both surfaces wet) indicate a mutual interference, at the trailing edg(s) of the leaf, between the vapour streams from opposite sides of the leaf. This interference forms an integral part of the transfer resistance of a leaf if both of its surfaces are active, but does not exist if only one of its surfaces is active (e.g. a hypostomatous leaf, which has stomata on its lower surface only).

Table 4.5 gives values of C_v determined, at several wind speeds, for two volatile liquids of low molecular diffusivity, namely bromobenzene, C_{bb}, and methyl salicylate, C_{ms}. Also included are the corresponding values of T, δT, T_L, δe, and E: ϕ was restricted to 0°. Each δe, equal to $e_s(T_L)$ (see 4.2(b)), was obtained from tabulated values of vapour pressure. Fig. 4.10 shows the graphical determination of E for methyl salicylate at u = 62 cm. sec.$^{-1}$ (Table 4.5). This Figure, which gives E close to 2×10^{-5} gm. sec.$^{-1}$

TABLE 4.4

$\phi = 0^{o}$	u cm. sec.$^{-1}$	19.8	41.0	72,3				159
	C_w^+	0.074	0.039	0.025				0.016
	u cm. sec.$^{-1}$	23.8	40.0	65.6	78.3		137	
	C_w^-	0.075	0.051	0.040	0.033		0.023	
$\phi = +23^{o}$	u cm. sec.$^{-1}$	18.0	47.6					150
	C_w^+	0.112	0.053					0.024
	u cm. sec.$^{-1}$	19.2	31.9	44.6	76.7	103		155
	C_w^-	0.068	0.042	0.032	0.024	0.021		0.016
$\phi = -23^{o}$	u cm. sec.$^{-1}$	20.7	42.4	69.0				144
	C_w^+	0.057	0.023	0.020				0.015
	u cm. sec.$^{-1}$	22.9	24.0	34.2	49.2	82.1		149
	C_w^-	0.079	0.079	0.062	0.053	0.039		0.024
$\phi = +90^{o}$	u cm. sec.$^{-1}$	23.4	45.7	72.0	86.0	96	119	146
	C_w^+	0.058	0.042	0.032	0.032	0.029	0.028	0.027
	u cm. sec.$^{-1}$	22.2	40.9	66.7		101		144
	C_w^-	0.053	0.030	0.019		0.018		0.018
$\phi = -90^{o}$	u cm. sec.$^{-1}$	20.4	27.7	40.6			124	
	C_w^+	0.039	0.033	0.029			0.013	
	u cm. sec.$^{-1}$	19.8	41.2			94		155
	C^-	0.093	0.064			0.041		0.031

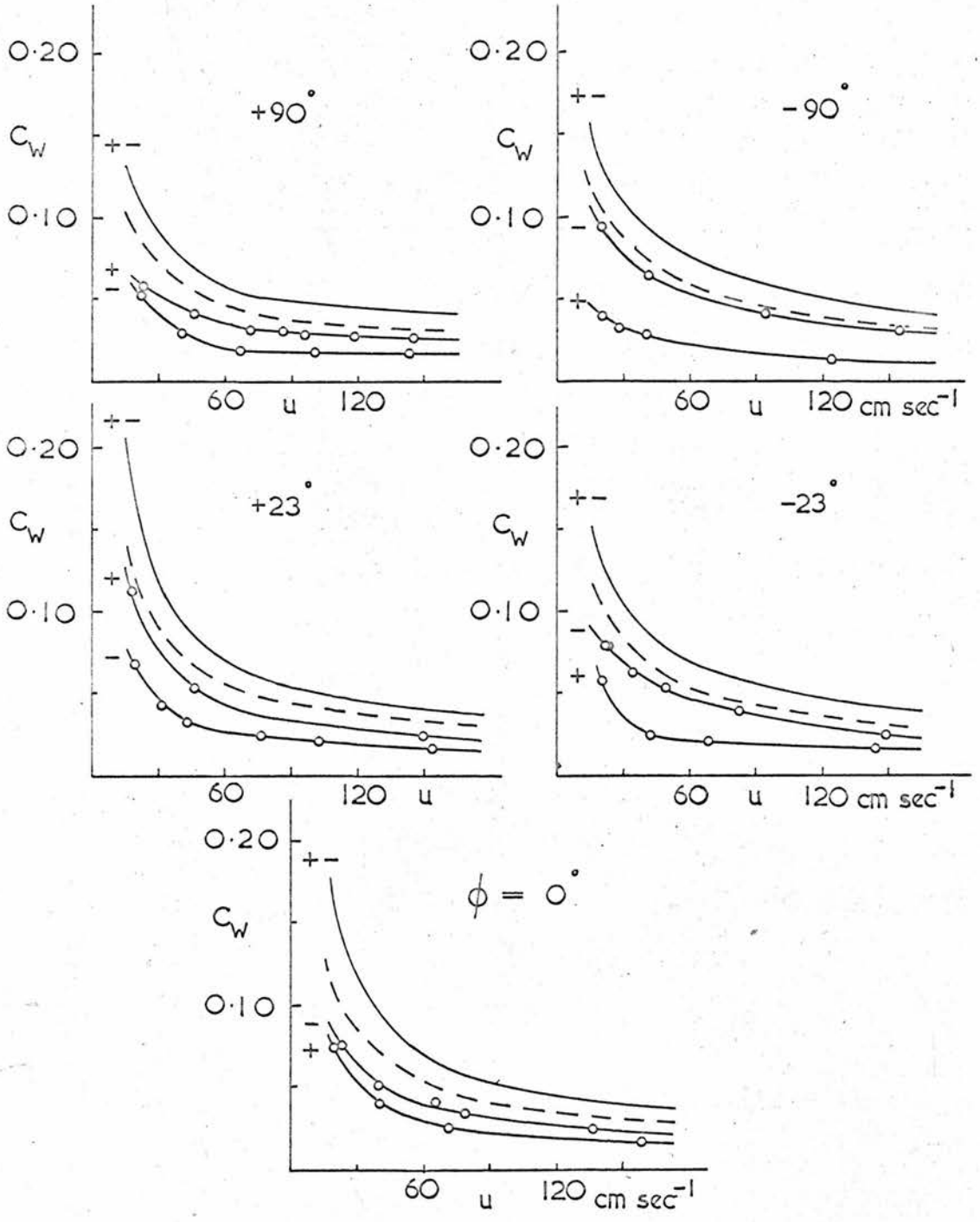

FIGURE 4.9 Transfer coefficients for water vapour versus wind speed for ϕ = -90°, -23°, 0°, +23° and +90°; from Table 4.4 .

\+ : for the leaf wetted on its concave face only.

\- : for the leaf wetted on its convex face only.

+- : the sum of + and - .

The broken curve (from Fig. 4.8) is the coefficient when both faces are wet.

TABLE 4.5

Liquid bromobenzene	u cm. $sec.^{-1}$	15.0	33.6	40.0	52.0	60
	T ^{o}C	18.2	23.4	18.0	21.7	14.0
	$(T-T_L)$ ^{o}C	1.7	2.0	1.4	1.7	0.7
	T_L ^{o}C	16.5	21.4	16.6	20.0	13.3
	δ_e mb.	3.30	4.42	3.32	4.03	2.63
	$10^4 \times E$ gm. $sec.^{-1}$	3.73	5.57	2.26	5.94	4.04
	C_{bb}	0.059	0.030	0.0253	0.0223	0.0205
	u cm. $sec.^{-1}$	107	122	134	142	
	T ^{o}C	21.6	21.6	20.7	16.5	
	$(T-T_L)$ ^{o}C	1.7	1.7	1.8	1.7	
	T_L ^{o}C	19.9	19.9	18.9	14.8	
	δ_e mb.	4.00	4.00	3.80	2.91	
	$10^4 \times E$ gm. $sec.^{-1}$	7.93	8.50	8.38	6.90	
	C_{bb}	0.0145	0.0137	0.0128	0.0132	
Methyl salicylate	u cm. $sec.^{-1}$	26.0	30.5	62	142	
	T ^{o}C	26.2	26.6	24.0	25.5	
	$(T-T_L)$ ^{o}C	0	0	0	0	
	T_L ^{o}C	26.2	26.6	24.0	25.5	
	δ_e mb.	0.189	0.196	0.157	0.177	
	$10^4 \times E$ gm. $sec.^{-1}$	0.194	0.194	0.206	0.357	
	C_{ms}	0.0322	0.0269	0.0172	0.0116	

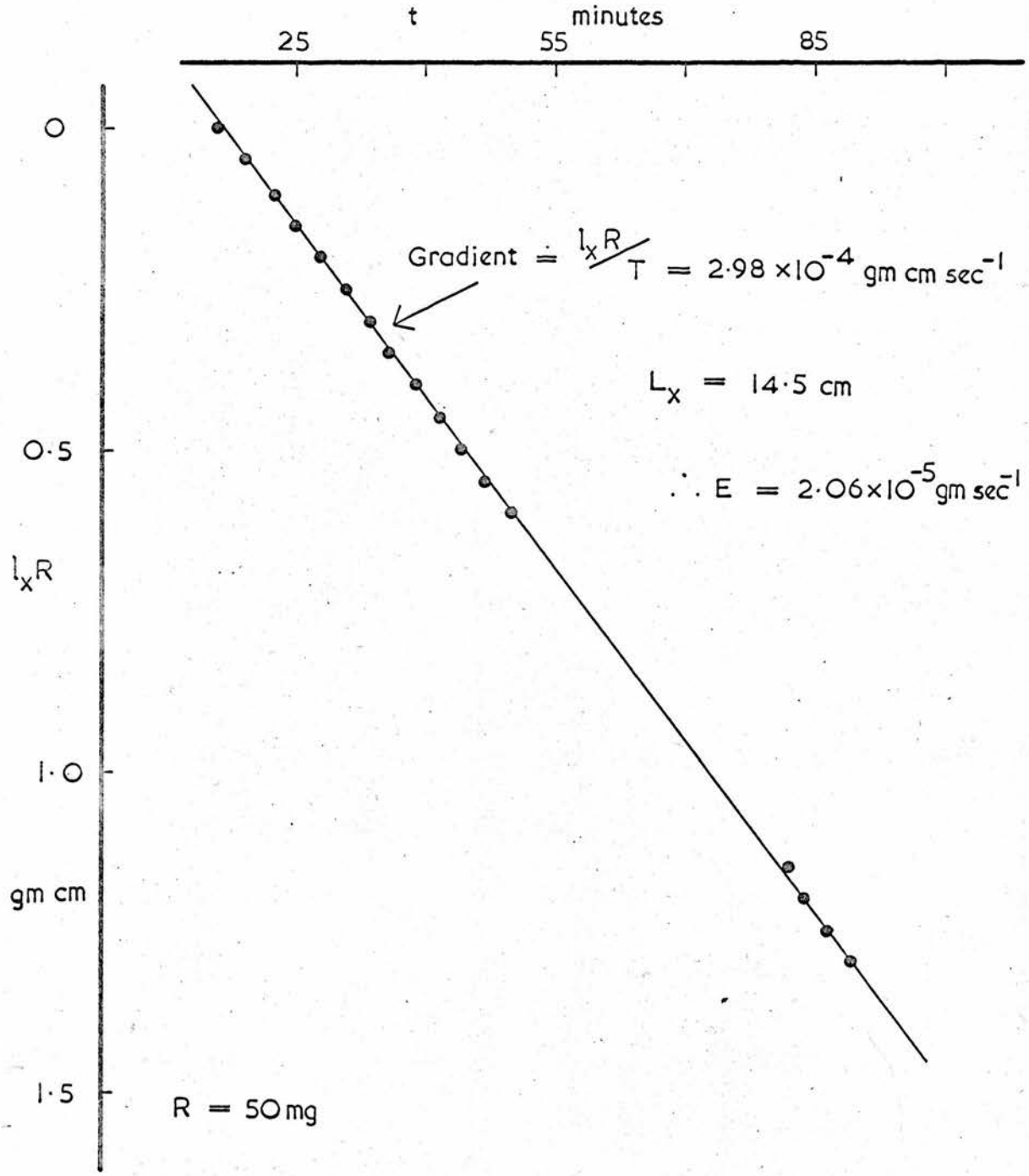

FIGURE 4.10 Determination of rate of evaporation from leaf.

Volatile liquid : methyl salicylate.
Wind speed, u : 62 cm. sec.$^{-1}$.
Leaf angle, ϕ : 0°.

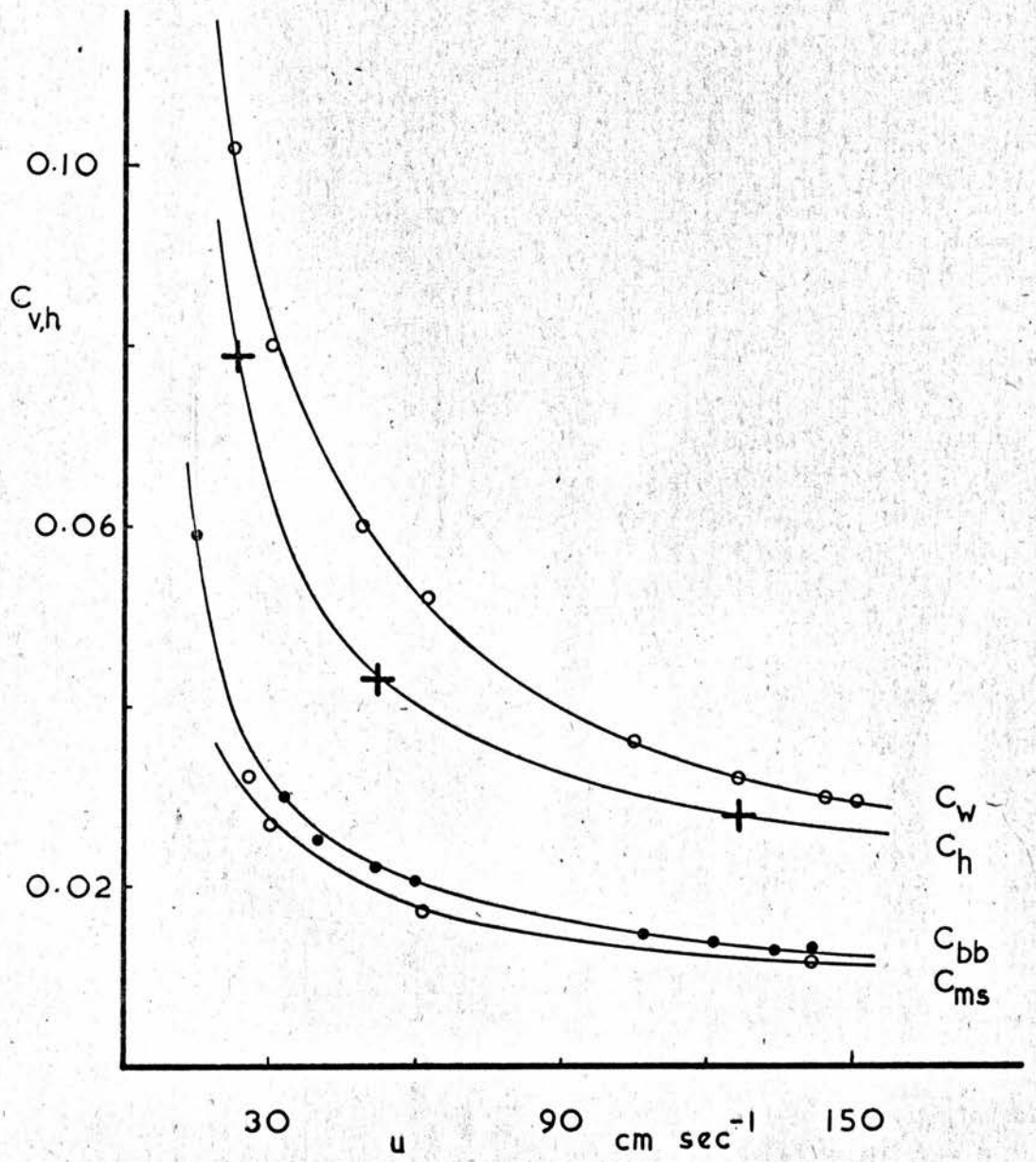

FIGURE 4.11 Transfer coefficients versus wind speed at $\phi = 0^{\circ}$ for water vapour C_w, bromobenzene C_{bb}, methyl salicylate C_{ms} and heat C_h ; from Tables 4.3, 4.5 - 4.7.

contrasts with Fig. 4.7 ($E = 1.5 \times 10^{-4}$ gm. sec.$^{-1}$) and demonstrates the versatility of the moment balance technique (see 4.2(b)).

Support for a relationship between C_v and molecular diffusivity D similar to Eq. (4.17) is given by the curves on Fig. 4.11, which shows the wind speed dependence (at $\phi = 0$) of C_w, C_{bb} and C_{ms}. The corresponding values of D are 0.24, 0.068 and 0.054 cm.^{2} sec.$^{-1}$ respectively, in air at 17°C.

4.3(c) Measured values of C_h

Table 4.6 and Fig. 4.12 show the calculation of C_h at the chosen (high) wind speed, u = 127 cm. sec.$^{-1}$ (see 4.2(c)). In Table 4.6(a) are the observed quantities $(T_{W1} - T)$, $(T_{W2} - T)$, $(\delta T)_i$, T, and W; and the corresponding values of K, (W - K), $(T_W - T)$ and $(T_L - T)$, equal to δT (Eq. (4.12)). Table 4.6(b) gives $(T_L - T)$ normalised to (W - K) = 97.0 mW., and consequent values of $(T_L - T_W)$ and $\bar{T}$, equal to $(T_L + T_W)/2$. In Fig. 4.12 the normalised values of $(T_L - T)$ are plotted against $(T_L - T_W)$ and a straight line drawn through the experimental points, to give $(T_L - T) = 1.14\ (8)$ °C when $T_L = T_W$, i.e. when R = 0.

The gradient of this straight line, $\dfrac{\delta(T_L - T)}{\delta(T_L - T_W)}$ must be proportional to the effective emissivity, e ,

TABLE 4.6(a)

$T_{w1}-T$ °C	$T_{w2}-T$ °C	T_w-T °C	$(\delta T)_i$ °C	T_L-T °C	T °C	W mW.	K mW.	W − K mW.
2.54	1.64	2.09	1.40	1.26	17.3	101.0	4.3	96.7
0.26	-0.38	-0.06	1.14	1.03	18.6	101.0	4.3	96.7
0.48	-0.16	0.16	1.17	1.05	18.6	101.0	4.3	96.7
0.63	0.43	0.53	1.20	1.08	19.1	100.3	4.3	96.0
1.26	0.68	0.97	1.24	1.12	19.1	100.3	4.3	96.0
3.74	2.06	2.90	1.46	1.31	14.2	100.0	2.4	97.6
3.19	1.93	2.56	1.43	1.29	14.2	100.0	2.4	97.6
1.71	1.00	1.35	1.30	1.17	16.1	99.7	2.4	97.3
-0.68	-1.16	-0.92	1.11	1.00	13.4	99.7	2.4	97.3

TABLE 4.6(b)

W − K mW.	T_L-T °C	T_L-T_w °C	$\bar{T}$ °C
97.0	1.26	-0.83	19.0
97.0	1.03	1.09	19.1
97.0	1.06	0.90	19.2
97.0	1.09	0.56	19.9
97.0	1.13	0.16	20.2
97.0	1.30	-1.60	16.3
97.0	1.28	-1.28	16.1
97.0	1.17	-0.18	17.4
97.0	1.00	1.92	13.4

From Fig. 4.12

$T_L - T = 1.15^{\circ}C$

when $T_L = T_w$.

Thus Eq. 4.18

with $H = W - K$

gives

$C_h = 0.028$

for $u = 127$ cm. sec.$^{-1}$.

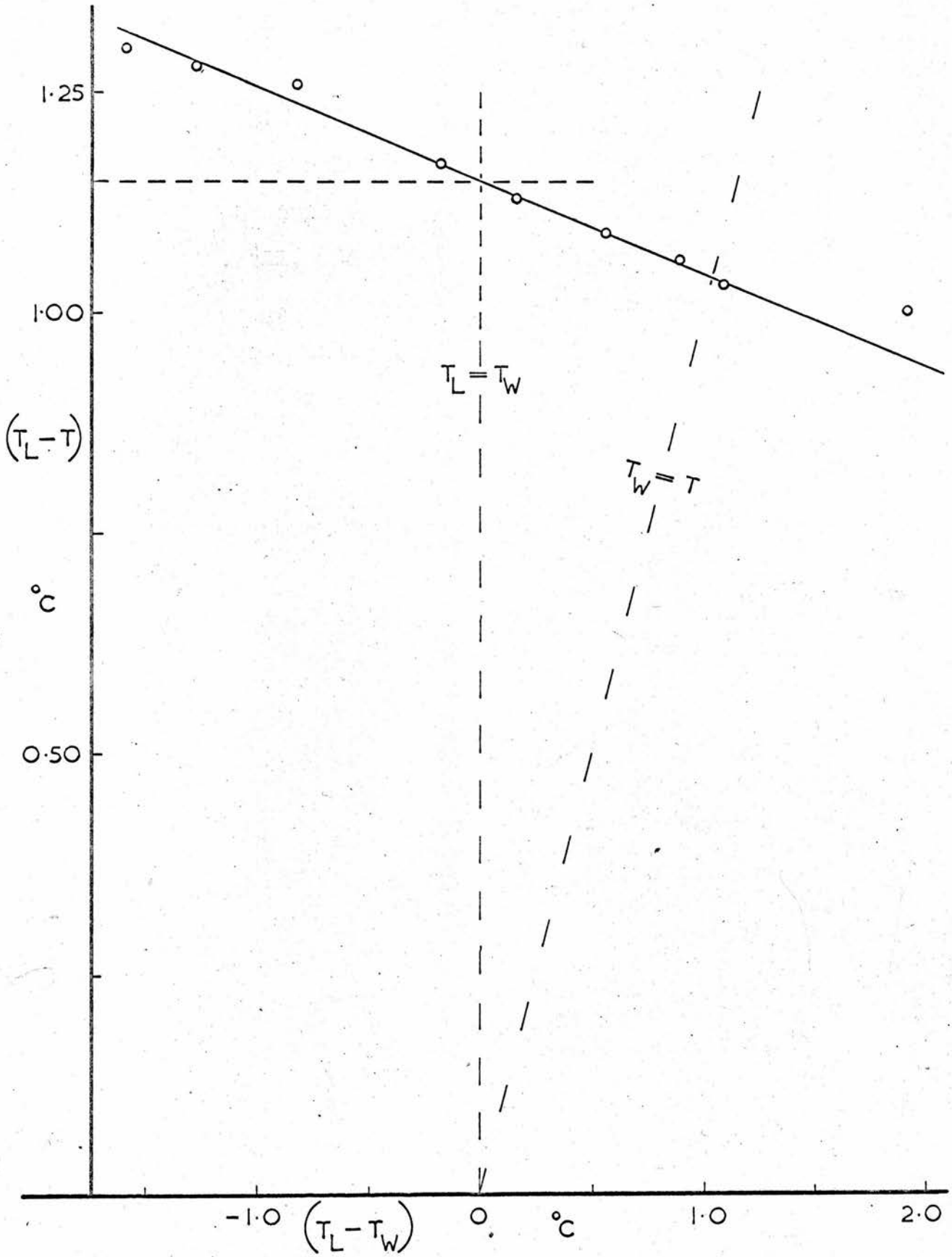

FIGURE 4.12 Leaf-air temperature difference (T_L - T) versus leaf-wall temperature difference $T_L - T_W$; from Table 4.6(b).

TABLE 4.7

u cm. sec.$^{-1}$	$T_{w1} - T$ °C	$T_{w2} - T$ °C	$T_w - T$ °C	$(\delta T)_i$ °C	$T_L - T$ °C	T °C	W mW.	K mW.
23.8	0.24	-0.40	-0.08	1.97	1.77	16.8	99.6	3.9
52.8	1.16	0.13	0.65	1.76	1.58	18.8	99.4	3.4

$T_L - T_w$ °C	$\bar{T}$ °C	R mW.	H = W-R-K mW.	C_h	u cm.sec^{-1}
1.85	17.7	16.3	79.4	0.079	23.8
0.93	19.9	8.3	86.7	0.043	52.8

of the leaf tunnel system. It can be shown, by combining Eqs, (4.7), (4.13) and (4.15) that with $\overline{T} = 17^{o}C$

$$e = -1.09\, u\, C_h \frac{\delta(T_L - T)}{\delta(T_L - T_W)} \qquad (4.18)$$

From Table 4.6, $C_h = 0.028$ at $u = 127$ cm. sec.$^{-1}$, and Fig. 4.12 gives $\frac{\delta(T_L - T)}{\delta(T_L - T_W)}$ equal to - 0.105, so that $e = 0.40$. This value of e was used, in Eq. (4.15), to give the values of R in Table 4.7. Otherwise, Table 4.7 is similar in form to Table 4.6, and shows the calculation of two further values of C_h.

Fig. 4.7 shows that the curve determined for C_h as a function of wind speed (at $\phi = 0$) is similar to the corresponding curves for the coefficients of vapour transfer; and that the magnitude of C_h is consistent with the size of the molecular diffusivity of heat, , equal to 0.205 cm.^{2} sec.$^{-1}$, in air at 17°C.

4.3(d) C_o, a generalised transfer coefficient for mass or heat.

The experimental results for C_v and C_h shown in Fig. 4.11 are re-plotted logarithmically in Fig. 4.13. When the free convection component of transfer from the leaf can be neglected, then C_v and C_h can be expected to be proportional to $u^{-\frac{1}{2}}$, from Eq. (4.17). The gradient of each broken curve drawn through the sets of

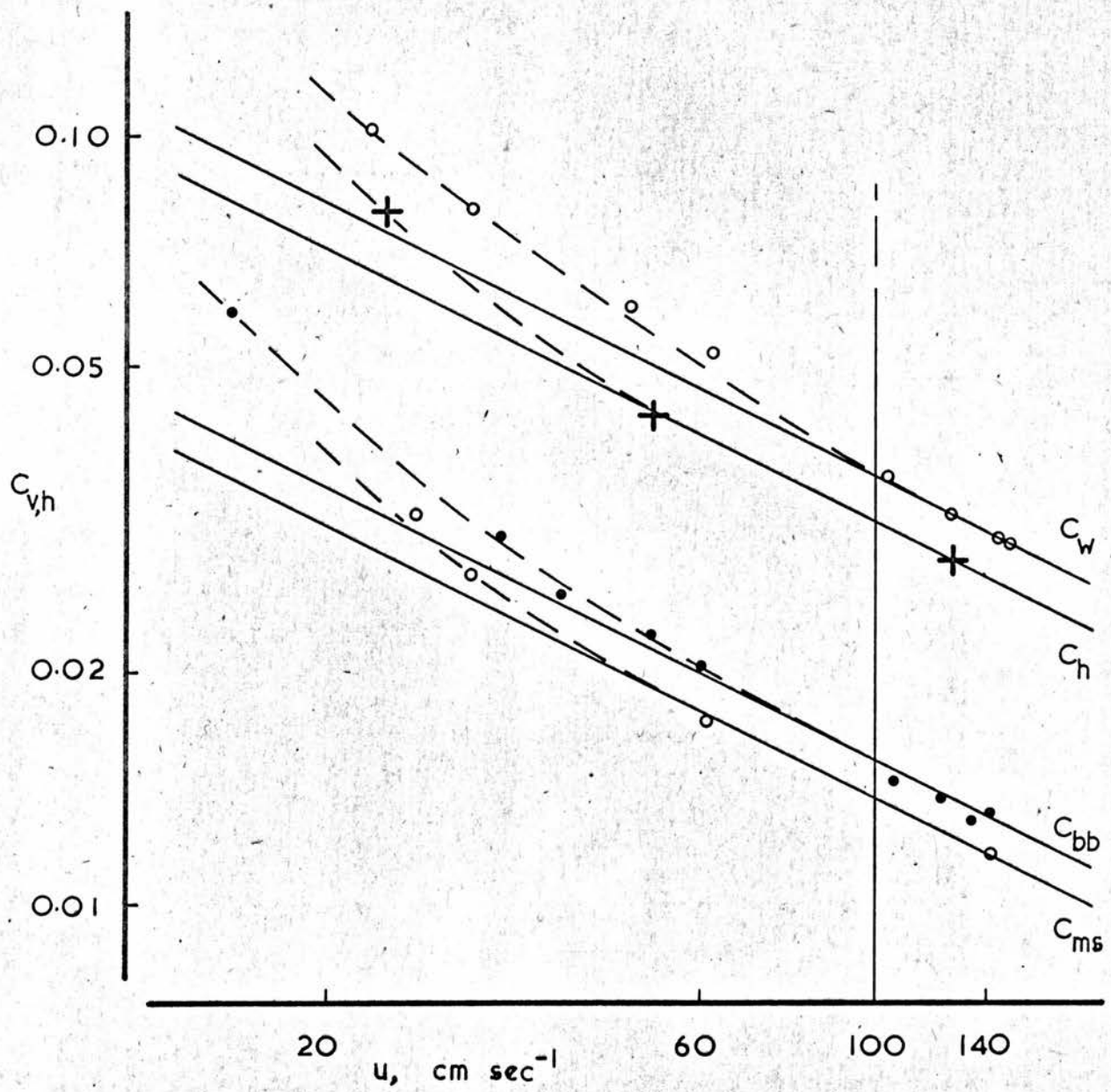

FIGURE 4.13 As in Fig. 4.11, but with logarithmic axes. The wind speed dependence of each transfer coefficient tends to $u^{-\frac{1}{2}}$ as u increases beyond a threshold value.

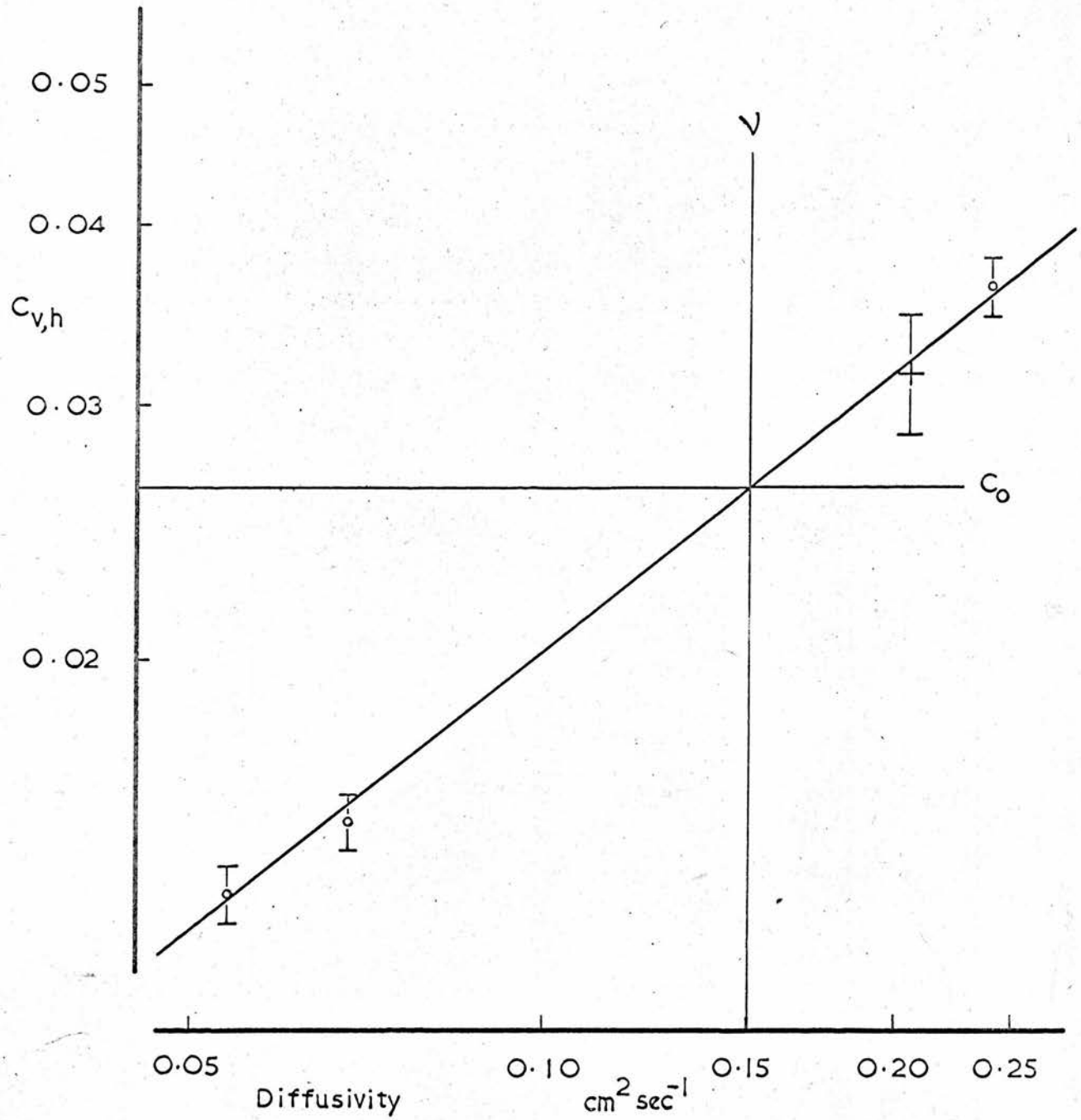

FIGURE 4.14 Transfer coefficients at u = 100 cm. sec.$^{-1}$ (from (Fig. 4.13) versus molecular diffusivity. The generalised coefficient C_o is defined at u = 100 cm. sec.$^{-1}$ for ν = 0.15 cm.^{2} sec.$^{-1}$.

experimental points on Fig. 4.13 does in fact approach the value $-\frac{1}{2}$ at a high enough wind speed. Above this (threshold) wind speed, which is greatest for water vapour, the ratio of the forces of buoyancy to the inertial forces acting on the air close to the surface of the leaf, given by the value of $((gd)/u^2)(\delta\rho/\rho)$, is estimated to be less than 10^{-3}. ($\delta\rho$ is the difference in density between air very close to the leaf surface and air in the free stream, and is a function of δT and $\delta\chi$: g is the acceleration due to gravity.) Solid lines of gradient $-\frac{1}{2}$ are drawn on Fig. 4.13 through appropriate points in each set to show that C_v and C_h are proportional to $u^{-\frac{1}{2}}$ when forced convection is the dominant transfer mechanism.

To determine the corresponding dependence of the coefficients on molecular diffusivity an intercept is drawn on Fig. 4.13 at the (arbitrary) wind speed $u = 100$ cm. sec.$^{-1}$. The resultant values of C are plotted against their respective molecular diffusivities in Fig. 4.14, which also shows the estimated experimental limits on each value of C : $\pm$ 5 per cent for each C_v, and $\pm$ 10 per cent for C_h. The line of gradient $^2/_3$ drawn through the experimental points on Fig. 4.14 confirms that the transfer coefficient of the leaf (at $\phi = 0^o$) is proportional to $D^{2/3}$ or $\kappa^{2/3}$.

A generalised coefficient, C_o, for forced transfer of mass or heat can thus be defined by writing

$$C_{v,h} = C_o \left(\frac{D,\kappa}{\nu}\right)^{2/3} \qquad (4.19)$$

where C_o equals C_v or C_h when D or κ equals ν. From Fig. 4.14 C_o can be found for $u = 100$ cm. sec.$^{-1}$, so that in general

$$C_o = 1.40 \left(\frac{ud}{\nu}\right)^{-\frac{1}{2}} \qquad (4.20)$$

Although C_o has been determined from results for transfer from the leaf at $\phi = 0$, it can be generalised to apply to transfer at any value of ϕ by taking the product C_o .(1 $\pm$ 10 per cent) to be independent of ϕ, as suggested by Fig. 4.6 (results for C_w at several values of ϕ).

4.4 The Difference between C_o and C_f

The skin friction drag coefficient of a thin flat plate in a tangential air-stream ($\phi = 0$) is equal to the coefficient for the transfer to or from the plate of a property with molecular diffusivity equal to the kinematic viscosity of air (see 4.3(b)). This equality fails when ϕ is non-zero, so that in general C_o can not, by appeal to analogy, be equated to C_f. However, a momentum transfer coefficient $(C_f)_o$ analogous to C_o could be derived from the scalar sum of the frictional forces on each element of the leaf surface. $(C_f)_o$ is equal to C_f only for a thin, flat leaf at $\phi = 0$. At all angles exceeding zero the scalar sum of these forces must exceed their vector sum resolved in the direction of the incident air-stream, so that $(C_f)_o$, and hence C_o, must exceed C_f. Thus the coefficient C_f can be

written

$$C_f = \beta C_o \qquad (4.21)$$

where β, which is less than unity, depends on wind speed and on ϕ.

This conclusion can be generalised to a natural rough surface whose coefficient of skin friction drag C_F, referred to the wind speed at a level z_n near the surface, would be over-estimated if it were assumed equal to the corresponding value of C_0 for the surface, as suggested by Barry (1965). However, for a given rough surface it may be legitimate to write

$$C_F = \beta C_0 \qquad (4.22)$$

where β, which must depend on the form and inclination (ϕ) of the roughness elements of the surface and on wind speed, can be expected to lie between 10^{-1} and unity. Assuming for a vegetated surface that $C_D(z_n)$ is of order $10\, C_0(z_n)$ (see Figs. 4.6 and 4.11 for the order of magnitude of C_d/C_o), then C_F must lie between $10^{-1}C_D$ and $10^{-2}C_D$, so that (of order) 95 per cent of C_D is most probably made up of "bluff-body" forces represented by C_B which is independent of wind speed. Although the remaining 5 per cent or so of C_D (represented by C_F) must vary with wind speed (approximately as $u^{-\frac{1}{2}}$), this (absolute) variation can reasonably be neglected; so that C_D itself can be considered independent of wind speed (provided surface geometry remains unchanged, see 1.1(b)).

Barry (1965) equates C_B to the difference between measured values of C_D and C_O. He says that "it is this "C_B" which may be expected to be a function of the roughness Reynolds' number," R_o, equal to $u_* z_o/\nu$. However, this is unrealistic, for z_o is directly related to the (total) roughness of the surface, specified by the (total) drag coefficient C_D. On two occasions Barry finds C_O to be greater than C_D, a result which he has to reject (as it implies negative C_B), but which supports Eq. (4.22).

4.5 Practical Aspects of the Results

4.5(a) The transfer resistance r of a single leaf in the field

Eqs. (4.19) and (4.20), combined with Eq. (4.2), yield

$$r_{v,h} = 1.84 \left(\frac{d}{u}\right)^{1/2} \left(\frac{D_{,K}}{\nu}\right)^{-2/3} \qquad (4.23)$$

which is the resistance to forced convective transfer of vapour or heat between an artificial bean leaf of dimension d and a wind-tunnel air-stream of speed u. This equation should give a close estimate of the resistance r of any leaf of chord d exposed in a crop canopy to a mean wind speed u, provided that the leaf does not flutter, that the boundary layers of adjacent leaves do not interfere and that u is large enough to promote fully forced convective transfer. This last condition is likely to be fulfilled in parts of the canopy where u

exceeds 50 cm. sec.$^{-1}$ (Monteith, 1965): thus Eq. (4.23) will tend to over-estimate r when u is less than 50 cm. sec.$^{-1}$. Any fluttering of the leaf, more likely at higher wind speeds, would again tend to reduce r, alternate sides of the leaf being exposed directly to the incident air-stream. However, consideration of Fig. 4.9 (effect of exposure on transfer from one or other side of the leaf) shows that the decrease in r due to fluttering is unlikely to be greater than about 25 per cent of r, and for low flutter frequencies is probably negligible. Interference between the laminar boundary layers of neighbouring leaves and direct sheltering of one leaf by another would, on the other hand, tend to increase the value of r over that predicted by Eq. (4.23) (see 5.4(a)). Turbulence in the canopy airflow is unlikely, in itself, to reduce any one of the resistances r_v, r_h, or r_d of a single leaf: the Reynolds' numbers involved, around 3000, are too small. When Smith and Kuethe (1966) introduced a turbulence level of 6 per cent into the previously smooth flow over a flat plate, they recorded a 25 per cent decrease in the resistance to the removal of heat from the plate at $R = 10^5$, but could detect no change at $R = 5000$.

Table 4.8 gives values of r in units of sec. cm.$^{-1}$ for water vapour, carbon-dioxide and heat, obtained from Eq. (4.23) ($d = 4$ cm., $\dot{u} = 75$ cm. sec.$^{-1}$). The values of r for heat and water vapour agree with the resistance

TABLE 4.8

	Water vapour	Carbon dioxide	Heat	Momentum
Molecular diffusivity $cm.^2\ sec.^{-1}$	0.24	0.14	0.20	0.15
ϕ	r sec. $cm.^{-1}$			
0^o	0.31	0.45	0.35	0.34
-23^o	0.31	0.45	0.35	0.12
$+90^o$	0.31	0.45	0.35	0.03

found by Impens (1964) for the transfer of heat or water vapour between an artificial bean leaf and the airflow within a canopy of beans (Phaseolus vulgaris); but are about twice as large as those suggested by Monteith (1965), who reviewed previous measurements of transfer resistance and chose those of Raschke (1956) to be most representative of leaves in the open air. Raschke's results were obtained from the heat exchange of a Canna indica leaf of length 34 cm. and chord, d, about 14 cm. The discrepancy of resistance is most likely a consequence of free convection from Raschke's leaves, exposed in bright sunshine.

The resistance of a hypostomatous leaf (4.3(b)) to water vapour or CO_2 transfer would be only about 50 per cent greater than that given by Eq. (4.23).

Table 4.8 includes measured values of the resistance, r_d, to the transfer of stream-wise momentum to the leaf at $\phi = 0^\circ$, -23°, and $+90^\circ$ (-23° is a likely "mean" value for ϕ within a canopy). Except for $\phi = 0^\circ$, r_d is much less than the corresponding resistances to mass or heat transfer (see 1.3(b)).

4.5(b) The psychrometric constant of a leaf

If evaporation from the leaf of a volatile liquid were maintained solely by transfer of sensible heat from the airflow then a unique relation would exist between δ_e and δ_T; introducing λ, the latent heat of

vaporisation of the liquid, Eqs. (4.6) and (4.7) could be combined in the psychrometric form

$$\delta e = \frac{C_h}{C_v} \cdot \gamma \delta T \qquad (4.24)$$

where $\gamma = (c_p p)/\lambda\varepsilon)$ and e_L/p is neglected in comparison with unity. Consideration of Eq. (4.19), or Fig. 4.14, shows that the ratio C_h/C_v can be replaced by $(\kappa/D)^{2/3}$. The true psychrometric constant of a leaf must therefore be written

$$A_L = \gamma \left(\frac{\kappa}{D}\right)^{2/3} \qquad (4.25)$$

This is identical to the result found by Kusuda (1965), who studied forced evaporation from a flat plate wet surface under adiabatic conditions. Using the value of κ/D equal to 0.85, quoted for water vapour by Kusuda, A_L = 0.59 mb. $^oC^{-1}$. This differs from the traditional value of the psychrometric constant γ, equal to 0.66 mb. $^oC^{-1}$, obtained on thermodynamic as distinct from kinetic grounds.

CHAPTER 5

APPLICATION TO A FIELD CROP

5.1 The 1966 Bean Crop at Rothamsted

5.1(a) Characteristics of crop and weather on July 7th

July 7th was chosen as a suitable day to study the transfer of momentum to the crop: temperate weather conditions coincided with the availability of all data relevant to the analysis. During daylight hours a moderate (west) wind blew across (as distinct from along) the rows of bean plants. This preferred wind direction ensured that, even although the canopy appeared to be completely closed, the wind would not persistently penetrate the canopy by blowing along between the rows. Total radiation measured for the day was only 229 cal. cm.$^{-2}$. (There were 7 oktas of cloud at 0900 hrs. g.m.t.): it is therefore likely that neutral stability conditions prevailed in the boundary layer flow above the canopy, so that Eq. (1.1) could be used without modification.

The height h of the crop was 118 cm. and the leaf area index L was 6.3 (cm.^{2} of one side of leaf per cm.^{2} of horizontal surface). Stratified area indices were available in the form $(\delta L)_i$, $(\delta S_t)_i$, $(\delta P_e)_i$ and $(\delta P_o)_i$ for leaf, stalk, peteole, and pod area, respectively, in each 20 cm. layer (i) of crop, working downwards from z = h. Each stratified index corresponds to

a value of $(A_i \delta z)_i$ in a finite difference form of Eq. (1.7) (see Eq. (5.1)). The indices are recorded in Table 5.1, and shown diagrammatically in Fig. 5.1.

5.1(b) Profiles of mean wind speed above and within the canopy

Mean wind speeds were available at x = 100, 125, 150, 200, 250, and 300 cm. in the form of the hourly wind run recorded from six (modified Sheppard type) cup anemometers. Corresponding hourly means at lower levels were derived from the chart records of four hot-bulb anemometers (Long, 1957) positioned at z = 5, 25, 50 and 75 cm. Table 5.2 gives the mean of each u(z) for each hour of July 7th: Fig. 5.2 shows the corresponding profiles of mean wind speed. Although the wind fetch over the bean crop was only about 30 metres, a similar surface roughness extended for some further distance upwind, so that the shape(s) of the measured profiles could be accepted as representative of the bean crop (or at least typical of the type of profile usually attributed to such a restricted expanse of crop).

The profiles were divided into six groups, A to F, for u(300 cm.) in each of the chosen ranges 57-75, 79-109, 152-164, 200-227, 259-278, and 293-304 cm. $sec.^{-1}$ in order. Table 5.3 gives the average values of u(z) for each group, at the same values of z as Table 5.2 for $z > h$ and at the same values of z as Table 5.1

TABLE 5.1

i	z cm	z_i cm	$(\delta L)_i$	$(\delta S_t)_i$	$(\delta P_e)_i$	$(\delta P_o)_i$
	118					
1	108	108	1.73	0.055	0.047	0
	98					
2	88	88	1.52	0.08	0.043	0
	78					
3	68	68	1.24	0.10	0.037	0.015
	58					
4	48	48	1.13	0.10	0.028	0.092
	38					
5	28	28	0.61	0.11	0.012	0.039
	18					
6	8	8	0.07	0.12	0.001	0
	0					

$$\text{Leaf area index} = \sum_{i=1}^{6} (\delta L)_i = 6.3$$

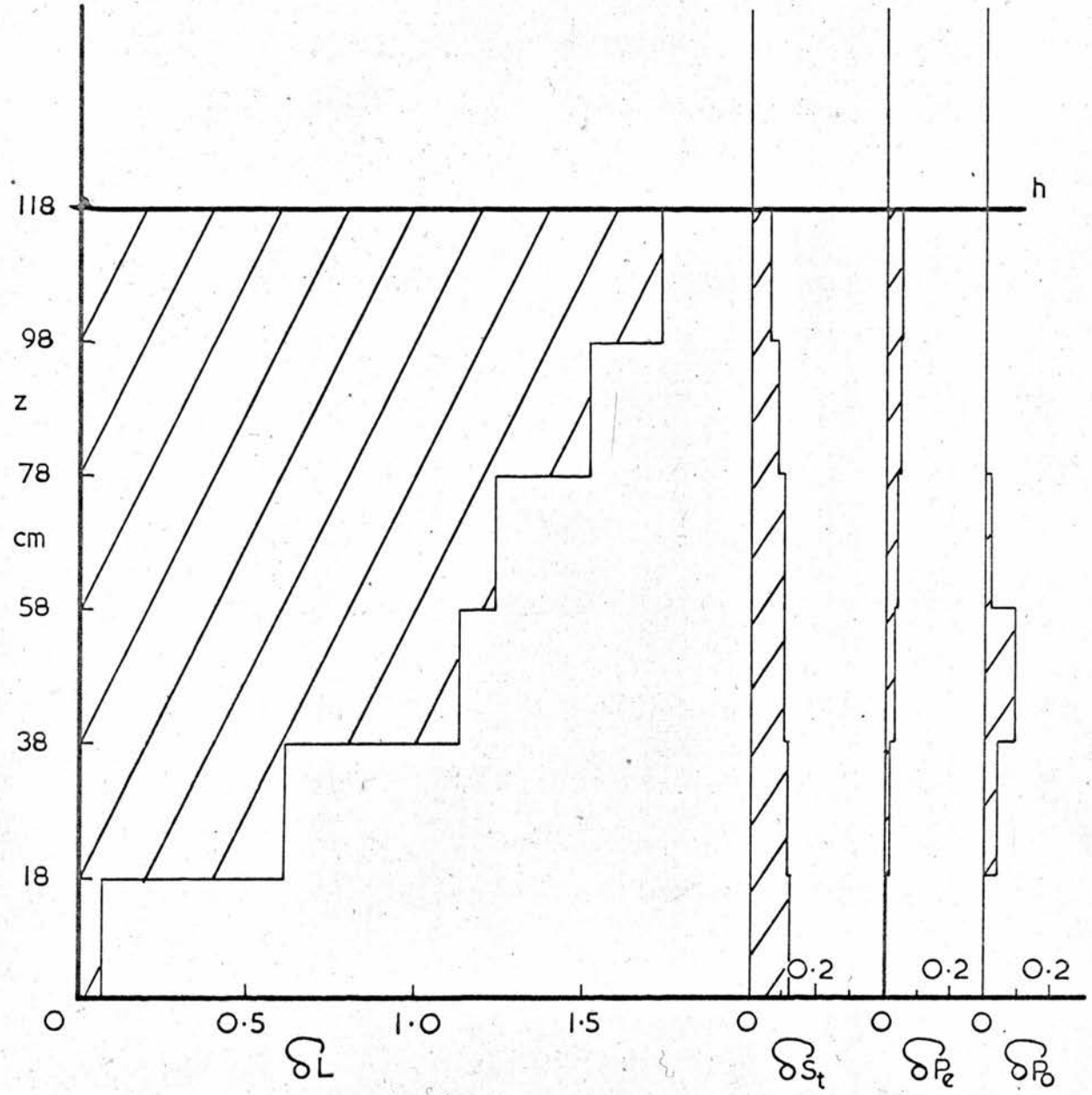

FIGURE 5.1 Stratified area indices; from Table 5.1.
δL: leaves. δS_t: stalks. δP_e: peteoles.
δP_o: pods.

TABLE 5.2

Z cm.	5	25	50	75	100	125	150	200	250	300	Group
G.M.T.	u cm. sec.$^{-1}$										
0											
1	6	6	7	5	-	15	16	23	61	67	A
2	6	6	7	5	-	-	17	19	51	57	A
3	7	7	7	6	-	22	19	31	68	74	A
4	9	9	9	9	15	33	37	51	86	94	B
5	9	9	9	9	-	26	26	33	63	65	A
6	9	9	10	11	20	47	58	79	102	109	B
7	15	15	16	19	37	70	98	119	143	152	C
8	22	23	23	29	50	94	133	163	185	200	D
9	24	25	26	30	59	99	140	172	197	209	D
10	25	30	31	40	79	130	181	218	251	270	E
11	25	30	33	44	72	122	167	209	238	259	E
12	25	33	36	46	69	125	177	218	251	272	E

TABLE 5.2 (Continued)

Z cm.	5	25	50	75	100	125	150	200	250	300	Group
G.M.T.	u cm. sec.$^{-1}$										
12											
13	29	40	42	49	71	122	172	211	240	259	E
14	30	43	45	54	87	137	196	239	272	293	F
	33	45	45	55	87	143	202	250	283	304	F
15											
16	32	42	42	50	76	123	184	225	256	278	E
17	25	28	28	37	69	112	161	196	225	241	-
	23	23	25	34	57	97	145	179	205	219	D
18											
19	22	23	24	32	64	102	148	181	209	227	D
20	15	15	17	20	42	71	103	128	154	164	C
	12	13	14	19	34	65	86	116	145	156	C
21											
22	9	9	10	9	15	24	29	43	74	79	B
23	10	12	12	11	15	27	29	51	74	79	B
	9	9	10	9	14	22	22	31	71	75	A
24											

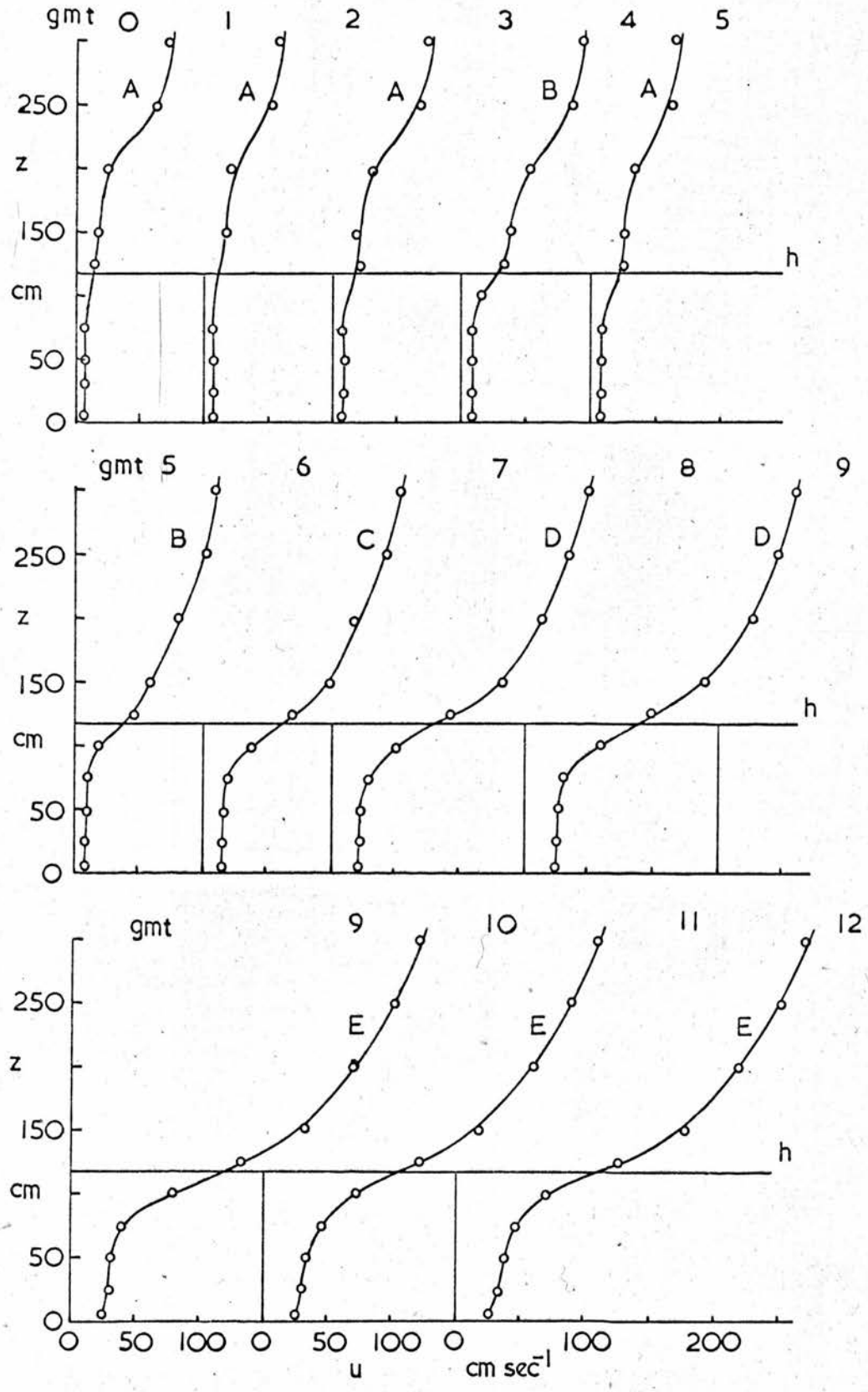

FIGURE 5.2 Profiles of hourly mean wind speed; 7th July 1966; from Table 5.2.

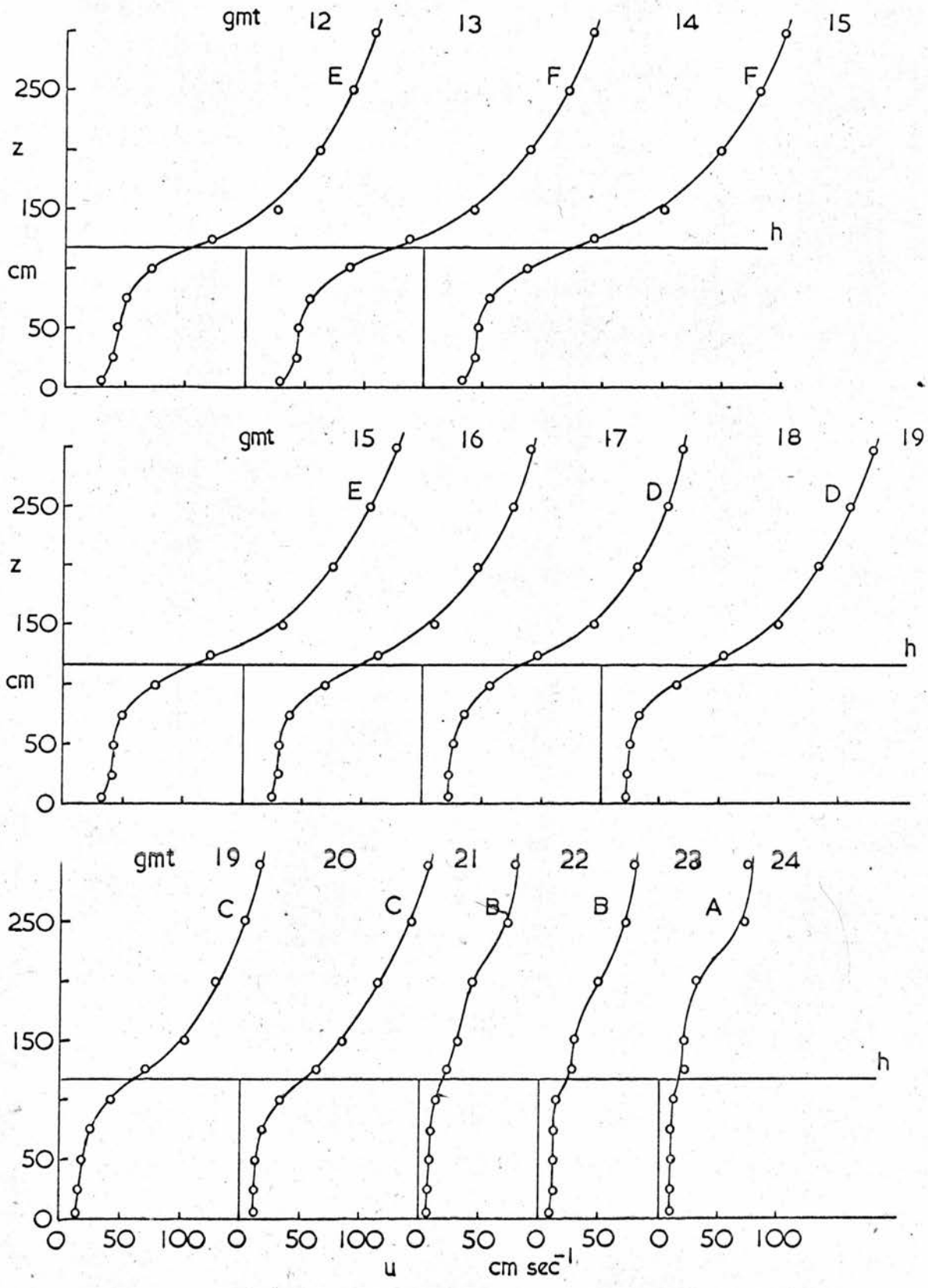

FIGURE 2(Contd.): Profiles of hourly mean wind speed; 7th July 1966; from Table 5.2.

TABLE 5.3

	Group	A	B	C	D	E	F
	z cm.	u(z) cm. sec.$^{-1}$					
	300	68	90	157	214	268	299
	250	63	84	147	199	247	278
	200	27.2	53	121	174	216	245
	150	20.0	38	96	142	176	199
i	125	19.6	33	69	98	125	140
	118	16.0	27.0	61	88	112	125
1	108	13.7	21.5	50	71	87 —	105
	98	11.4	16.0	39	55	72	85
2	88	9.4	13.1	31.6	46	61 —	74
	78	7.6	11.9	24.2	35	49	62
3	68	7.5	11.0	21.4	31	45 —	56
	58	7.5	10.5	18.7	26.5	40	49
4	48	7.5	10.0	17.2	25.2	38 —	47
	38	7.4	9.5	15.7	24.0	35	46
5	28	7.4	9.0	15.2	23.2	34 —	44
	18	7.4	8.5	14.7	22.5	33	42
6	8	7	8	12	20	25 —	30

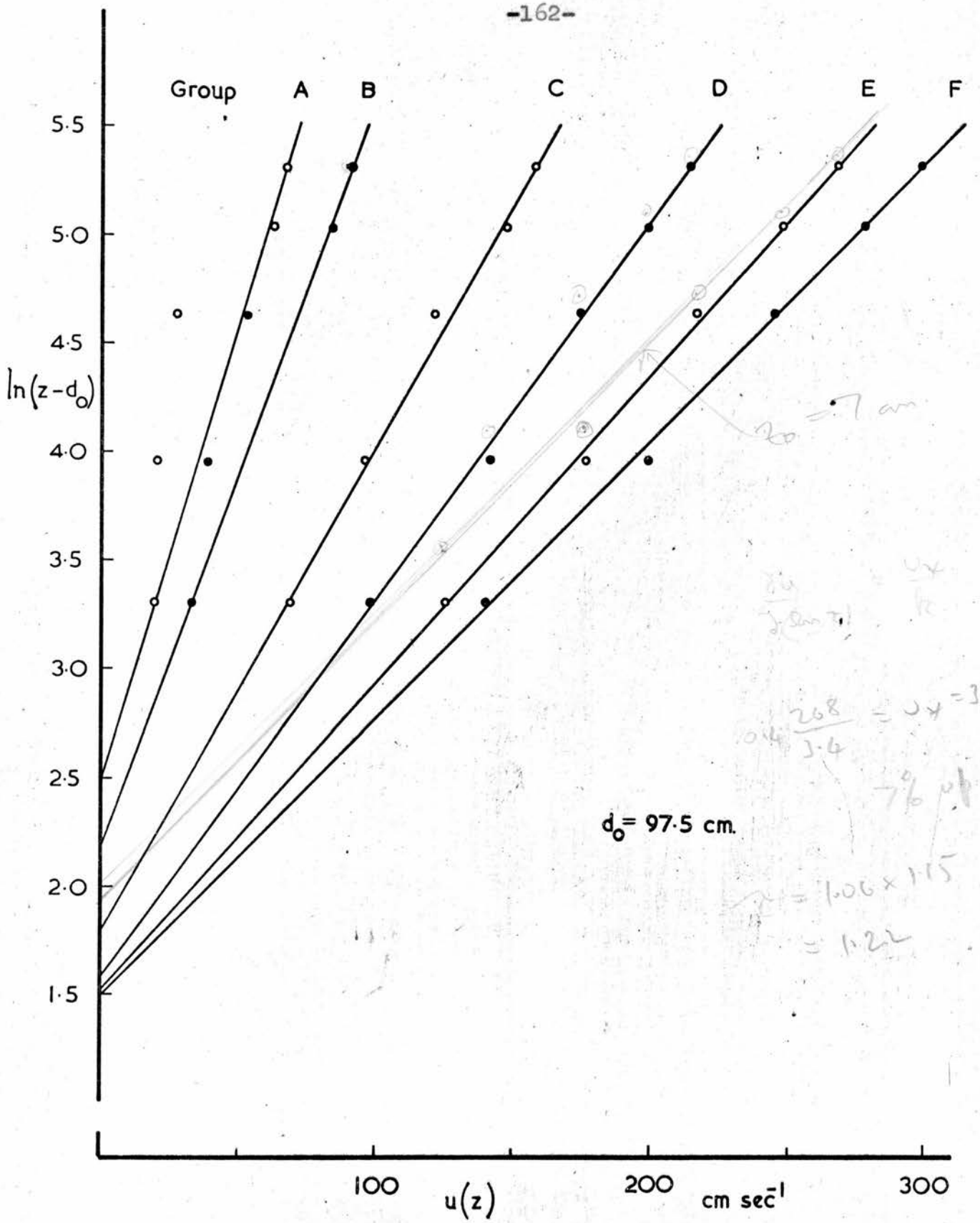

FIGURE 5.3 $\ell n(z - d_o)$ versus $u(z)$; from Table 5.3.

for $z < h$: the latter values of $u(z)$ were obtained from Fig. 5.2.

5.2 Wind Drag on the Crop

5.2(a) Calculation of the shearing stress τ in the flow above the crop

For each wind speed group, $\ell n(z - d_o)$ was plotted against $u(z)$, $z > h$, for each of d_o equal to 90, 95, 100 and 105 cm. Neglecting groups A and B, for which the lower recorded wind speeds were unreliable owing to stopping of the cups, the intermediate value of d_o, equal to 97.5 cm., was found to give a good straight line fit between $\ell n(z - d_o)$ and the observed values of $u(z)$ (1.1(c), 3.3(a)) for each of the other wind speed groups. Due to the non-ideal nature of the field data (which Fig. 5.3 demonstrates) this determination of d_o is subject to a large uncertainty (say $\pm$ 10 cm.). However, it was not unreasonable to assume d_o independent of wind speed and equal to 97.5 cm. - at least as a first approximation (see 5.3(d)).

Figure 5.3 shows, for each wind speed group, $\ell n(z-d_o)$ plotted against $u(z)$ for $d_o = 97.5$ cm. For groups C, D, E and F the best line was drawn by eye, while for groups A and B the line was ruled through the points appropriate to $z = 125$ and $z = 300$ cm. only. A value of u_* was derived from the gradient of each line (Eq. (3.7))

TABLE 5.4

Group	A	B	C	D	E	F
u_* cm. sec.$^{-1}$	9.5	11.4	17.9	23.4	29.5	31.8
z_o cm.	12.2	9.0	6.0	4.8	4.6	4.5
$u(h)/u_*$	1.69	2.37	3.40	3.76	3.80	3.93
$u(d_o+150$ cm.) cm. sec.$^{-1}$	62	90	152	210	265	295

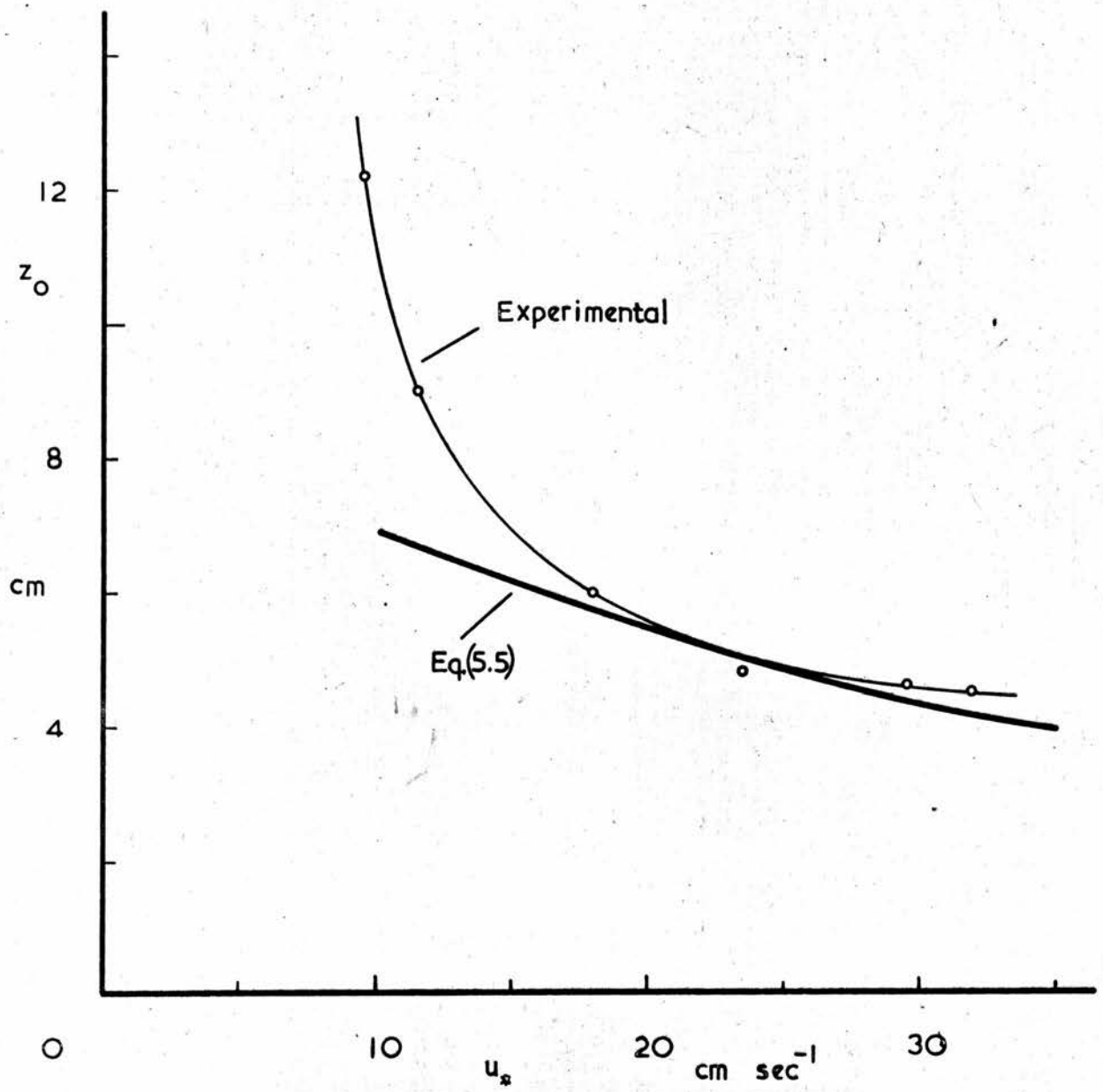

FIGURE 5.4 Measured behaviour of z_o with u_* ; from Table 5.4: and the predicted "maximum possible" rate of decrease in z_o with u_* ; from Table 5.12.

and the corresponding values of z_o from the intercepts on the $\ell n(z - d_o)$ axis. Table 5.4 records these values of u_* and z_o, together with the values of the dimensionless resistance $u(h)/u_*$ and the reference wind speed $u(d_o + 150 \text{ cm.})$ appropriate to each wind speed group: the roughness length z_o is shown plotted against u_* in Fig. 5.4. The experimental points on this Figure compare favourably with those on Figure 3 of Monteith's (1963) paper, where the roughness length of the 1961 bean crop at Rothamsted is shown plotted against $u(d_o + 1.5 \text{ metres})$ as a reference wind speed. Both Figures indicate an increase in roughness length as wind speeds fall - an increase most marked, however, in the wind speed range ($u_* < 15$ cm. sec.$^{-1}$; $u(d_o+150 \text{ cm}) < 150$ cm. sec.$^{-1}$) where the very nature of the field data (groups A and B) precludes any meaningful determination of z_o. It is possible, therefore, that such high values of z_o at low wind speeds are spurious (see (5.3(c)).

Each value of u_* in Table 5.4 was used in Eq. (1.2) together with ρ equal to 1.22×10^{-3} gm. cm.$^{-3}$, to determine a value of the shearing stress τ in the following Table.

TABLE 5.5

Group	A	B	C	D	E	F
τ dyne cm.$^{-2}$	0.11	0.16	0.39	0.67	1.06	1.23

5.2(b) Calculation of the drag f on an "equivalent" 1 cm.^{2} column of crop.

Eq. (1.17) was written in the finite difference form

$$f = \rho \sum_{i=1}^{6} u_i^2 \left[(\delta L)_i . C_d(u_i, \phi) + ((\delta S_t)_i + \frac{2}{\pi}(\delta P_e + \delta P_o)_i . C'_d \right]$$

$$= (\text{drag on leaves, } f_L) + (\text{drag on stalks, peteoles and pods, } f_S)$$

(5.1)

where $C_d(u_i, \phi)$ is the drag coefficient, available from Fig. 4.6, of a typical (average size) bean leaf, and C'_d is a drag coefficient representative of cylindrical objects at Reynolds' numbers between 10^2 and 10^3: for simplicity C'_d was assumed independent of wind speed, and equal to 0.5. The factor $2/\pi$ recognises the random orientations of the peteoles and pods in comparison with the stalks, which latter are generally vertical and therefore normal to a horizontal flow.

Taking the stratified area indices from Table 5.1 and each u_i from Table 5.3, and choosing -23° as a reasonable mean value for ϕ within the canopy, f_L and f_S were calculated for group E in Table 5.6, to give f equal to 4.4 dyne cm.$^{-2}$, or over four times the corresponding value of τ. Considering the relative sizes of f_L, f_S and τ, it was not possible to choose ϕ so that f would be equal to τ.

However, if the conclusion of Section 3.2(b) regarding drag coefficients within the canopy is accepted, and if each u_i can be regarded as a good measure of the mean speed of the wind blowing past each bean plant at the level z_i, then the above discrepancy between f and τ can be explained in terms of a shelter effect alone; many of the individual leaves and much of each stalk and peteole system being effectively sheltered by leaves immediately to windward.

Before values of $K_M(z)$ within the canopy could be determined, some plausible means had to be found to incorporate the effect of shelter into the calculation of f, in such a way that f would be equal to τ.

5.2(c) The "shelter factor" p, equal to f/τ

The ratio between the force (per cm.^{2}), f, calculated from Eq. (5.1) and the shearing stress τ was named the "shelter factor", and given the symbol p.

As a first approximation, the actual force on each layer $(\delta z)_i$ of crop was defined to be f_i/p, (Table 5.6), and Eq. (1.18) was used in finite difference form to determine $\tau(z)$ at several levels within the canopy. These values of $\tau(z)$ were then inserted in Eq. (1.19), together with appropriate $\partial u(z)/\partial z$ deduced from Table 5.3, to give the "first estimates" of $K_M(z)$, for group E, which are plotted against z in Fig. 5.5, (1).

The major assumptions embodied in the preceding determination of $\tau(z)$ are:

TABLE 5.6 Group E $\phi = -23^{\circ}$; p = 4.25

z cm.	i	u_i cm. sec.$^{-1}$	$C_d(u_i)$	$(f_L)_i$ dyne cm.$^{-2}$	$(f_S)_i$ dyne cm.$^{-2}$	f_i dyne cm.$^{-2}$	f_i/p dyne cm.$^{-2}$	$\tau(z)$ dyne cm.$^{-2}$	$\frac{\partial u(z)}{\partial z}$ sec.$^{-1}$	$K_M(z)$ cm.^{2} sec.$^{-1}$
118								1.060		
108	1	87	0.115	1.84	0.39	2.23	0.525	0.780	2.00	319
98								0.535	1.32	333
88	2	61	0.120	0.82	0.24	1.06	0.250	0.385	1.13	279
78								0.285	0.79	296
68	3	45	0.125	0.38	0.17	0.55	0.129	0.212	0.45	386
58								0.156	0.37	345
48	4	38	0.130	0.25	0.15	0.40	0.094	0.103	0.28	301
38								0.062	0.20	254
28	5	34	0.135	0.11	0.10	0.21	0.050	0.031	0.14	181
18								0.012	0.42	23
8	6	25	0.145	0.01	0.04	0.05	0.012	-	-	-

3.41	1.09	4.50	1.06	1.06
f_L	f_S	f	f/p	$\tau(h)$
	dyne cm.$^{-2}$			

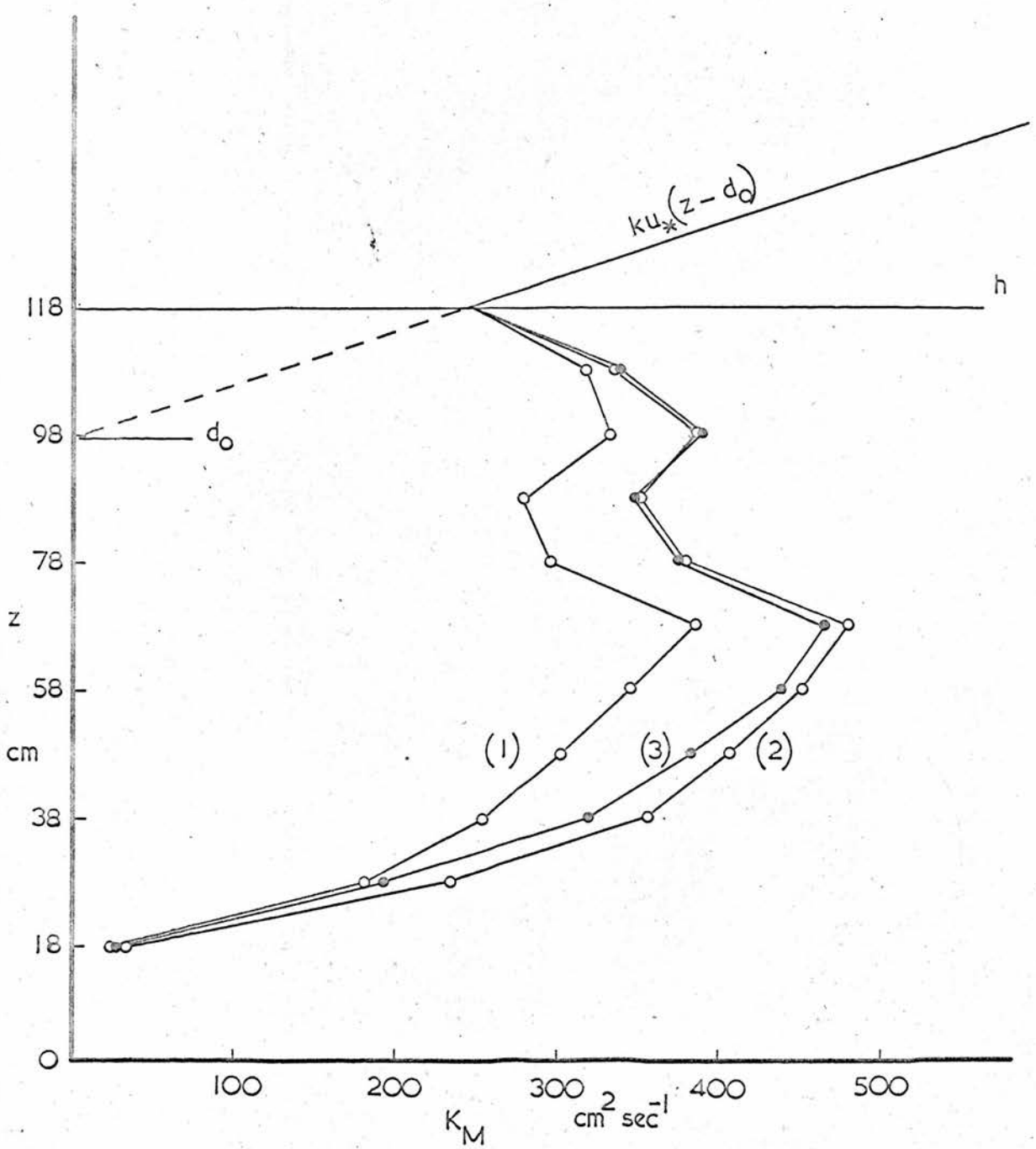

FIGURE 5.5 Measured values of $K_M(z)$ within the canopy (group E wind speeds):

(1) ϕ = constant = -23°, p = constant = 4.25 ; Table 5.6.

(2) ϕ = constant = -23°, $p = p(u_i)$; Table 5.8.

(3) $\phi = \phi(u_i)$, $p = p_o$ = constant = $3.71 \doteq 4$; Table 5.9.

(i) that ϕ has the same mean value, -23°, at all levels in the canopy;

(ii) that p has the same value, 4.25, at all levels in the canopy, and

(iii) that p is the same for stalks etc. as it is for leaves.

Included in (ii) is the assumption that p is independent of the local densities of crop elements (specified by $(\delta L)_i$, $(\delta S_t)_i$ etc.), an assumption which, although obviously weak (p must tend to unity in sparse foliage), defies objective investigation, and is incorporated, together with assumption (iii), in the following analyses. However, (i) and (ii) could be investigated; for these assumptions require, or imply, that neither ϕ nor p should change with wind speed: accordingly, p was calculated (Table 5.7) for each wind speed group for each of three chosen (constant) mean values of ϕ, namely -37°, -23° and 0°. (Obviously p depends on the choice of ϕ in Eq. (5.1)). Requisite values of $C_d(u_i,\phi)$ were derived from Fig. 5.6 (prepared from Fig. 4.6 and additional data). Fig. 5.7 shows p plotted against the chosen, reference, wind speed u_{98} = u(98 cm.), for each ϕ, and demonstrates marked dependence of the "shelter factor" not only (inevitably) on the arbitrary choice of ϕ, but also on wind speed. By equating u_{98} to u(z) within the canopy, this experimental correlation between

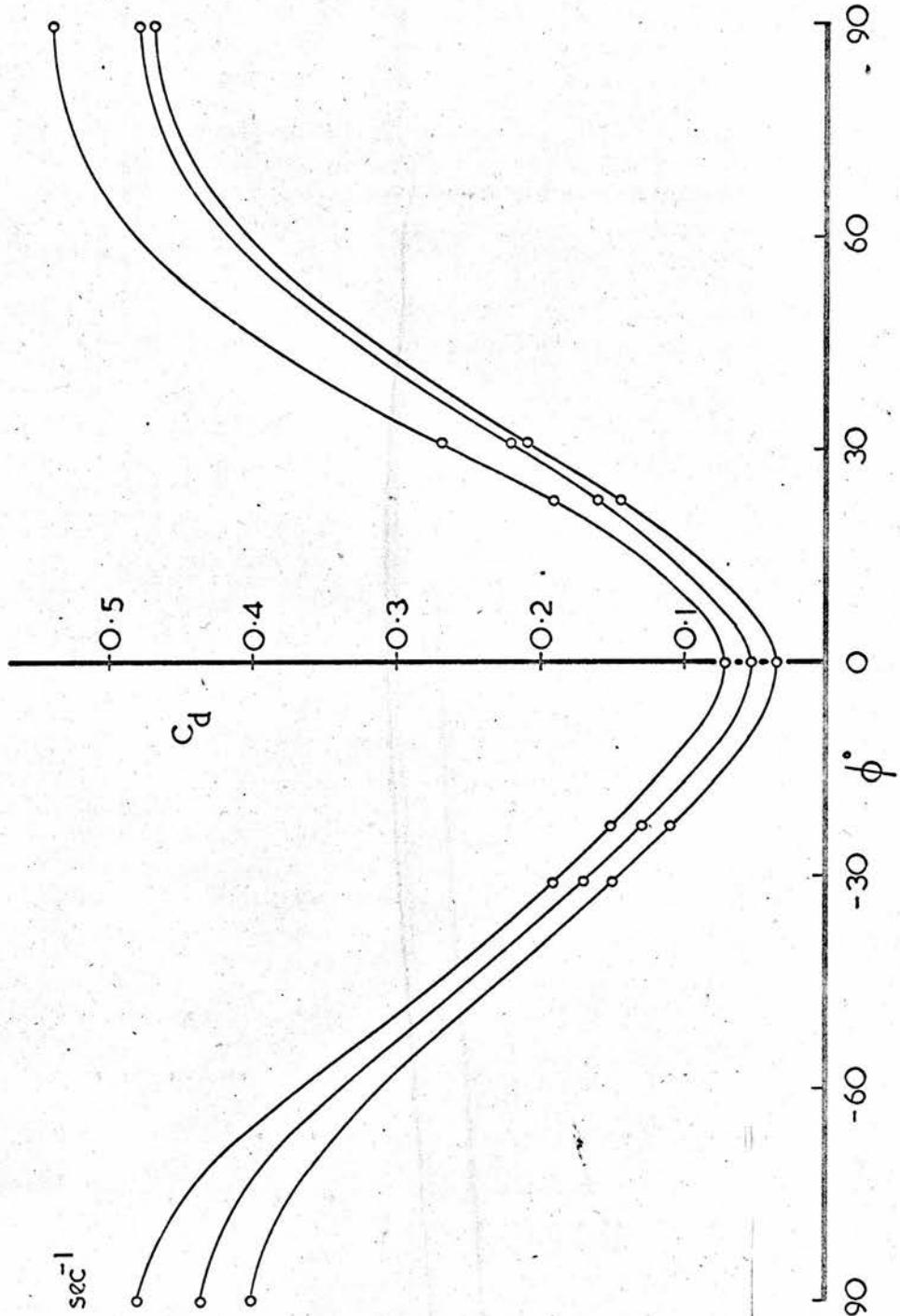

FIGURE 5.6 C_d as a function of ϕ at several wind speeds.

TABLE 5.7

ϕ	Group	A	B	C	D	E	F
-	f_S dyne cm.$^{-2}$	0.036	0.067	0.29	0.62	1.09	1.67
-	τ dyne cm.$^{-2}$	0.11	0.16	0.39	0.67	1.06	1.23
-	u_{98} cm. sec.$^{-1}$	11	16	39	55	72	85
-37°	f_L dyne cm.$^{-2}$	0.25	0.49	1.98	3.74	5.95	8.50
-23°		0.14	0.26	1.09	2.10	3.41	4.87
0°		0.085	0.13	0.45	0.77	1.17	1.61
-37°	$f = f_L + f_S$ dyne cm.$^{-2}$	0.286	0.557	2.27	4.36	7.04	10.17
-23°		0.176	0.327	1.38	2.72	4.50	6.54
0°		0.121	0.197	0.74	1.39	2.26	3.28
-37°	$p = f/\tau$	2.60	3.48	5.82	6.51	6.64	8.28
-23°		1.60	2.04	3.54	4.06	4.25	5.30
0°		1.10	1.23	1.90	2.07	2.13	2.67

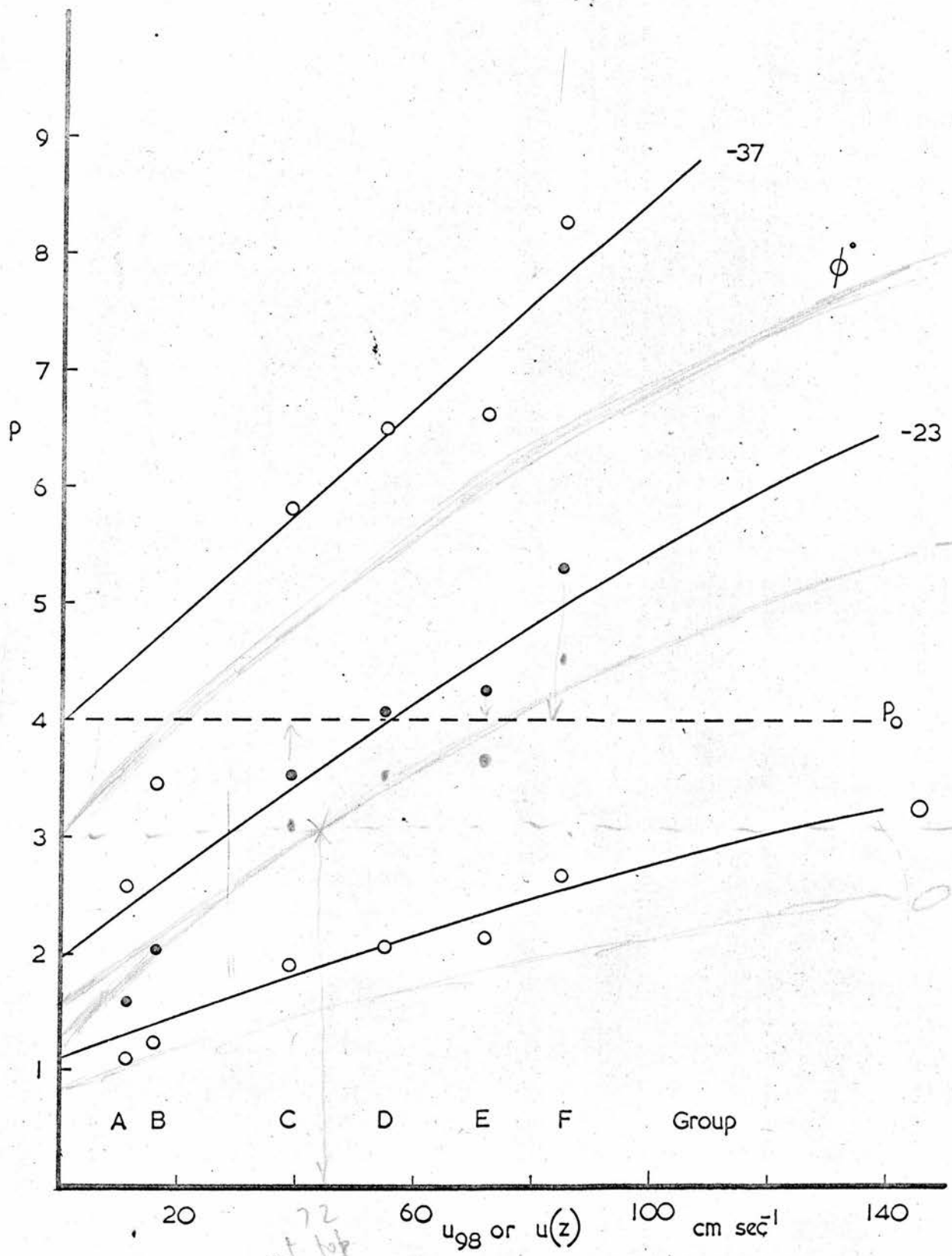

FIGURE 5.7 The "shelter factor" p versus the reference wind speed u(98 cm.); from Table 5.7. The "true" shelter factor p_o is shown equal to 4.

TABLE 5.8 Group E $\phi = -23^{\circ}$; $p = p(u)$ from Fig. 5.7

z cm.	i	f_i dyne cm.$^{-2}$	u_i cm. sec.$^{-1}$	$p_i(u_i)$	f_i/p_i	$\tau(z)$ dyne cm.$^{-2}$	$\frac{\partial u(z)}{\partial z}$ cm. sec.$^{-1}$	$K_M(z)$ cm.^{2} sec.$^{-1}$
118						1.060		
108	1	2.23	87	5.1	0.439	0.820	2.00	335
98						0.621	1.32	386
88	2	1.06	61	4.2	0.256	0.485	1.13	352
78						0.365	0.79	379
68	3	0.55	45	3.6	0.157	0.275	0.45	501
58						0.208	0.37	462
48	4	0.40	38	3.4	0.121	0.140	0.28	407
38						0.087	0.20	357
28	5	0.21	34	3.2	0.069	0.040	0.14	235
18						0.018	0.42	35
8	6	0.05	25	2.9	0.018	-	-	-

p and u_{98} for different wind speed groups was translated into a variation of p with $u(z)$ within any one wind speed group (i.e. profile), and used in Table 5.8, again for group E with $\phi = -23^{\circ}$, to obtain revised values of $\tau(z)$ and $K_M(z)$: each p_i, equal to $p(u(z_i))$, was obtained from Fig. 5.7 and applied to the appropriate value of f_i so that the sum $\sum_{i=1}^{6} (f_i/p_i)$ was equal to τ. Those values of $K_M(z)$ are shown in Fig. 5.5, (2), to be significantly greater than the original values (1).

However, it is likely that the calculated increase in p with u_{98} was more an artefact of holding ϕ constant than a result of a real increase in shelter effect with wind speed. It therefore seemed more plausible to attribute this calculated increase in p to a real decrease in ϕ with wind speed, due to streamlining, and the following form of analysis was investigated.

5.2(d) The "true" shelter factor p_o

The introduction of a "true" shelter factor p_o, assumed independent of wind speed, enabled the use of Fig. 5.7 to derive a likely rate of decrease in ϕ with wind speed. A line was drawn through each set of points on Fig. 5.7, little weight being placed on the points representing groups A and B. The line for $\phi = -37^{\circ}$ was restricted to pass through $p = 4$ at $u_{98} = 0$, and this value was assigned to p_o. The subsequent inter-

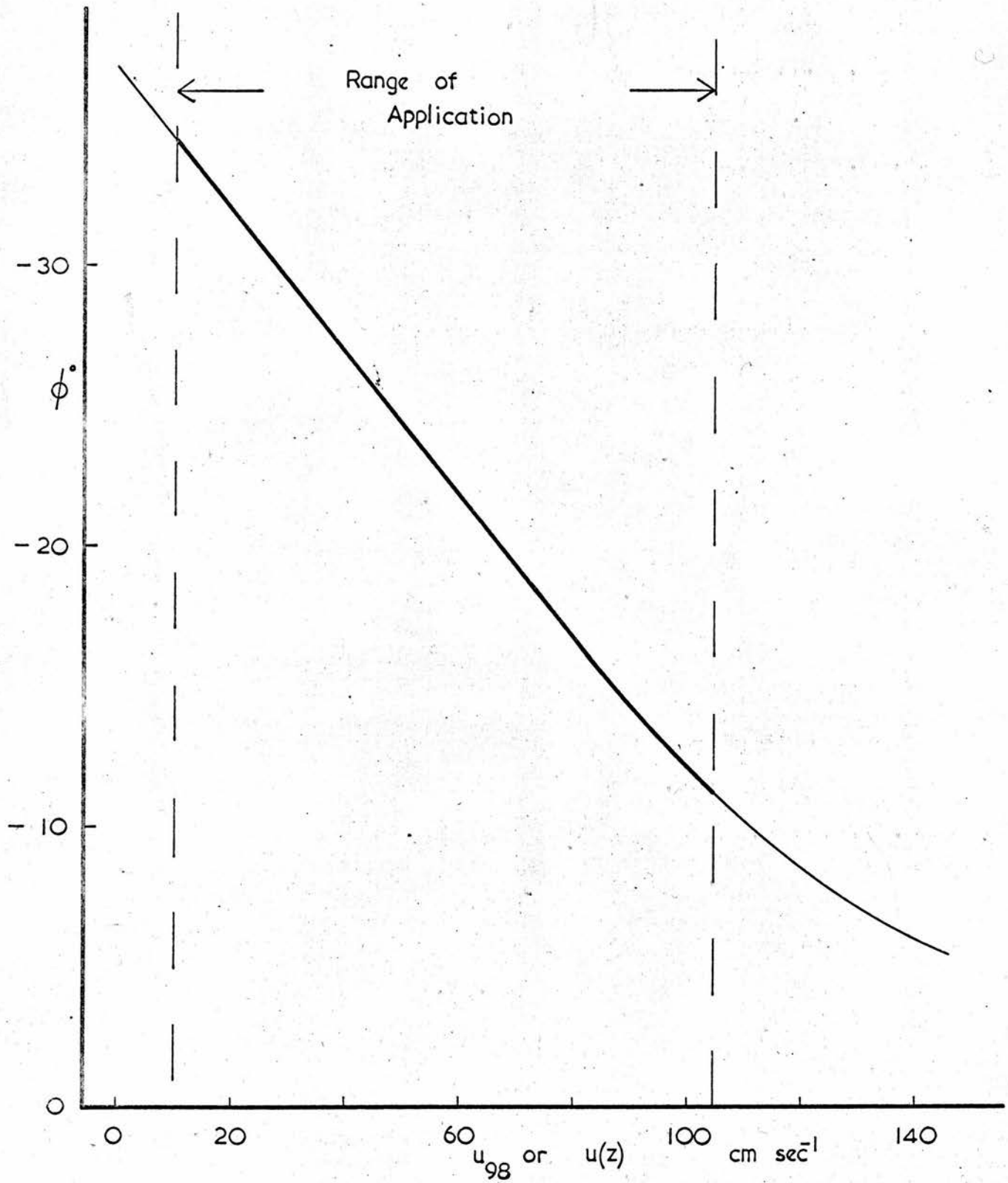

FIGURE 5.8 Variation in ϕ with u(98 cm.) predicted by Fig. 5.7 when $p = p_o = 4$.

TABLE 5.9 Group E $\phi = \phi(u)$ from Fig. 5.8; $p = p_o$, (actual value of p_o was 3.71).

z cm.	i	$(f_S)_i$ dyne cm.$^{-2}$	u_i cm. sec.	$\phi_i(u_i)$ deg.	$C_d(\phi_i, u_i)$	$(f_L)_i$ dyne cm.$^{-2}$	f_i dyne cm.$^{-2}$	f_i/p_o dyne cm.$^{-2}$	$\tau(z)$ dyne cm.$^{-2}$	$\frac{\partial u(z)}{\partial z}$ sec.$^{-1}$	$K_M(z)$ cm.^{2} sec.$^{-1}$
118									1.060		
108	1	0.39	87	-15	0.076	1.21	1.60	0.432	0.822	2.00	337
98									0.628	1.32	390
88	2	0.24	61	-22	0.11	0.75	0.99	0.267	0.480	1.13	348
78									0.361	0.79	375
68	3	0.17	45	-26	0.14	0.43	0.60	0.162	0.267	0.45	486
58									0.199	0.37	440
48	4	0.15	38	-27	0.15	0.30	0.45	0.121	0.131	0.28	384
38									0.078	0.20	320
28	5	0.10	34	-28	0.16	0.14	0.24	0.065	0.033	0.14	193
18									0.013	0.42	25
8	6	0.04	25	-31	0.18	0.01	0.05	0.013	-	-	-

-178-

section of the line $p_o = 4$ with the line for $\phi = -23^\circ$ occurred at $u_{98} = 55$ cm. sec.$^{-1}$, and with the line for $\phi = 0^\circ$ would occur at some very high wind speed. On this basis the curve on Fig. 5.8 was drawn: and the demonstrated decrease in ϕ with u_{98} was translated into a decrease in ϕ with $u(z)$ within the canopy. (N.B. the assumption $\phi = -37^\circ$ when $u_{98} = u(z) =$ zero is not inappropriate: it can be shown that the mean value of $\sin \phi$ for a large number of leaves in a bean canopy under calm conditions is about 0.6, for which $\phi = -37^\circ$).

In Table 5.9, again for group E, each $(f_L)_i$ was calculated using the appropriate value of $C_d(u_i, \phi)$ derived from Fig. 5.6 when $\phi = \phi(u_i)$ from Fig. 5.8. Each value of f_i was then divided by p_o (here "adjusted" to 3.71) so that the sum $\sum_{i=1}^{6} f_i/p_o$ was equal to τ. The resultant values of $K_M(z)$ are shown in Fig. 5.5,(3) to be again (as (2)) about 30 per cent greater than the original values ((1)).

The form of analysis most in accord with reality probably lies between the two preceding forms; a decrease in ϕ with wind speed less than suggested by Fig. 5.8 being accompanied by an increase in the "true" shelter factor p_o to account for progressive bunching of leaves as wind speeds increase.

5.3 Properties Determined for the Bean Crop

5.3(a) $K_M(z)/u_*$ within the canopy

The form of analysis investigated in Section 5.2(d), Table 5.9, was adopted to determine values of $K_M(z)/u_*$ within the canopy for groups C, D, E and F. The results are presented in Table 5.10 and Fig. 5.9.

Above the canopy $K_M(z)/u_*$ is equal to $k(z - d_o)$, Eq. (1.15), and is independent of wind speed (provided d_o is, or is assumed, independent of wind speed.). Fig. 5.9 shows the behaviour of $K_M(z)/u_*$ within the canopy to be broadly similar to that determined for the artificial crop (Fig. 3.18): i.e. $K_M(z)/u_*$ is approximately constant between $z = h$ and $z =$ (about $h/4$), but about 45 per cent greater than $K_M(h)/u_*$ from Eq. (1.15) (see 3.4(a)).

5.3(b) The resistances $\bar{R}_D$ and $\bar{r}_d/S_d$

The heavy line drawn on Fig. 5.9 was assumed to define $K_M(z)/u_*$ as a function of z. The method of Section 3.4(b) was then used, in Table 5.11, to obtain a first estimate of the canopy resistance $\bar{R}_D$ for a chosen wind speed group, group E. Each $u_*(R_D)_i$ in Table 5.11 is the integral of $u_*/K_M(z)$ between $z = z_i$ and $z = h$. By weighting each $u_*(R_D)_i$ with the corresponding value of the "true" force f_i/p_o, from Table 5.9, and dividing by the value of u_* appropriate to group E, namely 29.5

TABLE 5.10

Group	C	D	E	F
u_*	17.9	23.4	29.5	31.8
z cm.	$K_M(z)/u_*$ cm.			
118	8.2	8.2	8.2	8.2
108	11.5	10.6	11.4	12.6
98	9.3	9.6	13.2	13.0
88	7.5	8.1	11.8	13.7
78	8.2	8.2	12.7	13.4
68	11.5	11.8	16.5	14.3
58	10.7	12.8	14.9	15.4
48	10.0	17.5	13.0	31.4
38	9.2	14.0	10.8	18.8
28	8.3	10.9	6.5	7.7
18	0.7	2.0	0.9	1.2
c cm.	90	88	85	83

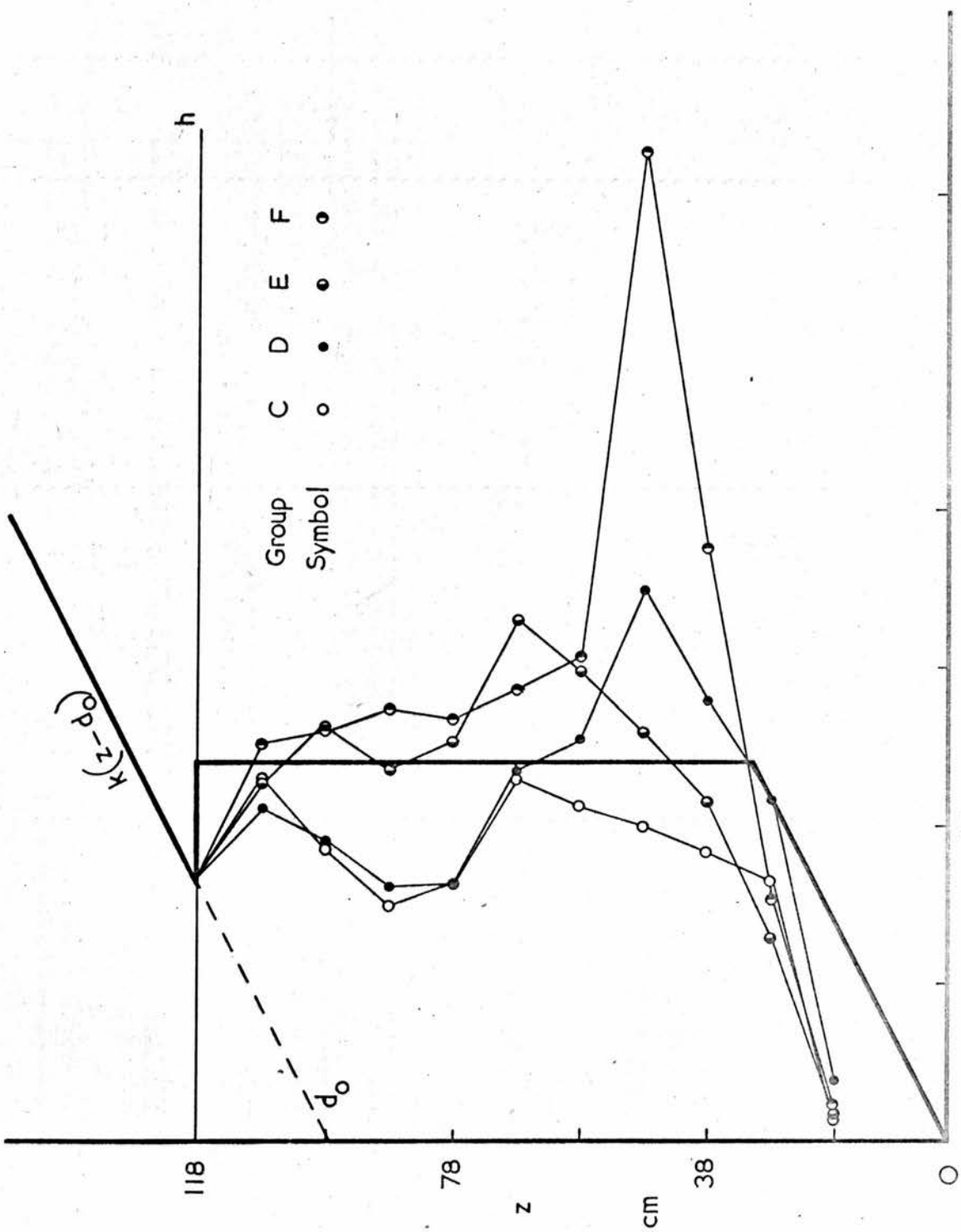

FIGURE 5.9 Measured values of $K_M(z)/u$ within the canopy; From Table 5.10.

cm. sec.$^{-1}$, the value 0.097 sec. cm.$^{-1}$ was found for $\bar{R}_D$, in comparison with $r_D(h)$ equal to 0.13 sec. cm.$^{-1}$ (derived from Table 5.4). However, a more reliable value for $\bar{R}_D$ (i.e. a value independent of measured $K_M(z)$) was determined using the indirect method of Section 3.4(c). Eq. (3.16) was written, with reference to Eq. (5.1), in the form

$$u_m^2(C_d(u_m,\phi(u_m))L/p_o + C'_d(S_t + \frac{2}{\pi}P_e + \frac{2}{\pi}P_o)/p_o) = u_*^2 \qquad (5.2)$$

(u_m is the fictitious uniform wind speed within the canopy which would give the same drag force as the original wind profile: i.e., same τ; same u_*; same z_o; only, a larger d_o.) The shelter effect is accommodated by dividing each area index by the "true" shelter factor p_o: the reduced index L/p_o, for example, could be considered the "effective" leaf area index for momentum transfer.

For wind speed group E : u_* = 29.5 cm. sec.$^{-1}$ and p_o = 3.71 (Table 5.9). Values of the area indices were derived from Table 5.1 and, using C'_d = 0.5, Eq. (5.2) was simplified to

$$u_m^2(C_d(u_m, \phi(u_m)) + 0.06) = 490 \qquad (5.3)$$

This equation was then solved by a method of successive approximations (involving Figs. 5.6 and 5.8) to give: u_m = 52 cm. sec.$^{-1}$; $\phi(u_m) = 22.5^\circ$; and $C_d(u_m,\phi(u_m))$=

= 0.125. Eq. (3.15) was then applied, with u(h) equal to 112 cm. sec.$^{-1}$ to give $\bar{R}_D$ = 0.07 sec. cm.$^{-1}$:- the canopy resistance at $u_* \doteq$ 30 cm. sec.$^{-1}$.

The resistance $\bar{r}_d/S_d$ of the crop elements themselves was obtained directly, being equal to u_m/u_*^2 or 0.06 sec. cm.$^{-1}$ (3.4(d)). However, as two types of crop element are recognised by the presence in Eq. (5.1) of two independent drag coefficients C_d and C_d', $\bar{r}_d/S_d$ must be a composite resistance, formed by suitable parallel combination of the resistance $(p_o\, r_d/L)$ for leaves and the resistance $p_o\, r_d'/(S_t + \frac{2}{\pi} P_e + \frac{2}{\pi} P_o)$ for stalks etc. Therefore, although the quantity $\bar{r}_d/S_d$ has meaning, neither $\bar{r}_d$ nor S_d can be given individual identity. It can however be shown, by the method of Section 3.4(d), that this composite resistance $\bar{r}_d/S_d$ is about two thirds of the mean value of $(p_o\, r_d/L)$ found if the drag on the leaves alone is considered.

5.3(c) Predicted variation in z_o with u_* (d_o assumed constant)

Using the value of the canopy resistance derived in the previous Section for $u_* \doteqdot 30$ cm. sec.$^{-1}$, namely $\bar{R}_D = 0.07$ sec. cm.$^{-1}$, Eq. (3.17) was written in the form

$$\frac{u(h)}{u_*} = 2.1 + \frac{u_* \bar{r}_d}{S_d} \qquad (5.4)$$ †

similar to Eq. (3.18) (see 3.4(e)). It was then assumed, for purposes of demonstration, that the "maximum possible" effect of streamlining on the behaviour of $\bar{r}_d/S_d$ would be to make this resistance independent of wind speed (i.e., the corresponding drag coefficient $\propto$ (wind speed)$^{-1}$); and in this way Eq. (5.4) was simplified to

$$\frac{u(h)}{u_*} = 2.1 + 0.06\, u_* \qquad (5.5)$$ †

from which the values of $u(h)/u_*$ recorded in Table 5.12 were calculated. The corresponding values of z_o, derived from Eq. (1.13) with $d_o = 97.5$ cm., were plotted on Fig. 5.4 to demonstrate the "maximum possible" rate of decrease in z_o with u_*. The "true" rate of decrease in z_o with u_* is likely to be even less than this, so that the markedly high values of z_o found by

† See Appendix

TABLE 5.11

i	$u_*(R_D)_i$	f_i/p_o dyne cm.$^{-2}$	$(f_i/p_o).u_*(R_D)_i$ dyne cm.$^{-2}$
1	0.83	0.432	0.36
2	2.50	0.267	0.67
3	4.17	0.162	0.68
4	5.83	0.121	0.70
5	7.50	0.065	0.49
6	10.8	0.013	0.14

$\overline{R}_D = \sum_{i=1}^{6} f_i(R_D)_i/f$; $u_* = 29.5$ cm. sec.$^{-1}$; so that

$\overline{R}_D = 0.097$ sec. cm.$^{-1}$

TABLE 5.12

u_* cm. sec.$^{-1}$	10	15	20	25	30	35
$\frac{u(h)}{u_*}$	2.7	3.0	3.3	3.6	3.9	4.2
z_o cm. (d_o = 97.5 cm.)	6.9	6.2	5.5	4.8	4.3	3.9

† See Appendix

experiment at low wind speeds must be regarded as spurious (5.2(a)).

The empirical Equation (3.9) gives z_o = 8.2 cm., in comparison with experimentally determined values around 5 cm.

5.3(d) Changes if d_o is equated to c.

Equality between the zero plane displacement d_o of a crop and the level of action c at which the wind drag can be considered to act on the crop was suggested in Section 3.3(f).

The level c was calculated for each of groups C, D, E and F, and is shown in Table 5.10 to fall from 90 cm. at group C wind speeds to 83 cm. at group F wind speeds, much below the constant value d_o = 97.5 cm. previously chosen (5.2(a)). However, it can be shown by redrawing Fig. 5.3 that d_o = c is little less consistent with the experimental data for groups C to F than is d_o = 97.5 cm. Some accompanying changes in results are:-

(i) z_o is essentially independent of u_*, and equals about 8 cm. (Eq. (3.9) gives about z_o about 12 cm.)

(ii) values for u_* increase by about 15 per cent, so that the value 3, in place of 4, can be assigned to the "true" shelter factor p_o.

(iii) $K_M(h)/u_*$, equal to $k(h - d_o)$, increases by

about 50 per cent, whereas values for $K_M(z)/u_*$ within the canopy increased by about 15 per cent, to become only some 10 per cent greater than $K_M(h)/u_*$ (5.3(a)).

The magnitude of these changes emphasises the need for care in choosing a value for d_o. It is suggested, if no "better" value can be deduced, that the 0.75h should be used for the zero plane displacement of a mature bean crop. (Here 0.75h = 89 cm.)

5.4 Estimated Resistance of the Crop to Mass or Heat Transfer

5.4(a) A value for B^{-1}

The canopy resistance to mass or heat transfer $\bar{R}_o$ was equated to the canopy resistance to momentum transfer $\bar{R}_D$ (see 1.3(d)) so that Eq. (1.33) could be written in the simple form

$$B^{-1} = u_* \left(\frac{\bar{r}_o}{S_o} - \frac{\bar{r}_d}{S_d}\right) \qquad (5.6)$$

Just as L/p_o has been considered (5.3(b)) as the "effective" leaf area index for momentum transfer to the crop, the corresponding quotient L/p'_o can be defined as the "effective" leaf area index for mass or heat transfer. If it is assumed that all exchange of water vapour, carbon dioxide and (even) heat between a bean crop and the atmosphere occurs via the leaves alone, then S_o in

Eq. (5.6) is simply equal to L/p'_o. The shelter factor p'_o for mass or heat must be close to, but less than, the shelter factor p_o for momentum. The estimated value 3 ± 1 was assigned to p'_o, in comparison with $p_o = 4$. The resultant value of S_o, namely 2.1 ± 0.7, was then used in Eq. (5.6) to determine a value of B^{-1} for the bean crop.

The mean resistance $\bar{r}_o$ was conveniently equated to $r_o(u(d_o))$, and found from Eq. (4.23) (with $u = 72$ cm. sec.$^{-1}$ from Table 5.3; $d = 4.0$ cm.; and D or $\kappa = \nu$), to be 0.43 sec. cm.$^{-1}$ at $u_* \doteq 30$ cm. sec.$^{-1}$. (N.B. $\bar{r}_o$ is independent of ϕ.) Finally with $\bar{r}_d/S_d$ equal to 0.06 sec. cm.$^{-1}$ from Section 5.3(b)., B^{-1} was found to have the value 4 ± 2. There are few determinations of the parameter B^{-1} for vegetated surfaces available for comparison. Chamberlain (1966) deduced $B^{-1} = 5$ for water vapour over grass - $z_o = 1$ cm., $u_* = 25$ cm. sec.$^{-1}$ - and calculated from data of Pasquill (1949) and Rider (1954) the respective values $B^{-1} = 5.7$ and 3.9 for heat over grass - $z_o = 0.3$ cm., $u_* = 25$ cm. sec.$^{-1}$.

It is encouraging to note, in terms of Section 1.3(c), that the value of B^{-1} determined here for a bean crop, for which $z_o \doteq 5$ cm., is at least experimentally indistinguishable from the above values determined for surfaces with roughness lengths an order of magnitude less. This may allow a universal value of B^{-1}, say 4, to be used with a certain measure of confidence over any suitably vegetated surface (provided u_* lies between 15

and 45 cm. sec.$^{-1}$, say).

This positive value for B^{-1} shows that the crop as a whole has a higher resistance to mass or heat transfer r_0 than it has to momentum transfer r_D. E.g. with $B^{-1} = 4$ and choosing $u(h)/u_* = 3.8$ from Table 5.4, Eq. (1.27) gives $r_0(h) = 2.1\, r_D(h)$.

Fig. 5.10 demonstrates that, when $K_0(z) = K_M(z)$, $u_* . r_0(z)$ exceeds $u_* . r_D(z)$ by B^{-1} at all levels within the logarithmic part of the boundary layer. The non-dimensional resistance $u_* . r_D(z)$ is given by Eq. (1.13), while the corresponding value of $u_* . r_0(z)$ can be written

$$u_* . r_0(z) = \frac{1}{k} \ell n \left(\frac{z - d_o}{z'_o}\right) \qquad (5.7)$$

where

$$z'_o = z_o e^{-kB^{-1}} \qquad (5.8)$$

is the roughness length for mass or heat transfer (introduced by Chamberlain). For positive B^{-1}, z'_o is always less than z_o : this is further manifestation that such surfaces are less conducive to (i.e. less "rough" for) mass or heat transfer than they are to momentum transfer. However, the physical significance of the length z'_o is, to quote Chamberlain, "not to be overstressed."

5.4(b) Estimation of "mean surface conditions" of temperature and vapour pressure

Monteith (1963) plotted $T(z)$ and $e(z)$ against $u(z)$ to define straight lines with intercepts T_s and e_s on the axis $u = 0$. These values of temperature and vapour pressure were then attributed to an effective crop surface positioned appropriately at $z = d_o + z_o$ (see also Penman and Long, 1960). Monteith endowed the effective surface with the physiological properties of a leaf and derived a formal expression for the "stomatal"* resistance r_s of a crop from the ratio $(e_s(T_s) - e_s)/$ (evaporative flux), where $e_s(T_s)$ is the saturated vapour pressure at the temperature, T_s : i.e. e_s and T_s were assumed to give an estimate of mean conditions of vapour pressure and temperature on the real crop surface. However, the above method took no account of the extra resistance encountered by mass or heat at a rough surface over that encountered by momentum (see 1.3(b), (c) and (d)); i.e. it contained the implicit assumption that $z_o' = z_o$, or rather, that $B^{-1} = 0$.

Consideration of Fig. 5.10 allows an improved estimate of e_s and T_s to be made from the intercepts of the wind versus property relationships, not on the line $u(z) = u(d_o + z_o) = 0$ as previously, but on the line

---

* Later called the "surface" resistance, Monteith (1965).

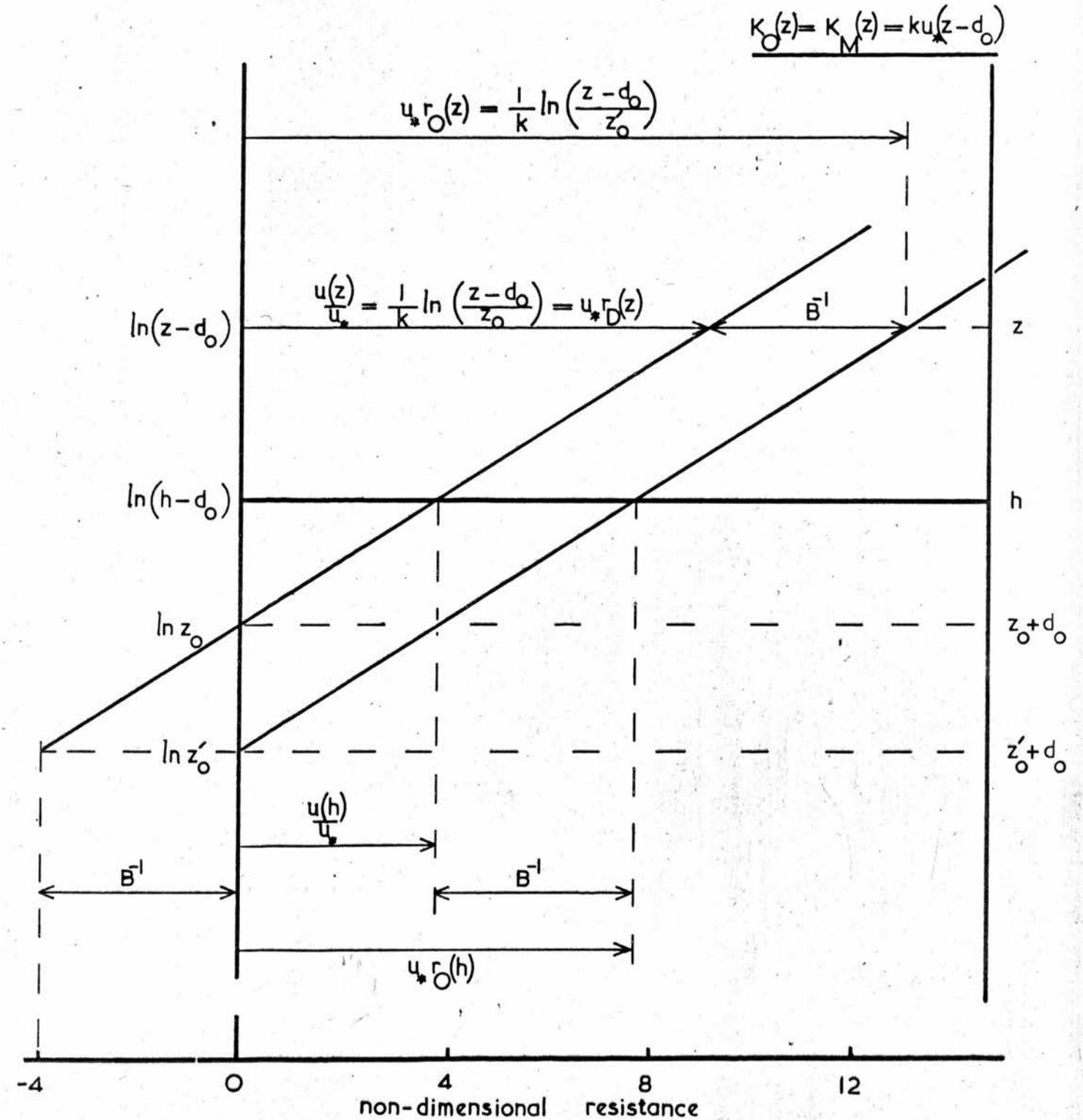

FIGURE 5.10 $\ell n(z - d_o)$ versus $u_* r_D(z)$ for momentum and $u_* r_O(z)$ for mass or heat: graphical representation of the parameter B^{-1}.

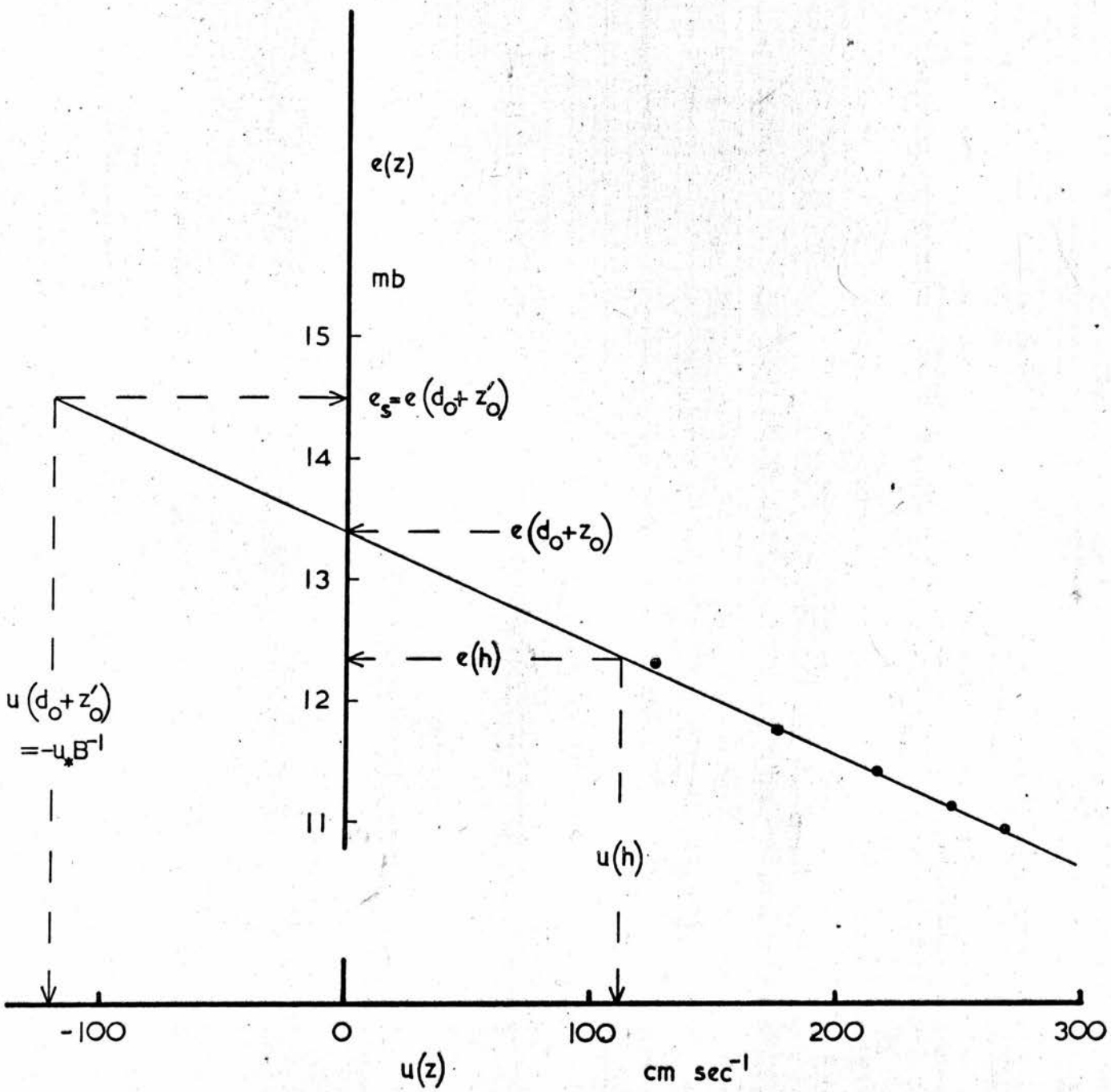

FIGURE 5.11 Vapour pressure e(z) verses wind speed u(z): a determination from Eq. (5.9) of surface vapour pressure e_s.

$$u(z) = u(d_o + z_o') = -B^{-1} u_* \qquad (5.9)$$

consistent with repositioning the effective surface at the level $z = d_o + z_o'$, where according to Eq. (5.7) the resistance $r_0(z)$ is zero.

In the example drawn in Fig. 5.11, a fictitious set of vapour pressures, $e(z)$, is plotted against the group E wind speed values, $u(z)$, from Table 5.3. With $u = 30$ cm. sec.$^{-1}$ and $B^{-1} = 4$, Eq. (5.9) gives $u = -120$ cm. sec.$^{-1}$: the intercept on this line of the straight line drawn through the points on Fig. 5.11 (assuming $K_V(z) = K_H(z)$) gives $e_s = e(d_o + z_o') = 14.5$ mb.; whereas on Monteith's simpler model, $e_s = e(d_o + z_o) = 13.4$ mb. (Compare differences with $e(h) = 12.3$ mb., for example.)

Some of the objections to Monteith's "stomatal" or "surface" resistance r_s (see Philip, 1966, and Monteith, 1963; Discussion) are removed if values of e_s and T_s defined by Eq. (5.9) can be used in its derivation. (With usual conditions of transpiration, such revised values of r_s would be about 50 to 75 per cent of the original values.) However, until likely differences between $\bar{R}_D$ and $\bar{R}_0$ can be included in an estimate of B^{-1} (i.e. a rigorous use of Eq. (1.33)), objections arising from differences in the vertical distributions of the sources and/or sinks of momentum, mass and heat cannot be answered.

N.B. it is the roughness length of a crop and not,

as suggested by Penman and Long (1960), its zero plane displacement which is modified (via Eqs. (1.33) and (5.8)) by any difference between the vertical distribution of the momentum sink within the canopy and the corresponding distributions of the sources and/or sinks of water vapour, carbon dioxide and heat.

CONCLUSION

This Section is not intended as a list of conclusions or results, each one of which is already recorded at an appropriate place in the text, but is selective in nature, treating only those points which allow further unification of the text, are worthy themselves of further emphasis, or in retrospect are in need of fuller explanation.

C.1 The Rough Surface - General

In Section 1.3(c), Eq. (1.24), the ratio μ is related to the parameter B^{-1} via the absolute constant E. The value of E will now be estimated, and used to find the value of B^{-1} corresponding to the transition to the "fully rough" flow regime.

For the elements of the artificial crop, $\mu \doteqdot 1.3$ over the range of Reynolds' numbers involved (Goldstein, 1938), and Eq. (1.34) gives $B^{-1} \doteqdot 0.5$ ($\overline{r}_o$ derived from data on heat exchange in Schlichting's treatise): so that $E \doteqdot 0.4$. Using the field value, $B^{-1} = 4$, proposed in Section 5.4(a), μ is found to have the value 10 for a vegetated surface - not substantially different from the order of magnitude implied for μ in Section 4.4.

The (element) Reynolds' number $R_c = 600$, defined in Section 1.1(c) to specify the transition to the "fully rough" flow regime, corresponds, for circular cylinders, to $\mu \doteqdot 5$ (Goldstein, 1938); so perhaps $\mu = 5$ is a

close enough estimate of the corresponding universal threshold value of μ (1.3(c)). With $E = 0.4$, this threshold is effectively specified by $B^{-1} = 2$ (provided $D_{,\kappa} = \nu$).

As a final example, $E = 0.4$ implies that for the rough glass plates used by Owen and Thomson (1963) $\mu \doteqdot 50$ when $u_* \doteqdot 25$ cm. sec.$^{-1}$.

C.2 The Crop

It has been demonstrated in the text, that $r_D(h)$ (the total resistance of a crop referred to $z = h$) can be consistently and properly separated into two (suitably defined) mean resistances $\overline{R}_D$ and $\overline{r}_d/S_d$, where $\overline{R}_D$ is a measure of the turbulent resistance of the canopy and $\overline{r}_d/S_d$ a measure of the resistance of the crop elements themselves; that the magnitude of $\overline{R}_D$ is in agreement with the corresponding values of $K_M(z)/u_*$ within the canopy - which values are significantly larger than those determined by Uchijima and Wright, for example - and also; that $\overline{R}_D$ and $\overline{r}_d/S_d$ are generally of comparable magnitudes. This last property lessens to some degree the effect of a change in $\overline{C}_d$, (equal to $1/\overline{u}\,\overline{r}_d$), on the value of z_o (see 3.4(a)); for z_o is related to (the sum) $r_D(h)$.

It is to be noted that the proposed empirical relation $z_o = k\,(h - d_o)$, Eq. (3.9), gives values of z_o nearer to those derived experimentally (3.3(b); 5.2(a)) than does Eq. (3.8).

C.3 The Leaf

It was first suggested by Cowan and Milthorpe (1967) that the "bluff-body" effect must result in r_d being significantly smaller than r_o for a leaf exposed within a crop canopy; and indeed the values found for the artificial leaf in Chapter 4 show that, except near $\phi = 0^o$, r_d is much smaller than r_o.

Sheppard (1958) implied that any relation employing vertical fluxes of vapour or heat to estimate surface conditions of vapour pressure or temperature must include the appropriate molecular diffusivity D or κ; and indeed the coefficient C_{vh} is found to be proportional to $(D, \kappa)^{2/3}$; so that, generalising to a natural rough surface, the appropriate value of n to be used in Eq. (1.23) or Eq. (1.24) is $2/3$.

However, owing to the uncertainty introduced by the effect of shelter into the derivation of a value for B^{-1} in the field (p_o for momentum; $p_o' < p_o$, for vapour or heat), the value $B^{-1} = 4$ is considered to apply to water vapour, CO_2 and heat over any vegetated surface. (Note: the source of this uncertainty is not doubt as to the "real" value of p_o (see 5.3(d), (ii)), but hinges on the choice of the ratio $p_o'/p_o = 0.75 \pm 0.25$ - a ratio which, however, is open to experimental investigation.)

C.4 Final Remarks

This thesis has been concerned to a relatively large extent with surface conditions, i.e. with the lower boundary conditions of the atmosphere. However, it is the various material fluxes across this lower boundary which are of prime concern; and only in as much as some advance has been gained in understanding the nature of the resistances presented to these fluxes, at this boundary, can any distinct claim to relevance be made. Nevertheless, it is hoped that the results of this work may have application in agriculture and in forestry - which latter offers considerable scope for further research into the properties of canopy flow.

APPENDIX JULY 1968

The assumption (p.105) that the product $u_* \bar{R}_D$ is independent of u_* is tenable only in terms of the physical model of a crop which it defines*, and breaks down on application to a real crop. A proper physical model includes the assumption that successive profiles should be geometrically similar in shape - not congruent as implied by the original model - so that $u_* \bar{R}_D$ and hence $u(h)/u_*$ must be proportional to $u_* \bar{r}_d / S_d$. Thus variation in z_o with u_* depends solely on the behavior of the mean drag coefficient $\bar{C}_d$ of a crop element and is more extreme than indicated in the original analysis.

Changes are

(i) that Eq. (3.11) is upheld and can be written as

$$C_D(h) = \left(\frac{\bar{u}}{u(h)}\right)^2 S_d C_d \qquad (3.12\text{-A})$$

which can be derived from Eq. (3.12) on the assumption that $\bar{u}$ is proportional to $u(h)$ ($\bar{u}$ is properly equal to u_m as defined on p.183);

(ii) that Eq. (3.17) is transformed into

$$\frac{u(h)}{u_*} = \frac{u(h)}{\bar{u}} \quad \frac{u_* \bar{r}_d}{S_d} \qquad (3.18\text{-A2})$$

* A comprehensive appendix is available from the author, Department of Meteorology, Drummond Street, Edinburgh, 8.

while Eq. (3.18) is replaced by

$$\frac{u(h)}{u_*} = 3.45\, u_* r_d(\bar{u})/s_d \qquad (3.18\text{-A})$$

(iii) that Eq. (5.4) becomes

$$\frac{u(h)}{u_*} = 2.2\, u_* \bar{r}_d/s_d \qquad (5.4\text{-A})$$

and Eq. (5.5)

$$\frac{u(h)}{u_*} = 0.13\, u_* \qquad (5.5\text{-A1})$$

It is plausible* however that $\bar{c}_d \propto 1/u^{\frac{1}{2}}$,

so that

$$\frac{u(h)}{u_*} = 1.26\, u_*^{\frac{1}{2}} \qquad (5.5\text{-A2})$$

For Fig. 3.15 and in Table 3.12 the u_* values were calculated from the forces f derived from moment balance readings and as such are somewhat incompatible with the values of u(z) used. However, when values of u_* are derived from the forces f_p calculated from the measured u(z) profiles these u_* are compatible with each u(z) and the resulting Fig. 3.15-A (p.201) is in agreement with Eq. (3.18-A).

* See foot-note p. 199

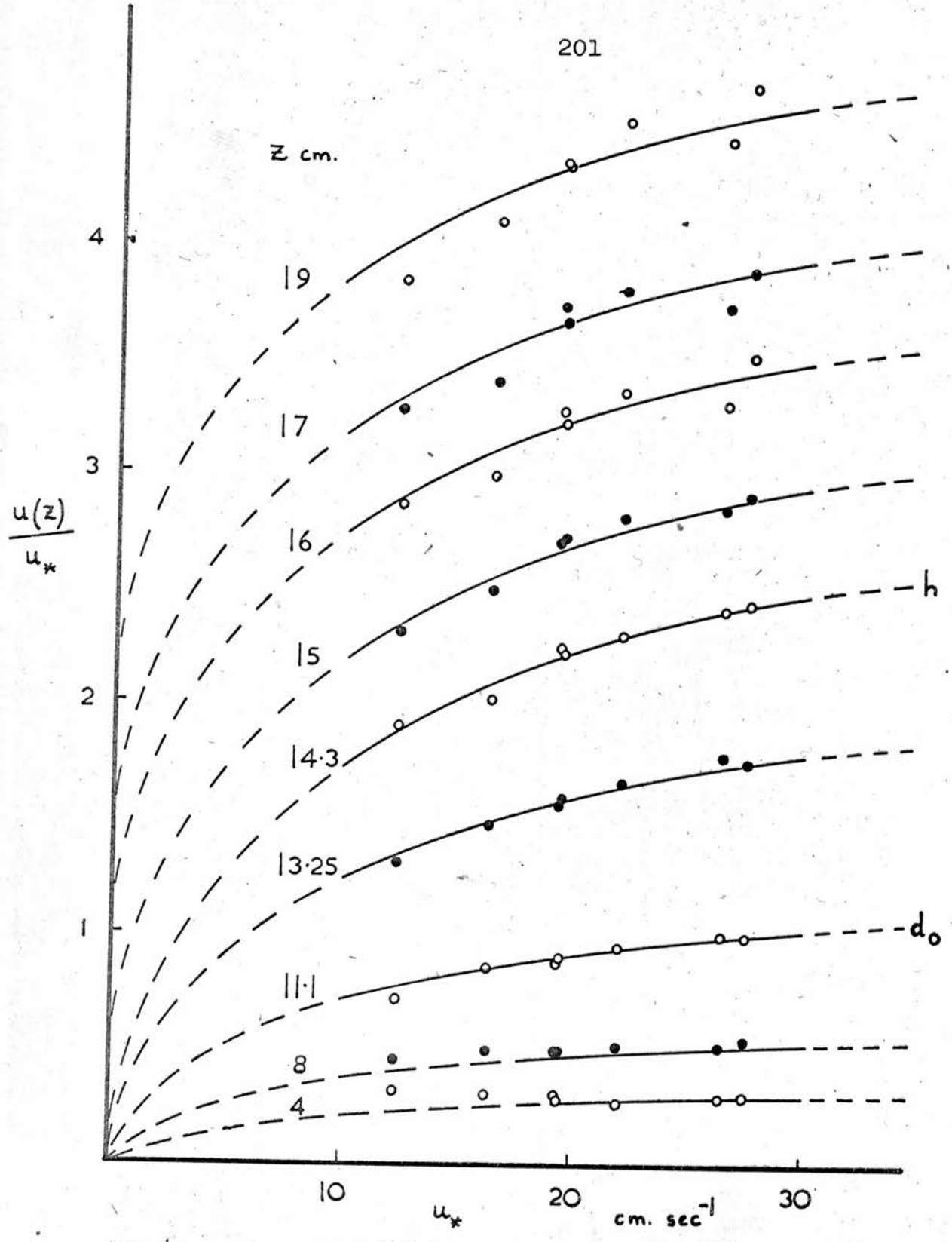

FIGURE 3.15-A $u(z)/u_*$ versus u_* from Table 3.12A (u_* derived from normalised f_p, not from f as Fig 3.15)